NANOSCALE MODEL CATALYSTS SUPPORTED BY METAL ORGANIC FRAMEWORKS

by

CYRIL YOUNG

A dissertation Submitted in the fulfilment of the requirements for the degree of

MAGISTER SCIENTAE

in the

DEPARTMENT OF CHEMISTRY
FACULTY OF SCIENCE

at the

UNIVERSITY OF THE FREE STATE

SUPERVISOR: PROF. ANDREAS ROODT

CO-SUPERVISOR: PROF. BEN BEZUIDENHOUDT

NOVEMBER 2009

Acknowledgements

I wish to express my gratitude:

To my heavenly father for the talents and capabilities he has bestowed on me and the opportunity to use them to explore is his wonderful creation.

Prof Andreas Roodt, who has mentored me for the duration of masters, thank you for your time, support and the enthusiasm. You have played a critical role in the development of chemistry ability and it has been a privilege to have you as a mentor.

Prof BCB Bezuidenhoudt, thank you for your help and input throughout the year.

The UFS inorganic group: Thank you all especially Nicoline, Theuns and Deon for your help, insight and friendship.

To my parents Elsabe' and Peter John Young; thank you for the sacrifices you have made to provide me with the opportunity to further my education. This could not have been possible without your love, support and understanding. To my brother P.J. and my sister Dina for your friendship and advice.

To Tharien who stayed by my side throughout the frustrating times. Your love and companionship means the world to me.

SASOL for financial support.

Table of Contents

Table of Contents

Table of Contents

Abbreviations

Symbol / Abbreviation	Meaning
Z	Number of molecules in a unit cell
Å	Angstrong
NMR	Nuclear Magnetic Resonanse spectroscopy
KMR	Kern Magnetiese Resonance spektroskopie
ppm	(Unit of chemical shift) parts per million
IR	Infrared spectroscopy
υ	Streching frequency on IR
MO	Molecular orbital
π	Pi
σ	Sigma
α	Alpha
β	Betha
γ	Gamma
λ	Wavelength
θ	Sigma
º	Degrees
ºC	Degrees celcuis
cm	Centimeter
g	Gram
M	(mol/L)
mg	Milli gram
h	Planck's contant
k_B	Boltzman's constant
T or temp.	Temperature
UV	Ultraviolet region in light specturm
Vis	Visible region in light spectrum
NaOH	Sodium Hydroxide
CO	Carbon monoxide
DMF	Dimethylformaldehyde
PVA	Polyvinyl acetate
MOF	Metal Organic Framework
ATR	Attenuated Total Reflectance
GC	Gas Chromatography
SEM	Scanning Electron Microscope
NaH	Sodium Hydride
K	Kelvin
Bpym	2,2-Bipyrimidine
PPh_3	Triphenylphosphine
Trif	Triflate ion
Daf	4,5-diazafluoren-9-one
NA	Nicotinamide

Abstract

The aim of this study was to use square planar platinum(II) and palladium(II) complexes for the synthesis of bridged complexes and as building blocks for the subsequent construction of two dimensional metal organic frameworks. For this purpose, pyrazine, 2,2'-bipyrimidine (bpym) and 4,4'-bipyridine (4,4-bipy) were chosen as rigid bridging ligands. 4,5-Diazafluoren-9-one (Daf) was used as a non-bridging ligand in some of the investigations. The optimum conditions for crystallization of these bridged species were determined in order to co-crystallize the complexes with synthesized crystalline inorganic supports, which consisted of titanium and tungsten oxide.

Characterization of the complexes was done by Infrared spectroscopy and Nuclear Magnetic Resonance spectroscopy (NMR). Single crystal X-ray crystallographic structure determinations of the following compounds were completed: *cis*-[$Pd(PPh_3)_2(Daf)_2$].-$(Trif)_2.CH_3NO_2$, *cis*- [$Pd_2BpymCl_4$].DMF and *cis*-[$Pd(PPh_3)_2(NO_3)_2$].$CO(CH_3)_2$.

cis-[$Pd(PPh_3)_2(Daf)_2$].$(Trif)_2.CH_3NO_2$ crystallized in the monoclinic space group *P*2/n with Z =4 in a unit cell with dimensions: a = 15.184(1) Å, b = 17.112(1) Å, c = 22.256(2) Å, α = 90 °, β = 99.676(4) °, γ = 90 ° at 100 K. Least-squares refinement led to a value of the conventional R index of 0.0750 and R_w = 0.1930 for 12345 reflections having $I > 2\sigma(I)$. The palladium ion is coordinated *cis* with two phosphorus and two nitrogen atoms. The formal geometry of the palladium center is square planar. In addition there is an interaction between uncoordinated nitrogen atoms of 4,5-diazafluoren-9-one ligand in the axial positions, which results in the formation of a pseudo octahedral structure. A 50% disorder is present on one of the phenyl rings and one of the triflate counter ions. The R_w value is high as the result of one carbon atom and its hydrogen atoms not being located on the disordered acetone solvate.

cis-[$Pd_2BpymCl_4$].DMF crystallized in the monoclinic space group *C*2/m with Z = 2 in a unit cell with dimensions: a = 10.73(7) Å, b = 14.24(8) Å, c = 5.938(2) Å, α = 90 °, β = 108.229(4) °, γ =

Abstract

90 ° at 100 K. Least-squares refinement led to a value of the conventional R index of 0.032 and R_w = 0.0893 for 1110 reflections having I > 2σ(I). The complex consists of two palladium centers linked by the 2,2'-bipyrimidine ligand. Each palladium atom is coordinated by two chlorido ions, two nitrogen atoms and has a square planar geometry. A 25 % disorder is found on the DMF solvate.

cis-[$Pd(PPh_3)_2(NO_3)_2$].$CO(CH_3)_2$ crystallized in the monoclinic space group *C*2/c with Z = 4 in a unit cell with dimensions: a = 40.343(2) Å, b = 9.749(1) Å, c = 19.78(1) Å, α = 90 °, β = 115.514(1) °, γ = 90 ° at 100 K. Least-squares refinement led to a value of the conventional R index of 0.0773 and R_w = 0.1873 for 8638 reflections having I > 2σ(I). The complex consists of a square planar geometry at the palladium center coordinated to two oxygen atoms and two phosphorus atoms in a *cis* fashion. The high R_w value is a result of one carbon and its hydrogen atoms not being located on the disordered acetone solvate.

A preliminary catalytic investigation was attempted using *cis*-[$Pd_2BpymCl_4$].DMF in Heck coupling and the Wacker oxidation process. However, no reproducible results were obtained due to infrastructural and time constraints.

Key terms:

Platinum

Palladium

Nanoparticles

Crystal structure

Supports

Metal organic frameworks

2,2'-bipyrimidine

Pyrazine

4,4-bipyridine

Catalysts

Opsomming

Die doel van hierdie studie was om vierkantig-planêre platinum(II) en palladium(II) brugkomplekse te sintetiseer en as boustene vir die daaropvolgende konstruksie-boustene vir tweedimensionele organometaalraamwerke te gebruik. Die starre vlakligande pyrasien, 2,2'-bipirimidien en 4,4'-bipiridien is vir hierdie doel gekies. 4,5-diazafluoren-9-one (Daf) is gebruik as 'n nie brugende ligand. Die optimum kondisies vir die kristallisasie van hierdie gebrugde spesies is bepaal om dit in opvolgende stappe met gesintetiseerde kristallyne anorganiese titaan- en wolframgebaseerde vaste steunraamwerke, te ko-kristalliseer.

Die komplekse is met behulp van Infrarooi- (IR) en kernmagnetiese resonansspektroskopie (KMR) gekarakteriseer. Suksesvolle enkelkristal X-straalkristallografiese struktuurbepalings is van die volgende verbindings gedoen: *cis*-[Pd(PPh_3)$_2$(Daf)$_2$].(Trif)$_2$.CH_3NO_2, *cis*- [Pd_2BpymCl$_4$].DMF en *cis*-[Pd(PPh_3)$_2$(NO_3)$_2$].$CO(CH_3)_2$.

cis-[Pd(PPh_3)$_2$(Daf)$_2$].(Trif)$_2$.CH_3NO_2 kristalliseer in die monokliniese ruimtegroep *P*2/n met Z=4 in 'n eenheidsel met dimensies: a = 15.184(1) Å, b = 17.112(1) Å, c = 22.256(2) Å, α = 90 °, β = 99.676(4) °, γ = 90 ° by 100 K. 'n Kleinste-kwadrate verfyning het 'n konvensionele R indeks van 0.0750 en R_w = 0.1930 vir 2345 refleksies met $I > 2\sigma(I)$ gelewer. Die palladiumatoom is in 'n vierkantig-planêre geometrie *cis* gekoördineerd deur twee fosfor- en twee stikstofatome. Daar is addisioneel twee ongekoördineerde stikstofatome van die diazafluooren-9-oon ligand in die aksiale posisies, wat 'n pseudo oktahedriese geometrie induseer. 'n 50% Wanorde in die pakking van een van die fenielringe sowel as in een van die triflaatanione is waargeneem. Die hoë R_w waarde is 'n gevolg van die feit dat een koolstofatoom van die wanordelik-gepakte asetoonoplosmiddel en die waterstofatome daarvan, nie geplaas kon word nie.

cis-[Pd_2BpymCl$_4$].DMF kristalliseer in die monokliniese ruimtegroep *C*2/m met Z = 2 in 'n eenheidsel met dimensies: a = 10.73(7) Å, b = 14.24(8) Å, c = 5.938(2) Å, α = 90 °, β = 108.229(4) °, γ = 90 ° by 100 K. Kleinste-kwadrate verfyning het 'n konvensionele R indeks van 0.032 en R_w = 0.0893 vir 1110 refleksies met $I > 2\sigma(I)$ gelewer. Die kompleks bestaan uit twee palladiummetaalsenters wat deur die 2,2'-bipirimidienligand gebrug word. Elke palladiumatoom

Opsomming

word deur twee chloridoligande en twee stikstofatome in 'n vierkantig-planêre geometrie gekoördineer. 'n 25 % Wanorde in die pakking van die DMF oplosmiddel is waargeneem.

cis-[$Pd(PPh_3)_2(NO_3)_2$].$CO(CH_3)_2$ kristalliseer in die monokliniese ruimtegroep *C*2/c met Z = 4 in 'n eenheidsel met dimensies: a = 40.343(2) Å, b = 9.749(1) Å, c = 19.78(1) Å, α = 90 °, β = 115.514(1) °, γ = 90 ° by 100 K. Kleinste-kwadrate verfyning het 'n konvensionele R indeks van 0.0773 en R_w = 0.1873 vir 8638 refleksies met I > 2σ(I) gelewer. Die kompleks besit 'n vierkantig-planêre geometrie rondom die palladiumatoom, gekoördineer deur twee suurstof- en twee fosforatome in 'n *cis* oriëntasie. Die hoë R_w waarde is 'n gevolg van die feit dat een koolstofatoom van die wanordelik-gepakte asetoonoplosmiddel en die waterstofatome daarop, nie geplaas kon word nie.

Die kompleks *cis*-[$Pd_2BpymCl_4$].DMF se katalitiese aktiwiteit is voorlopig in die Heck koppelingsreaksie en Wacker oksidasieproses geëvalueer, maar geen herhaalbare resultate is as gevolg van infrastruktuur- en tydsbeperkings verkry nie.

Sleutelterme:

Platinum

Palladium

Steunraamwerke

Organometaalraamwerke

2,2’-bipirimidien

4,4’-bipiridien

Pyrasien

boustene

katalitiese

Boustene

1 Introduction and Aim

1.1 Introduction

The burden of an ever-growing human race has drawn an enormous amount of resources from the earth. Mankind is living in a time where it is confronted by the consequences of the rapid rate at which it is using fossil fuels and other natural resources. Consequently, the human race stands at a point where it has to develop ways in which to conserve energy and the environment. One way in which this can be achieved is through the development of better catalysts for industrial processes.

A catalyst, by definition, is a chemical compound that increases the reaction rate of a chemical reaction, but is not consumed in the process[1]. Figure 1.1 illustrates how a catalyst lowers the activation energy of a chemical reaction and by exploiting this principle, one is able to save time, money and energy.

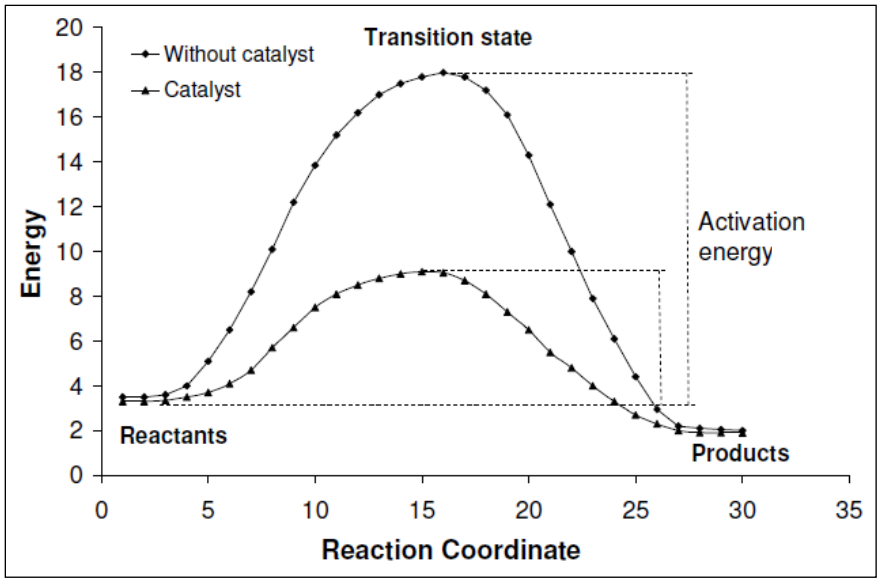

Figure 1.1: Illustration of the lowering of activation energy of a reaction by a catalyst.

Chapter 1

Although a wide variety of metals are used in catalysis today, the platinum group metals show the most promising catalytic properties. The platinum group metals consist of platinum, palladium, osmium, rhodium, iridium and ruthenium. Except for Russia, which produces the most palladium, South Africa is the largest producer of all platinum group metals[2]. Platinum group metals catalyze a large number of chemical reactions in the chemical industry such as hydrogenation, oxidation reactions and methanol reforming. Platinum and palladium are of particular interest as they are very similar in nature. Palladium is the more reactive of the two, unfortunately also with regards to decomposition reactions[3]. Both these metals form square planar compounds which are of interest for this study. Their wide variety of applications as catalysts also provide the possibility to test the catalytic activity effectively and easily.

1.2 Brief overview of catalysis

Metal catalysts were unknowingly used since the early 1800's. In 1818 L. J. Thenard announced his discovery of, "a chemical substance that can speed up a chemical reaction without itself being chemically changed[4]." The word "catalysis" was first formulated by Berzelius in 1836. Although he did not have a molecular understanding of the working of a catalyst, he was able to correlate that some reactions were driven by a 'catalytic force'. At the end of the eighteenth century scientists started to focus their research on the decomposition of chemical materials in the presence of various metals. It was consequently discovered that the decomposition of certain compounds resulted in the formation of different products. Later Humphrey Davy discovered that platinum and palladium were catalysts for the oxidation of coal. He also noted that copper, silver and gold did not catalyze the process. Davy however, was not able to postulate the correct theory on the working of catalysts. In 1834 Faraday proposed the theory that in order for a catalyst to work successfully in a reaction, both reactants had to simultaneously adsorb to the catalyst's surface. However, he did not explain the catalytic action. Later on Ostwald proposed: 'a catalyst does not influence the thermodynamic equilibrium of the reactants and products but affects the rate of the chemical reaction[5].'

In the early 19th century industrial scale reactions started to include catalysis, mainly in the wine and beer industry. Also, inorganic oxidation processes like the Deacon process in which HCl was oxidized for chlorine production were developed. Later, van't Hoff developed the equilibria theory which was the basis for the development of catalysts. By the start of the twentieth century, chemical catalyzed processes had been developed for the production of sulfuric acid and ammonia. Ammonia was produced on a large scale in the 1st world war and sulfuric acid was used in the mining industry[6].

Today catalysis is used in the chemical industry in a large number of processes[2]. It plays a critical role in the production of feed-stocks used in the production of commodities that are consumed by the public every day. However, catalysts are far from reaching their fullest potential and there remain a vast number of undiscovered areas in this research area.

1.3 Heterogeneous *versus* Homogeneous Catalysis

Catalysis is mainly divided into homo- and heterogeneous catalysis processes and both of these have advantages and disadvantages. Homogeneous catalysis has a major problem with regard to separation, it is expensive, energy intensive and the catalysts contaminate the products. However, it shows better specificity, controllability and reproducibility. Heterogeneous catalysts, on the other hand, have greater thermal stability[7] and even though some metal particles are lost due to leaching, the catalysts tend not to plate out as in the case of homogeneous catalysts. The catalysts are also less sensitive to oxygen and moisture. Even though heterogeneous catalysis by definition points towards the deposition of a catalyst, usually a metal complex, on an inert support it is often over-looked that the support may be able to increase the efficiency of a catalyst. The conformation of the support at the catalytic site may be in such a way as to benefit the process. The organic functional groups that are bound to the metal complexes also bond covalently to the support, which in turn can alter the stereochemistry of the metal complex in a beneficial way. Supports can alter the equilibrium between the metal ion and its ligands in such a way as to improve selectivity. Lastly, certain compounds tend to be stabilized by supports. This is beneficial as certain unstable compounds that show catalytic activity, which in other ways would have gone to waste, can be utilized on supports[8].

1.4 Catalyst supports

Two major types of supports have been developed. In the first category, the metal complex is linked to a support *via* attachment of the support to one of the ligands that are bonded to the metal. In the second category, the ligands that bond to the metal center are displaced by reacting with the support. The ligands are substituted by the groups that are found on the surface of the support. Both of these attachments have their advantages and disadvantages.

1.4.1 Organic Polymer Supports

A large number of organic polymers have been developed to serve as catalyst supports. This includes polystyrene, polypropylene, polyacrylates and polyvinyl chlorides. As with most things, these supports have their advantages and disadvantages. Polymer supports have the following advantages.

- Polymer groups are easily functionalized.
- The supports are mostly inert and do not take part in the chemistry that occurs at the catalytic site.
- The supports can also be synthesized in a wide variety of ways. Consequently, one can control the porosity and surface area of the support. This is usually done by increasing or decreasing the degree of cross linking.

Unfortunately, the supports exhibit poor mechanical properties and are destroyed under the harsh conditions found in industrial reactors. Polymer supports also have poor heat transfer properties[8].

1.4.2 Inorganic Supports

A few inorganic supports such as silica, alumina, glasses, metal oxides and zeolites have also been developed. Inorganic supports are better suited to industrial reactions than their organic counterparts as a result of better mechanical properties[9]. These compounds also display better thermal stability and reasonable heat transfer properties. Zeolites containing a wide variety of

pore size and pore distributions are currently being used. Most inorganic supports contain hydroxyl groups on their surfaces. These groups are used to attach the metal complex to the support [8].

1.5 Aim of this study

In most of the industrial processes making use of heterogeneous catalysis today, the catalyst is prepared and then placed on a support. Most of these supports have micro-pores into which the catalyst is deposited. However, the processes currently used lack the ability to control the dispersion of metal particles throughout the support. Consequently, metal particles are not evenly dispersed and tend to cluster. Temperatures in industrial reactors tend to be in excess of 200^{o} C and under these conditions small nano-sized metal particles fuse to form larger metal conglomerates. Since catalysis takes place at the surface of the metal particles, catalytic rates are dependent on the number of metal particles available. Once the metal particles fuse, there are fewer sites available for catalysis and hence a loss of activity.

The following aims were set for this study:

1. Synthesize two dimensional square planar palladium and platinum metal organic systems, which can be developed into frameworks that can theoretically be used to control the positioning of the metal atoms when adding the catalyst to the support.

2. Synthesize crystalline inorganic supports.

3. Develop the optimum conditions for the crystallization of the synthesized molecules.

4. Characterization of these complexes by means of single crystal X-ray crystallography, IR and NMR. i.e. utilize crystal engineering principles to produce catalysts.

5. Attempt to co-crystallize the compounds together with crystalline inorganic supports.

6. Test catalytic activity of complexes before and after co-crystallization in order to determine the change of activity by the addition of a support.

Chapter 1

(1) Swaddle, T. *Inorganic chemistry: an industrial and environmental perspective*; Academic Press: San Diego, **1997**.

(2) Kettler, P. B. *Org. Process Res. Dev.* **2003**, *7*, 342-354.

(3) Tsuji, J. *Palladium reagents and catalysts: new perspectives for the 21st century*; Wiley: Hoboken NJ, **2004**.

(4) Robertson, A. J. B. *Platinum Metals Review* **1975**, *19*, 42–47.

(5) Lindström, B.; Pettersson, L. J. *Cattech* **2003**, *7*, 130–138.

(6) Van Santen, R. *Catalysis: an integrated approach*; 2nd ed.; Elsevier: Amsterdam; New York, **1999**.

(7) Bhaduri, S. *Homogeneous catalysis mechanisms and industrial applications*; Wiley-Interscience: New York, **2000**.

(8) Hartley, F. *Supported metal complexes: a new generation of catalysts*; Kluwer Academic Publishers: Dordrecht; Boston; Hingham MA U.S.A., **1985**.

(9) Clark, J.; Royal Society of Chemistry (Great Britain) *Clean synthesis using porous inorganic solid catalysts and supported reagents*; Royal Society of Chemistry: Cambridge, **2000**.

2 Literature Study of Platinum and Palladium Nanoparticles in Catalysis

The term "nano" is the prefix used to denote the minus 9th power of ten. A nanometer corresponds to a billionth of a meter. Investigations of particles in this size regime have led to development of nanocatalysts. These catalysts are used in processes like *inter alia* hydrogenation, hydrosilylation and carbon- carbon bond formation reactions[1]. In many of these processes the exact detail of the kinetic mechanism at nano-level is not yet understood completely. However, with better quality analytical techniques such as Scanning Tunnel Microscopy, Atomic Force Microscopy, laser tweezers and X-ray Diffractometry becoming available in recent times, scientists have been given the opportunity to gain better understanding of these systems[2]. Ultimately, the word "nano" has become synonymous in a number of different disciplines, including physics, electronics and chemistry.

2.1 The importance of catalysis

Developing and industrialized countries rely heavily on the production of large scale and fine chemicals and in most cases the chemical industry forms a vital part of the economies of these countries. The variety of chemicals that are produced either for large scale applications or household use is vast and contributes to the accepted way of life. Catalytic processes are used in fuel processing, petroleum refining and the conversion of syngas ($CO + H_2$). Unfortunately, the production of these chemicals is not without consequence, since a large quantity of chemical waste is generated. These waste products tend to have adverse effects such as global warming, acid rain and climate changes on the environment. This led to the introduction of legislation that called for the redesign of the chemical industry to attain the so called, "triple bottom line", which calls for the consideration of social, economical and environmental factors in the chemical industry.

Chapter 2

Large quantities of waste are generally generated from the stoichiometric reactions used in the production of chemicals. One way in which these waste products can be reduced is through the introduction of catalytic processes. Catalysis and more specifically, heterogeneous catalysis, provides scientists the opportunity to recover, regenerate and re-use catalysts. Unfortunately, heterogeneous catalysis can be plagued by poor selectivity, which can generate additional waste products. On the other hand, heterogeneous catalysis forms an essential part of the fine chemical industry. Transportation fuels, high temperature lubricants, chlorine-free refrigerants, stain-resistant fibres, high-strength polymers, and many thousands of other products are all synthesized by making use of some sort of catalyst. The chemical industry is not the only industry that exploits the benefits of catalysis. The pharmaceutical industry employs precious metal catalysts like palladium, platinum and gold in the synthesis of desired compounds. The Buchwald Hartwig, Heck, Kumada, Negishi, Nozaki Hiyama, Sonogashira, Stille, Suzuki Miyaura, and Tsuji Trost are some of the coupling reactions that make use of palladium as a catalyst in the pharmaceutical industry[3,4].

The majority of the processes used in the chemical industry involve the use of high surface area supports onto which nanoparticles can be deposited. These supports, which are discussed later, play a vital role in the performance of heterogeneous catalysts as well as nanocatalysts. The term ‘nanocatalyst’, was developed to describe the unique reactions that occur when making use of these nanoparticles as catalysts. In order for a catalyst to be considered a nanocatalyst, it has to fulfill the following characteristics;

- The valence electrons of the particle are extremely confined, leading to chemical and physical properties, which are not present in bulk form.
- The nanoparticles adsorb to specific areas of the utilized support. This adsorption process changes the intrinsic properties of these particles to a large extend.

Nanocatalysts exhibit large quantum size effects and structural fluxionality. These factors can be exploited for atom by atom design of these moieties. Cluster size can be controlled to tailor catalysts with different activity, selectivity and specificity.

2.2 Brief overview of nanotechnology and nanoparticles

The exact origin of nano-materials is unknown, although some research suggests that nanoparticles date back to 400 A.D. where Roman glass makers made coloured glass containing nanoparticles[5]. During the eighteenth and nineteenth century photography made use of light sensitive silver nanoparticles to produce the pixels on a photograph. This technique was further developed to produce the first colour photograph in 1861. In 1857, Michael Faraday published a paper that sought to explain the colour found in church windows. Later, Faraday also successfully synthesized gold nanoparticles by the reduction of tetrachloroaurate with phosphorus. Richard Feynman published a book in 1960 in which he alluded to the use of nanoparticles in computer and biological systems. Although scientists investigated small metal particles in the 1950's and 1960's not much came of their investigations. During this period electron paramagnetic resonance was employed to characterize particles on a nanometer scale. This technique was used to characterize colloids, which were produced by the thermal decomposition of solids containing positively charged metal ions. The structural aspects of these ions were further investigated during the 1970's by making use of mass spectrometry.

Throughout the 1980's several developments were made in microscopy, which gave rise to the Scanning Electron Microscope and the Atomic Force Microscope. Due to the development of new analytical tools like these, scientists gained understanding of entities on a smaller and smaller scale[6]. In 1981, methods were developed to produce nanoparticles by making use of focused lasers that melted metals into plasma. Bönnemann[7] introduced a method to produce nanoparticles by making use of metal salts, molecular stabilizers and a reductant. Figure 2.1 shows a nanoparticle stabilized after the reduction of its metal chloride salt in the presence of the tetra-N-butylammonium cation. Other methods like the thermal decomposition of metal(0) species in the form of metal carbonyls in the presence of stabilizing polymers, were also developed during this time.

Chapter 2

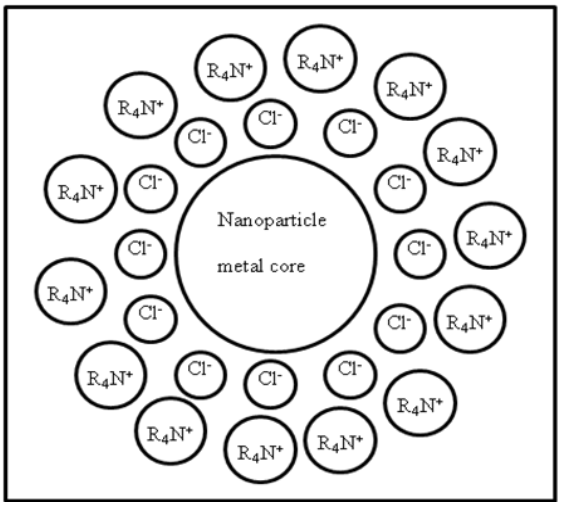

Figure 2.1: nanoparticles. Nanoparticles are stabilized by metal salts and stabilizers[7].

In the 1990's, attention was drawn to fluorescence, self assembly and molecular switches in small metal particles. In 1996, major institutions started funding nanotechnology initiatives which led to a global trend towards the exploration of this phenomenon. Consequently, by 2002 more than 37 global companies were funding some or other form of nano-initiative. Figure 2.2 illustrates the global surge in spending towards nanotechnology from 1997 onwards.

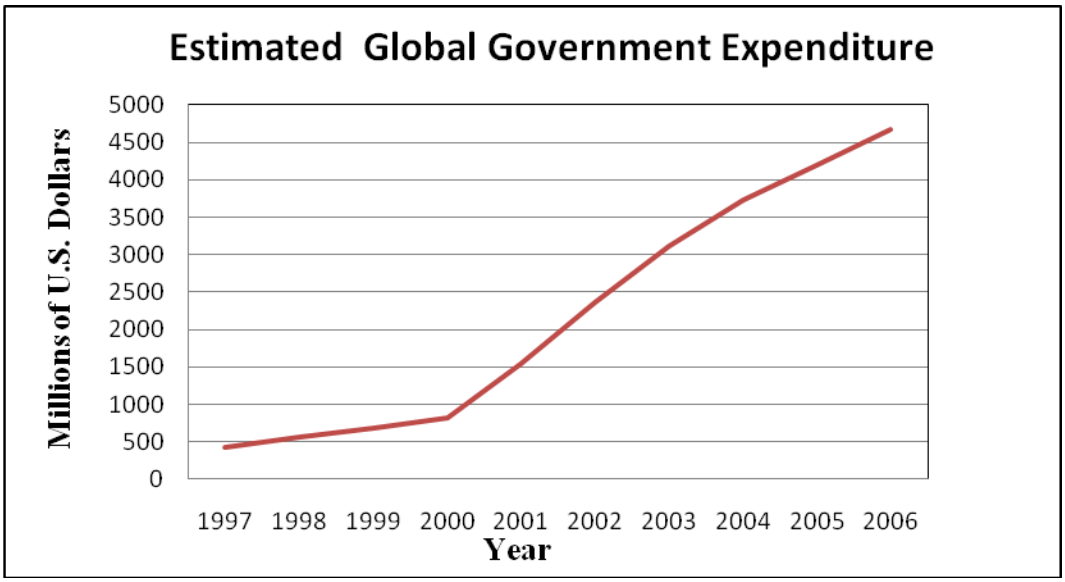

Figure 2.2: Estimated Global expenditure on nanotechnology research and development from 1997 to 2006.

Chapter 2

The number of different techniques that were developed for the synthesis of nanoparticles in the last 10 years is vast, but four major categories can be differentiated [8].

- **Wet Chemical processes;** this area employs colloidal chemistry, hydrothermal methods, sol-gels, and precipitation processes. Precise solutions of different ions are mixed under controlled conditions to yield insoluble particles that precipitate from solution. The precipitates are then collected and dried. This process does have a number of advantages. The equipment needed for synthesis is relatively cheap, easy to obtain and the process can be used to synthesize inorganic and organic moieties. Particle size and mono-dispersion of particles can be controlled by this method. However, yields may be low and bulk production can become costly.

- **Mechanical processes;** this technique makes use of grinding, milling and mechanical alloying. A course powder is physically eroded into finer and finer powders by planetary or ball mills. The advantage of this technique is that it is simple and cheap, provided that a course feedstock can be synthesized. Unfortunately, there can be agglomeration of particles, poor particle size distribution and contamination of particles from the equipment.

- **Form-in-place processes**; vacuum deposition, lithography and spray coatings are used to synthesize nanoparticles. These processes are very useful in the production of nano-structured layers and coatings, but can also be employed in the synthesis of nanoparticles. These processes are plagued by inefficiency.

- **Gas phase synthesis**; a variety of techniques like flame pyrolysis, electro-explosion, laser ablation, high temperature evaporation and plasma synthesis are used in the synthesis of nanoparticles. Each of these techniques can be applied in the production of a wide range of materials, provide clean controllable conditions and each one has their own drawbacks and advantages.

It is clear that there are various ways in which nanoparticles can be synthesized. The key to success is finding the method that will produce the desired catalysts with regards to efficiency and selectivity. From the above it is obvious that the development of effective processes is hampered by financial and environmental restrictions.

2.3 Nanoparticles in heterogeneous catalysis

The term ‘‘catalysis’’ was introduced by Berzelius in 1836. He used the term to classify chemical reactions where the progress of the reaction is affected by the addition of substances, which do not form part of the reaction products. Heterogeneous catalysis is a process where the catalyst and reactants are in a different phase. In most cases, the catalysts are in the solid phase and the reactants are in liquid or gas phase. Heterogeneous catalysis is utilized because it has the following distinct advantages:

- Solid catalysts tend to be non-corrosive.
- When using heterogeneous catalysis, a wide range of pressures and temperatures can be applied to the system according to the desired outcome.
- Separation of catalyst and feed is easy and inexpensive.

The term “nanocatalyst” in a sense forms part of the heterogeneous catalysis definition, but it can be seen as border lying towards homogenous catalysis. After World War II heterogeneous catalysis development was slow in relation to homogenous catalysis. This was due to the poor selectivity achieved in heterogeneous catalysis and the poor understanding of the mechanisms which were present in the catalytic systems. Homogeneous catalysis provided outstanding selectivity and efficiency, but the catalysts themselves suffered from poor thermal stability and the separation of catalysts from products was problematic[7]. Energy and environmental constraints required catalysts that could be recycled efficiently and effectively, consequently the development of heterogeneous catalysis was induced. In 1940, Nord first employed nanoparticles as catalysts in the reduction of benzene. Hydrogen transfer between benzene and cyclohexane, as well as oxygen transfer between CO and CO_2 by making use of gold nanoparticles was reported by Parravano in 1970. The reaction that started giving scientists

insight into the working of nanoparticles was performed by Haruta[6]. He made use of gold nanoparticles supported on metal oxides to oxidize CO with O_2 at low temperatures. This reaction revealed to scientists that it was in fact the particle size which was crucial to the catalytic process. During the 1970's and 1980's Bond and Sermon made use of gold nanoparticles for olefin hydrogenation reactions.

Gold was not the only metal that was employed for nanocatalysis. Hirai made use of rhodium nanoparticles that were synthesized using NaOH as a reducing agent in aqueous methanol. By putting $RhCl_3.3H_2O$, under the above mentioned reaction conditions, he was able to synthesize PVA stabilized rhodium nanoparticles that were smaller than any reported before. In the early 80's Maire's group made use of micelles for the catalytic hydrogenation of unsaturated substrates. This technique was developed by Fendler[9] who investigated nanoparticles in constrained environments like micro-emulsions, micelles, inverse micelles and vesicles. Hirai and Toshima collaborated to produce the platinum nanoparticles that were stabilized by surfactants. The nanoparticles were produced by reducing K_2PtCl_6 photochemically. In 1986 Lewis reported the colloidal mechanism of olefin hydrosilylation by employing silanes and a range of metals like cobalt, nickel, platinum and palladium. During the 90's Toshima furthered this research and investigated the use of polymers as stabilizers during the formation of nanoparticles. He also explored bimetallic systems of gold and platinum[10]. This gradual investigation of nanoparticles started to yield a better understanding of the catalytic systems. Catalysts were developed for a range of processes like redox reactions, photocatalysis, oxidation, hydrogenation reactions and carbon-carbon bond formation reactions.

As mentioned previously, heterogeneous catalysis used to lack in terms of selectivity and efficiency in many areas. Fortunately, transition metal nanoparticles and the developments throughout the 80's and 90's have given scientists the opportunity to eliminate these problem areas. Transition metal nanoparticles are clusters containing thousands of metal atoms, stabilized by ligands, polymers and dendrimers that protect their surfaces. These particles mimic metal surface activation and in so doing, have the ability to introduce efficiency and selectivity into heterogeneous catalysis. Previous studies have indicated that even though these metal clusters contain nanoparticles with a variety of sizes, the particles ranging from 1-10 nanometers are responsible for the catalytic process. The nanoparticles partaking in the catalytic process consist

of small crystallites that contain active sites where atom molecule interaction results in accelerated reaction rates[11]. Zeolites are often employed as supports for these catalysts in order to provide a pathway of access to the reactants. As a result of the major thrust towards nanocatalysis, the number of catalysts that have been developed are too many to discuss here. Table 2.1 illustrates a selected few of these reactions that make use of nanoparticles. These reactions are applied to a number of different substrates in chemical synthesis.

Table 2.1: Reaction where nanocatalysts are employed[7].

Reactions that employ nanoparticles as catalysts.
Hydrogenation: olefins, dienes and alkynes.
Heck C-C coupling: olefins.
Suzuki C-C coupling.
Sonogashira C-C coupling.
Stille C-C coupling.
Negishi C-C coupling.
Kumada C-C coupling.
Dehydrohalogenation of aryl halides.
Amination of aryl halides and sulfonates.
Hydrosilylation.
Coupling of silanes.
Hydroxycarbonylation of olefins.
[3 + 2] Cycloaddition.
McMurry coupling.
Oxidation: CO, amines and ethene.
Amination.
Carbonylation: aryl halides and methanol.
Allylic alkylation.
Hydroconversion of hydrocarbons.
Combustion: alkanes, arenes, alcohols.
Methanol reforming.

2.4 Platinum and Palladium in catalysis

Palladium was discovered by William Hyde Wollaston in 1803 and can be identified as a lustrous silver white metal. It has an atomic number of 46, an atomic mass of 106.42 and is found in group ten on the periodic table. Palladium forms part of the platinum group metals and can have oxidation states of 0, +1, +2, +4, and +6. Although it was previously believed that a +3 oxidation state exists, it was proven incorrect by XRD analysis, which confirmed the formation of a palladium dimer formation rather than a +3 oxidation species. Palladium(II) in the most common oxidation state and the complexes formed are mostly square planar. It has an ionic radius of 0.64 Å with 6 natural isotopes; Pd-102 (1.02 %), Pd-104 (11.15 %), Pd-105 (22.34 %), Pd-106 (27.33 %), Pd-108 (26.47 %), Pd-110 (11.73 %). Palladium has a melting point of 1554.9 ^{o} C and a density of 12.023 g.cm^{-3}. It is reasonably soluble in sulfuric , nitric and hydrochloric acid. Palladium remains stable in air at ambient temperatures. It has a very high affinity for hydrogen and can absorb up to 900 times its own volume at ambient temperature, which makes it ideal for hydrogen storage. It is mined mainly by Russia, South Africa and Canada and usually occurs with the other platinum group metals. It is estimated that palladium has an abundance of 0.015 mg/kg earth crust, which is roughly three times more than platinum. Even though the bulk of it that is mined each year is used in the catalytic converters found in exhaust systems, palladium is also a valuable catalyst in other chemical reactions. Palladium alloys find a wide variety of applications in dentistry and electronics. In medicine, palladium alloys are also used in the replacement of damaged bones and joints[12].

Of all the transition metal catalysts, palladium displays the most versatility when applied to carbon-carbon bond formation reactions. The ability to tolerate an abundance of functional groups is the major contributing factor in this area. The highest reactivity amongst the platinum group metals is displayed by palladium. Another factor that one needs to mention is the fact that reactions can be catalyzed by palladium without protecting functional groups and the catalysts are relatively stable in the presence of oxygen and moisture. However, palladium is a scarce metal and it is expensive. In organic synthesis Pd(0) and Pd(II) salts are employed as catalysts. Palladium chloride and palladium acetate are commercially available salts, which can be used as catalysts. These palladium(II) salts can be used as a source of palladium(0) which is usually

generated *in situ* to prevent the deactivation of the catalyst in the absence of substrate. Phosphines are often employed to prevent deactivation[13]. In a typical palladium catalyzed reaction there are five major steps that occur in the catalytic cycle (Figure 2.3).

1. Oxidative addition: This is the addition of the H-X molecule to the palladium, which results in the cleaving of the covalent bond and the formation of two new bonds. In the process palladium(0) is oxidized to palladium(II).
2. Insertion: This is the process whereby a molecule is inserted between the R group and the palladium center.
3. Transmetallation: The palladium center is alkylated by a M'-R" group which results in the transfer of the X group, which is attached the palladium center in the oxidative addition process, to another metal species.
4. Reductive elimination: This is effectively the reverse of the oxidative addition step. It results in the loss of two ligands and the reduction of the palladium center to palladium(0).
5. β -H elimination: This involves the elimination of hydrogen from the carbon situated in the β position from the palladium center. This give rise to a palladium hydride and an alkene.

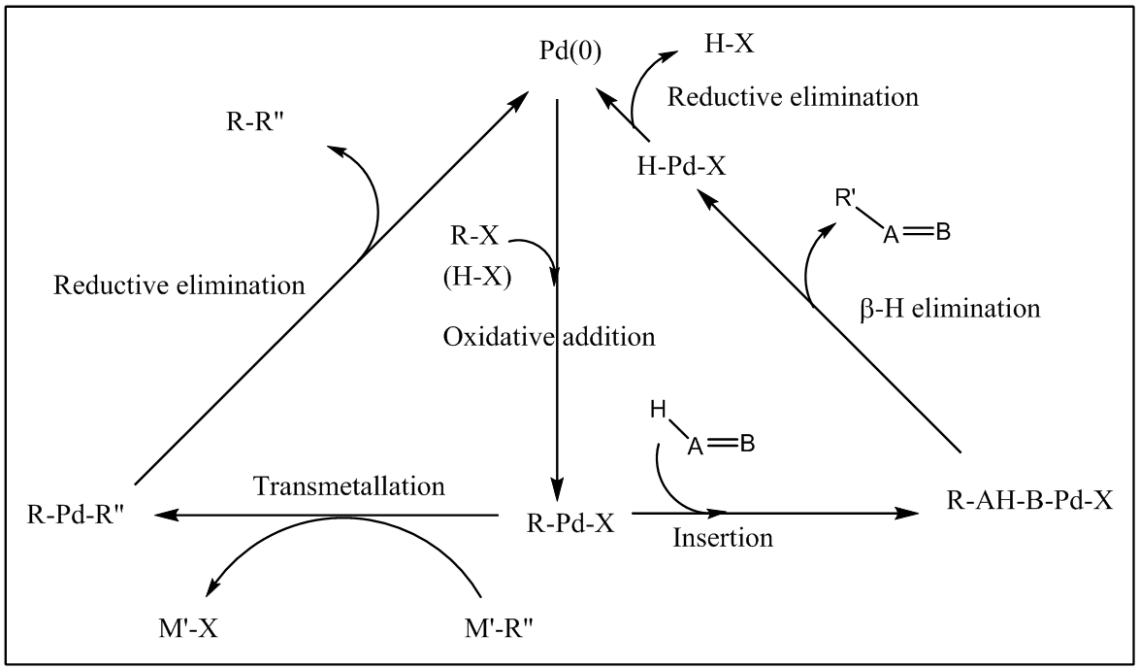

Figure 2.3: Illustration of the catalytic cycle for palladium catalytic systems[13].

Researchers are not sure when exactly platinum was discovered, but it was used by the Egyptians and Indians to make smaller jewellery items. In 1736 A. de Ulloa, a Spanish astronomer, observed an unworkable metal, platinum, in the now Columbian gold mines. Ulloa later also introduced the metal to Europe where at the time it was known for its poor workability as a result of its high melting point. Platinum falls in group ten on the periodic table, has an atomic number 78 and an atomic weight of 195.08. It is a grey, white metal which is malleable, ductile and dense. Platinum has a melting point of 1768.3 ℃, and a density of 19.77 $g.cm^{-3}$. The following oxidation states can be accommodated by platinum: +6, +5, +4, +3 , +2, 1, -1, -2. Of these the +2 and +4 oxidation states are the most common. The ionic radius of the Pt^{4+} and Pt^{2+} species are 0.63 Å and 0.60 Å respectively. Platinum is fairly resistant to nitric and hydrochloric acid but can be dissolved by utilizing aqua regia. Excellent resistance to chemical attack and its high thermal stability has been exploited by industrial applications. Platinum, like palladium, is also largely mined in Russia, South Africa and Canada. The earth's crust contains roughly 0.005 mg platinum per kilogram. Catalytic converters which are found in the exhaust systems of cars also employ platinum together with palladium to reduce the toxicity of exhaust gases. Other applications include the construction of high temperature furnaces and jet engine parts.

Platinum, like palladium, tends to show an affinity towards CN^- compounds, rather than oxygen or fluorine[14].

The supported platinum catalyst however tends to be more advantageous than the unsupported colloids. Larger surface areas which relate to more active sites and greater efficiency towards catalyst recovery are mentioned as reasons for this observation. Although the supported catalysts are more useful, it is important to control which support is used and how the support interacts with the metal nanoparticles. Alumina and carbon are the most common supports for platinum catalyzed reactions. Most of these catalysts are attached to the supports by impregnation. Platinum oxide mixed with other platinum group metals like rhodium, iridium and ruthenium are employed as catalysts for hydrogenation[15]. The activity of supported platinum catalysts is dependent on the support that is used. A study performed by Maxted[15] found the following series to exist; $ZrO_2 > ThO_2 > Cr_2O_3 > CeO_2 > 2Cr_2O_3 > MgO$. Zirconia and thoria were the most promising supports and the activity that was attained was an order of magnitude greater than with unsupported platinum catalyst. Alumina with small pores, gave roughly the same activity as the zirconia support.

In both platinum and palladium the 2+ cations are of interest for the application of this literature study. Pd^{2+} and Pt^{2+} are both "soft" acids that form stable complexes with a variety of donor atoms such as phosphorous, sulphur and nitrogen. Platinum is the less labile of the two metals and is often investigated more for this reason[16]. Square planar complexes are usually found in d^8 metal centers with large crystal field splitting energies. The ligands bonded to the metal center in a square planar geometry lie in the x and y plane. Square planar geometries are typically formed in metal centers where the d_{x2-y2} is much higher in energy than the other four d orbitals. The d_{xy} orbitals lie in the plane of the ligands but, are located between the ligands which make the electron repulsion less than in the case of the d_{x2-y2} orbitals. The remaining three d orbitals are lower in energy than the d_{xy} orbitals because they point out of the plane of the metal-ligand plane. The d_{z2} is slightly higher in energy when compared to the d_{xy} orbitals due to a small band of electrons that circle the metal center[16].

2.5 Nanoparticle supports

2.5.1 General

Porous supports are used in heterogeneous catalysis for a variety of reasons, and it is important to understand the mechanism, which is present in heterogeneous catalysis in design of these supports. The mechanism can be divided into five major steps.

1. Substrate diffusion
2. Substrate adsorption
3. Surface reaction
4. Product desorption
5. Product diffusion

During the catalytic process substrate and product molecules diffuse in and out of the pores. Although smaller pores provide higher textile strength and larger surface areas, diffusion can be hindered. This results in concentration gradients that reduce the efficiency and effectiveness of catalysts. The synthesis of small metal particles drastically increases the number of active sites at which the catalytic process can occur. It can, however be difficult to ensure that these metal particles remain dispersed in solution and to prevent these particles from being leeched with the products. Consequently, the use of insoluble supports has provided scientists with the capability to achieve both of these important aspects namely, dispersion and high surface area. The solid supports typically contain micro-pores into which the catalysts can be adsorbed. The micro-pores also give the supports a high surface area which will achieve a high number of active sites. Some of the first supports that were used, relied on physisorption to attach the catalyst to the support. Unfortunately, this meant that some of the catalyst's active particles were lost due to leeching. Later, methods were developed to attach the metals to the support chemically. This provided more stable compounds and removed the leaching problem, however other challenges were created. The characteristics of the free metal particle could not be considered to be the same as that of the attached metal particles. It was also important that the molecules should be attached far enough from one another and that the support's bridging groups did not deter the active site in any way[17].

The heterogeneous catalyst could also be prepared by pre-reacting the catalysts with the support. Typically, aluminium chloride, a Lewis acid, will be reacted with a hydroxylated material like silica gel to form an $OAlCl_2$ species. A multi-stage route, in which silanes are grafted onto the solid support, are more commonly employed in the synthesis of heterogeneous catalysts. In some cases, the silanes already contain the catalyst, but the catalyst can also be attached at a later stage. Unfortunately, a limited number of silanes are available; consequently these silanes need to be modified after being grafted. The most commonly used silane is 3-aminopropyl (trimethoxy)silane which is relatively inexpensive and behaves like an amine functionality which can be altered according to needs. This approach does have drawbacks. The altering of the silane can result in the formation of surface species as a result of the fusion of successive Si-O-Si groups.

Another approach, which is less common, is the chlorination of the surface of the silica support. Organometallic reagents are then reacted with the chlorines for attaching the catalyst to the support. This method allows for the attachment of catalysts in various modes with a fairly stable bond. The formation of unwanted surface species is also prevented. Organic polymers are also employed as supports for heterogeneous catalysis and the attachment of catalyst follow similar procedures. In heterogeneous catalysis, supports can be divided into organic and inorganic supports. Organic supports include cross-linked polystyrenes and ion-exchange resins. These polymers can have various orientations like linear, cross-linked and membrane-like. Although soluble polymers are available, there tend to be problems with catalyst removal. Cross-linked polymers are used the majority of the time and tend to be in the form of resin beads with sizes that range from 10 μm to 1 mm.

Since this project is in the field of inorganic chemistry, it was decided to focus the main part of this section on inorganic supports. A whole range of inorganic materials posses the appropriate characteristics needed for a heterogeneous support. These materials include silicas, aluminas, carbons, montmorillonites, zeolites, aluminosilicates and more complex heteropolyacids. These materials are porous in nature, which provides the desired large surface area for heterogeneous catalysis. The pore size can vary between 0.3 nm in zeolites to 100 nm in silicas. The inorganic supports can be sub-classified into crystalline, amorphous and flexible layered structures. The

crystalline supports have a very narrow pore size distribution and are found mainly among the zeolites. Silicas tend to form amorphous structures in which a large range of pore-size distributions can occur. Montmorillonites are utilized for layered applications. The discovery of hexagonal mesoporous silicas has provided scientists with the ability to grow pores to any desired size. Table 2.2 summarizes the most of the common supports and their basic properties.

Table 2.2: Supports[18].

Support	**Basic Properties**
Silica gels	Inexpensive and available. Contain surfaces that are highly hydroxylized with a mesoporous structure. These supports are associated with broad pore sizes; they are easily functionalized and used in halogenation and silylation.
Structured silicas	Hexagonal mesoporous silicas are prepared via sol-gel techniques to yield extremely high surface area supports. They have a narrow pore size distribution and tend to be less hydrophobic than normal silicas.
Montmorillonites	Employs natural clays with swelling capabilities that yield microporosity. Pillard clays tend to have large pores and acid treatments are used to form mesoporous species.
Aluminas	These supports are available in acid, base and neutral form and have moderate surface areas.
Zeolites	These supports are microporous in nature and have a tight pore size distribution. Zeolites are highly structured and have large surface areas. Small pore sizes may result in diffusional problems in liquid-phase systems.
Other materials	Other materials that have been explored include charcoal and calcium fluoride. The charcoals have large surface areas but functionalization of the surfaces is complex. The calcium species have low surface areas but are used for their inertness.

2.5.2 Crystalline Titanium Dioxide

Nanocrystalline titanium oxide displays remarkable physical and chemical properties. Consequently, these particles can be applied in a variety of areas such as gas sensors, pigments, catalysts, photovoltaic cells and as precursors to mesoporous supports. The particle size, size distribution, morphology, crystallinity and phase of titanium oxide can be altered according to the desired application. Titanium oxide exists in two phases namely, anatase and rutile. In bulk, the rutile phase is thermodynamically favoured, however calculations performed by Zhang and Banfeild have indicated that when titanium crystals are smaller than 14 nm anatase is in fact the favoured phase[19]. Crystalline anatase exhibits more photolytic activity than rutile, which is more thermodynamically stable than anatase. Particle size is believed to be the most important factor to control when tailoring titanium nanoparticles for certain applications. Mechanical strength, electronic characteristics, magnetic properties and optical activity are influenced by the size of the nanocrystallites. As a result of this, there have been numerous investigations on how to control particle size. Many studies on the effects of temperature, pH and additives on the influence these entities have in the synthesis of titanium dioxide have been performed[,20,21,22,23].

In the work of Coville[22] palladium was supported on nanotubular titanium oxide and showed favourable catalytic activity for hydrogenation reactions. The kinetics that accompanies the formation of titanium dioxide was also investigated to gain insight into the formation of the different phases[24]. Due to the multi-functionality of titanium oxide crystallites a variety of methods for the preparation of the compounds have been investigated. These methods comprise of flame synthesis, ultrasonic irradiation, chemical vapour synthesis and sol-gel processes. Although these methods are successful, special machinery and specialized equipment is required for the synthesis process. Niederberger however, developed a much simpler methodology for the synthesis of crystalline titanium oxide[25,26,27] at low temperatures. The particles show high surface areas and particle size can be controlled through the variation of mole ratios and temperature. This methodology is particularly useful in the context of this project.

2.6 Metal organic frameworks

Metal organic frameworks (MOF) are defined as a polymeric, porous material in which the metal atoms are linked to each other by some or other organic bridging ligand. These compounds typically contain inner "pores" into which other guest molecules can be trapped[28]. The size and shape provide selectivity towards which molecules or atoms can be incorporated. Once this process is complete the guest can be chemically altered. This principle is currently employed in catalytic cracking and xylene isomerisation. Research on metal organic frameworks has increased dramatically since the early 1990's as illustrated by Figure 2.4. The early pioneers of this research namely, Robson, Moore, Yaghi, and Zaworotko eluded to the wide diversity of these compounds[28]. Theoretically there exists a wide choice of metals with an even larger amount of bridging ligands, which can be used to alter the structural, magnetic, electrical, optical, and catalytic properties of these compounds according to the desired effect. Although these metal organic frameworks provide diversity, there remain various challenges with regard to synthesis.

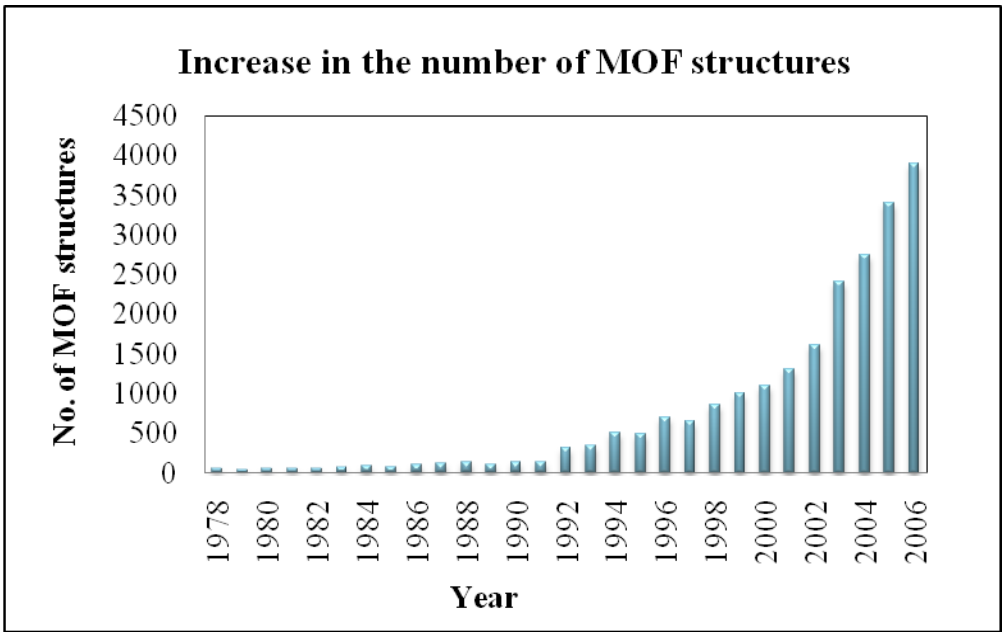

Figure 2.4: MOF structures from 1978 to 2006 obtained from the CSD[29].

Chapter 2

The design of metal organic frameworks principally forms part of another discipline namely, supra-molecular chemistry. Although this term is generally used to describe the organization of molecules into larger structures through the utilization of weak reversible interactions such as hydrogen bonding, π stacking and van der Waals forces, coordination of bridging ligands to metal centers are also classified under this term. This can be said since some ligand-metal interactions posses a reversible (lability) character. This is essential in classifying multinuclear coordination structures under the term supra-molecular chemistry. One of the attractive features of supra-molecular chemistry is that the larger structures that are formed by the assembly of metals and ligands result in the formation of new species that do not show the same properties as the sum of their constituents[30].

Although π-stack and van der Waals forces can be exploited in the construction of metal organic frameworks in supra-molecular chemistry it becomes difficult to achieve exact control over these. Coordination chemistry, provides scientists with the opportunity to firstly predict the possible arrangement of molecules and then, to a certain extent, controllably synthesize desired molecules. The late transition metals are prime candidates for the use in metal organic frameworks as a result of their well understood geometries and coordination modes. Another critical factor in the design of molecules is the lability of the employed ligands since the reversible bond formation allows the system to reach thermodynamic equilibrium.

Two major approaches to the synthesis of multinuclear species have been developed, namely controlling the bonding vectors among the building blocks or controlling the overall symmetry of the starting materials. In the bonding vectors approach metals and ligands are represented as angular and linear species. These species are combined to form two or three dimensional units. The "molecular library" that exists can be used to construct a variety of species respectively. Figure 2.5 and Figure 2.6 illustrate the combination of different subunits that can be used to obtain a variety of different metal organic frameworks[31].

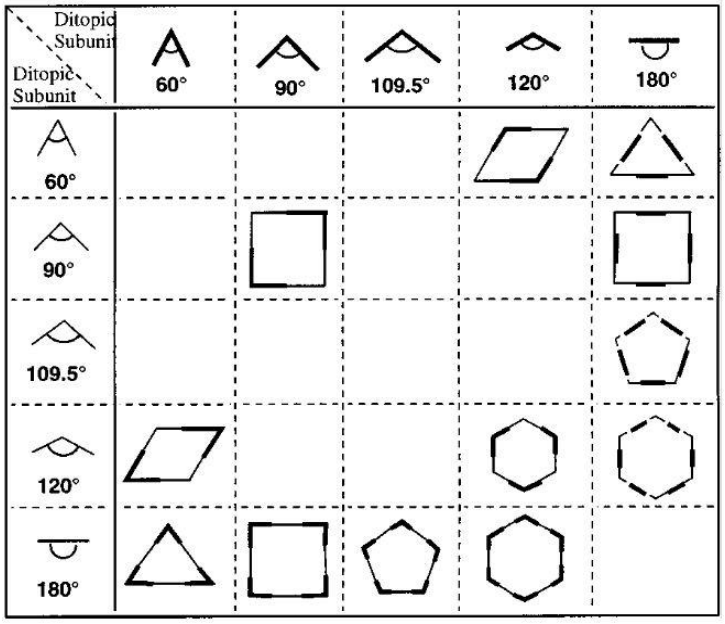

Figure 2.5: The molecular library of cyclic moieties constructed from building blocks[31].

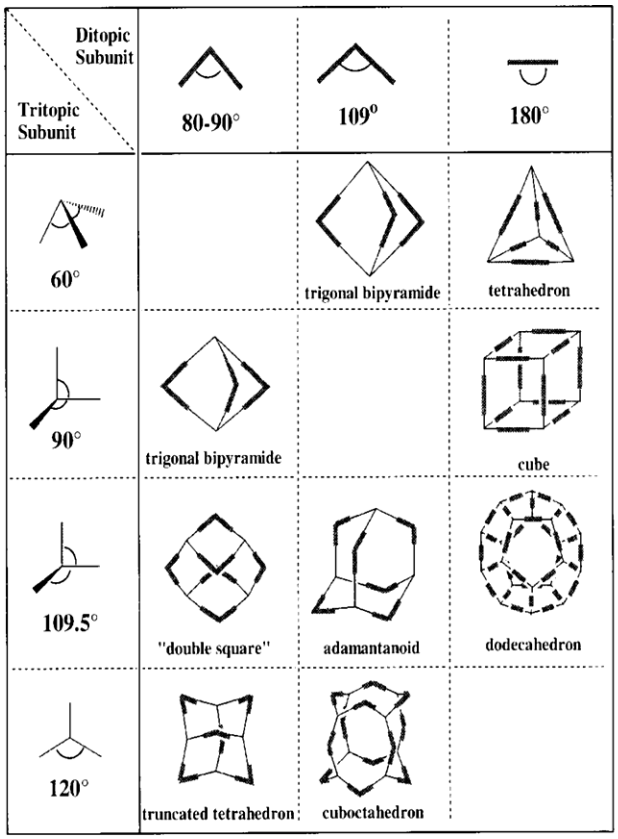

Figure 2.6: Three dimensional assemblies constructed from the molecular library[31].

The symmetry interaction approach simply breaks target assemblies into symmetry elements. These elements must then combine to form a tetrahedral structure. Raymond and co-workers reported the synthesis of a M_4L_6 moiety by the combination of pseudo octahedral metals as corner units and trigonal trisbidentate ligands for the tetrahedral faces[32]. Four-coordinate square planar or six-coordinate octahedral configurations have been reported. Ligands with various coordination modes are used and capping molecules are exploited to prevent the formation of oligomers.

Although it was previously mentioned that the lability is important in supra-molecular chemistry, certain metal ions such as Ti(IV), Cr(III), Co(III), and Pt(II) can be forced to form super molecules by manipulating the reaction conditions to reach the thermodynamic equilibrium[30]. The overall architecture of the species is typically controlled through ligand design and the exploitation of certain oxidation states in metals, which have an affinity for specific bonding modes.

2.7 Bridging ligands in polymetallic systems

In order to achieve specific assemblies, it is important to have the metal centers at specific distances from each other in a metal organic framework. This can be achieved by using different bridging ligands. These ligands have the ability to couple metal centers using a donor atom to form a covalent bond between the ligand and the metal centers. Typically, these ligands contain π-systems which allow for π back bonding and less commonly, π bonding. This usually results in the stabilization of the metal-ligand bond. Bidentate ligands typically bond two metal centers together by means of two donor atoms being attached to each metal. These bidentate ligands are commonly developed for supra-molecular chemistry where they are used to link metal centers that result in the formation of metal organic frameworks. There are some factors that need to be taken into consideration when investigating these bridging ligands. The ligand determines the spatial orientation and the degree of electronic coupling to the metal center. The spatial orientation of the ligand in the bridged metal systems is determined by the shape of the ligand, its rigidity and the coordination geometry (Figure 2.7).

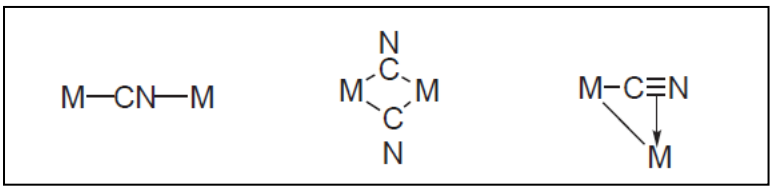

Figure 2.7: Example of the different spatial separations achieved by different bridging modes, CN^- as an example.

Electronic coupling can be promoted by the bridging ligand but is dependent on the degree of aromatic conjugation of the ligand. The electronic coupling changes the properties of the metal centers in such a way that they differ significantly from the original metal species. Unconjugated ligands are used to bring metal centers into close proximity but no electronic coupling exists. Not all bridging ligands are found in between metal centers. In some cases, the bridging ligands tend to promote metal-metal interactions. In these systems the bridging ligands lead to uncoupled electronic properties[33].

A wide variety of bridging ligands exists and many of these ligands are used for different applications. Nitrogen based bridging ligands are particularly useful for the construction of transition metal frameworks because most transition metals bond to nitrogen successfully. Figure 2.8 illustrates a few examples of the different nitrogen bridging ligands that are already used in metal organic frameworks[31]. Some ligands (**2, 3** and **5**) are more flexible than others as a result of the absences of double and triple bonds. These ligands tend to form metal organic frameworks with a twisted orientation to accommodate steric hindrances. The other rigid ligands (**1, 4, 6, 7, 8,** and **9**) tend to form metal organic frameworks, which are planar and almost two dimensional when coordinating with d^8 metal species. As the aim of this project is to attach two dimensional metal organic frameworks to inorganic supports, 4,4'-bipyridine, (**4**) 2,2'-bipyrimidine (**6**) and pyrazine (**9**) were chosen to be investigated. The flat, planar complexes have the potential to be attached to the surface of the support due to the interaction of the oxygen groups on the support with the vacant orbital on the metal center. Secondly as a result of these bridging ligands the distances between metal centers can be controlled and optimum dispersion can be attained. Thirdly, the conjugation which is present in the metal organic framework could serve to activate the metal centers for catalysis. Finally, the vacant orbital which points upward from the support provides the substrate, in the catalysis process, with "access" to the metal center. The individual properties of the chosen ligands are discussed in the following sections.

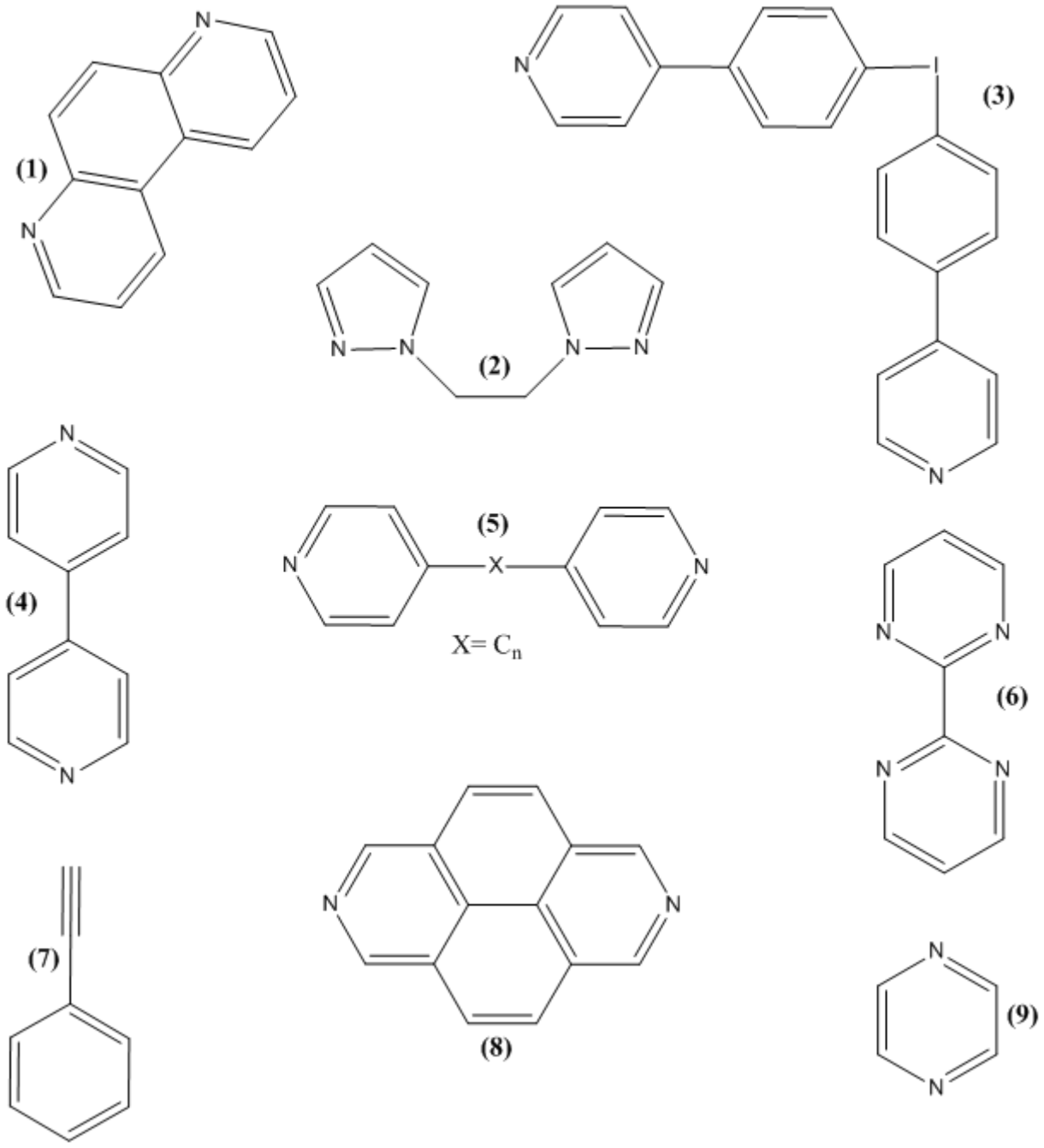

Figure 2.8: Selected nitrogen based bridging ligands used in the construction of metal organic frameworks. (1) 4,7-phenanthroline, (2) 1,2-di(1H-pyrazol-1-yl)ethane, (3) Bis(4-phenylpyridine) iodate, (4) 4,4'-bipyridine, (5) dipyridin-4-ylmethane (X=CH_2), (6) 2,2'-bipyrimidine, (7) ethynylbenzene, (8) benzo[*lmn*][3,8]phenanthroline, (9) Pyrazine.

2.7.1 2,2'-Bipyrimidine

2,2-Bipyrimidine (bpym) is a beige solid with a molecular mass of 158.16 g/mol and a melting point of 112 - 116 ℃. It is a bidentate ligand that can be used to link two metal centers with four equivalent nitrogen atoms, as indicated in Figure 2.9. This ligand removes any stereoisomerism and shows remarkable stability in acidic media[34]. The platinum complex of 2,2-bipyrimidine is used as a catalyst for methane functionalization reactions, which are performed in oleum. Bly and Mellon[35] first synthesized 2,2-bipyrimidine by means of the Ullmann coupling of 2-bromopyrimidine in the presence of metallic copper. The synthetic yield was low and the procedure was later improved by Vlad and Horwath[34].

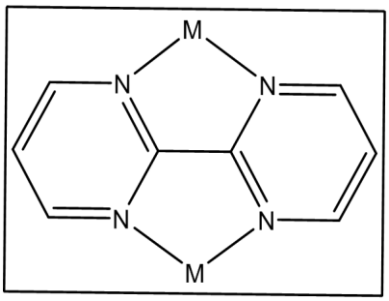

Figure 2.9: Two metal centers (M) linked by 2,2-bipyrimidine.

The coordination of 2,2-bipyrimidine to certain metal centers does alter its reactivity. Typically, coordination to the first pair of nitrogen atoms leads to the withdrawal of electron density from the remaining two nitrogens in the conjugated system. Consequently, the bacisity of these nitrogens and their coordination ability is decreased. Homobimetallic and heterobimetallic complexes linked by 2,2-bipyrimidine can be synthesized. Akiko Inagaki[36] *et al.* used 2,2'-bpym as a bridging ligand to join a photo active ruthenium(II) center to a palladium(II) center (Figure 2.10). The ruthenium is activated by UV light and as a result of the conjugated system the palladium center is then also activated as catalyst.

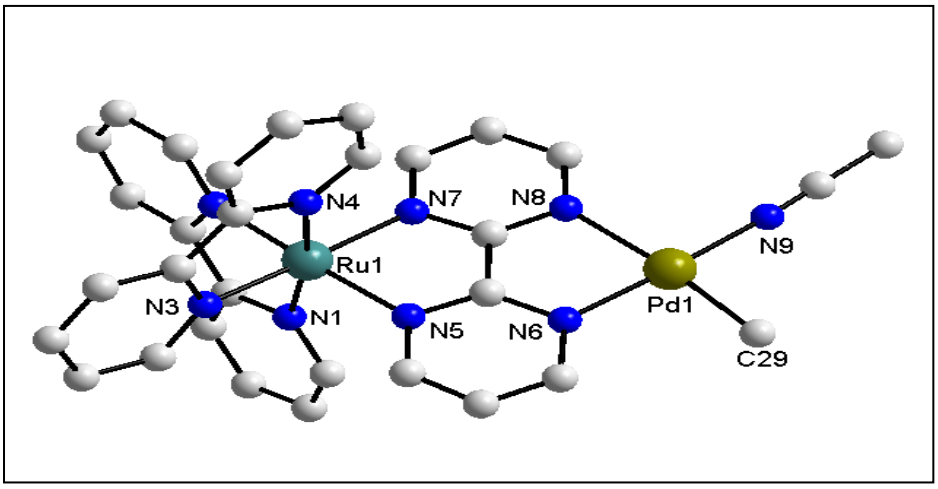

Figure 2.10: Crystal structure of ruthenium(II) and palladium(II) bridged by bpym.[36]

Platinum(II) and platinum(IV) metal centers have also been linked using 2,2-bpym[37,38]. Other heterobimetallic systems include Ru/Rh[39], Ru/Re[40], Ru/Ir[41], and Ru/Pt[42]. 4,4'-bipyridine which is discussed later has been used, by Benkstein[43] *et al.*, in combination with bpym to form the rectangular species shown in Figure 2.11.

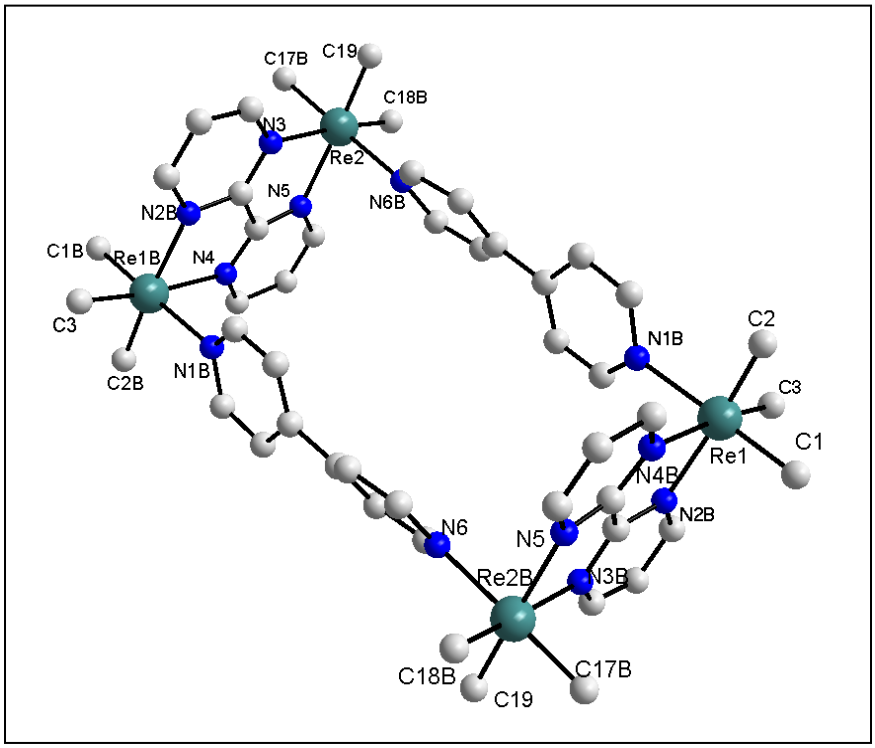

Figure 2.11: Crystal structure of a rectangular metal organic framework constructed from 2,2-bypyrimidine, 4,4-bipyridine and a rhenium metal center[43].

2,2-Bipyrimidine is a useful tool to place metal centers in close proximity of each other and to form a conjugated link between the two metal centers. When using d^8 metal species the complexes are limited to linear structures. The introduction of more than one bypm molecule can be complex as it involves the formation of polymers if suitable capping ligands are not used. The disadvantage of this ligand is the loss of bacisity of the nitrogens once a metal center has bound to the first pair of nitrogen atoms.

2.7.2 Pyrazine

Pyrazine (Figure 2.12) is a heterocyclic aromatic ring with better π accepting capabilities than pyridine. It can be identified as a colourless crystalline compound with a molecular mass of 80.09 g/mol that melts at 54 - 56 ° C. Generally, pyrazine is used as a monodentate bridging ligand that facilitates π mediated metal-metal interactions. Platinum, molybdenum and ruthenium have been linked by making use of pyrazine. Bridged metal centers tend to be coplanar with the pyrazine ring. This results in significant electronic coupling between the two metals.

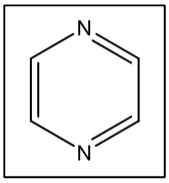

Figure 2.12: Illustration of the pyrazine bridging ligand.

Pyrazine is the smallest and most rigid bridging ligand employed in the synthesis of metal organic frameworks. Four platinum(II) centers linked by pyrazine have been reported[44,45]. Single crystal X-ray studies of the compound confirmed the two dimensional nature of the complex. This is more clearly illustrated in Figure 2.13. Willermann also successfully combined platinum and silver by making use of pyrazine to form a similar square shaped species.

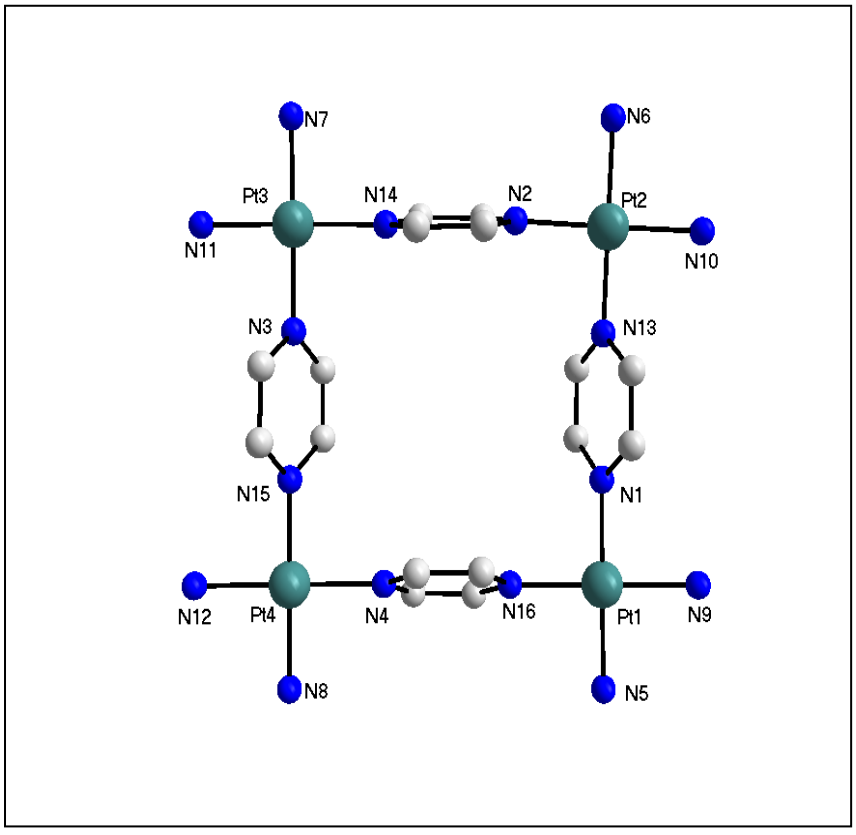

Figure 2.13: Crystal structure of platinum(II) metal centers linked by pyrazine bridging ligands[45].

Triangular shaped frame works have also been constructed using pyrazine and platinum as reported by Schweiger[46]. It should be noted however, that the formation of the square species is favoured above that of the triangular one. Electronic properties and entropy play a major role in the formation of triangular entities.

2.7.3 4,4'-Bipyridine

Bipyridine ligands are ligands with nitrogen atoms occupying various positions on the heterocyclic ring. Combinations such as 4,4'-bipyridine 3,4'-bipyridine and 4,4'-bipyridine have been studied as bridging ligands. 4,4'-Bipyridine (Figure 2.14) is a beige coloured, crystalline compound with a molecular mass of 156.18 g/mol and a melting point of 109 - 112°C. It is typically used to increase the distance between metal centers in bridged complexes. It can be synthesized in high yields from the reaction of 4-bromopyridine with NaH, $Ni(O_2CHCH_3)_2$, $NaOC(CH_3)_3$, and PPh_3 in $(CH_3OCH_2)_2$ at 45 ^{o} C. X-ray crystal structure investigations have shown that 4,4'-bipyridine can form coplanar complexes in which electronic interactions between metal centers are achieved through the overlap of the π-orbitals. 4,4'-Bipyridine also introduces the ability to vary the distance between metals. This is readily achieved by the introduction of spacer groups between the rings. However, even though the metal centers are found further apart it becomes increasingly difficult to control the conformation of these species.

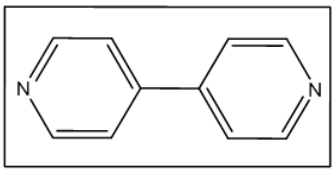

Figure 2.14: Illustration of 4,4-Bipyridine bridging ligand.

Of the three selected ligands, 4,4'-bipyridine has been exploited the most in the synthesis of metal organic frameworks. Platinum and palladium metal organic frameworks constructed with the aid of 4,4'-bipyridine typically form square shaped metal organic frameworks. Stang[47] used this ligand to synthesize platinum and palladium metal organic frameworks with a variety of phosphine substituents on the metal centers. Similar work was performed by Uehara[47], who used

nitrogen based ligands and synthesized the triangular as well as square shaped metal organic frameworks illustrated in Figure 2.15 and Figure 2.16. Various other authors have reported square metal organic frameworks by utilizing 4,4'-bipyridine[48,49,50,28].

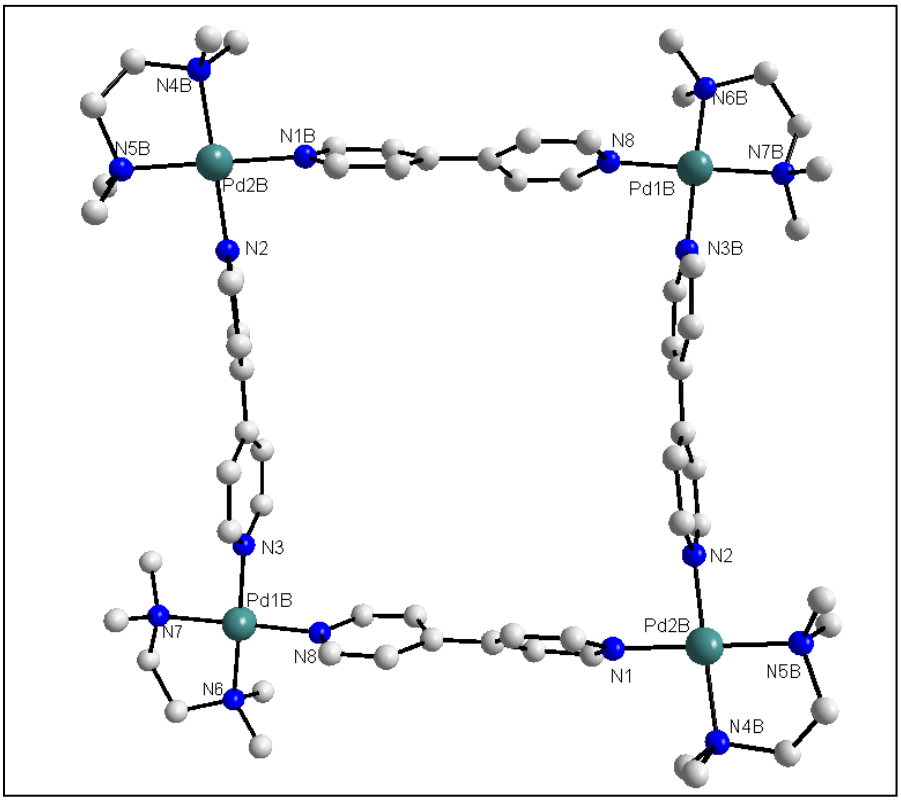

Figure 2.15: Crystal Structures of a square metal organic framework, utilizing a palladium(II) metal center, synthesized by Uehara[51].

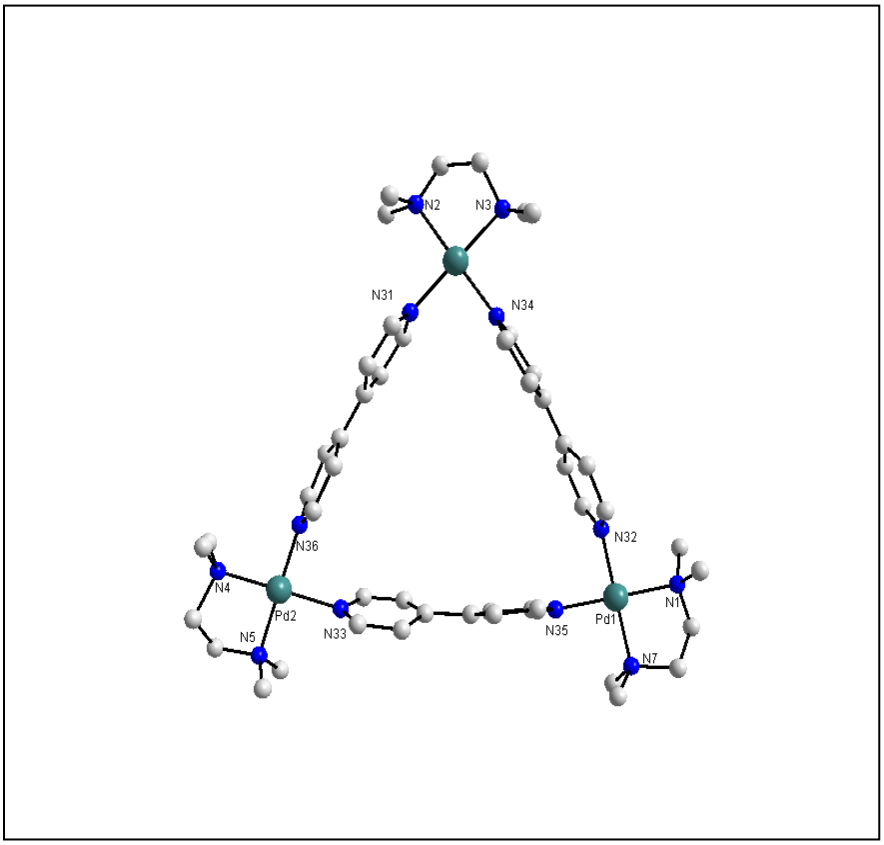

Figure 2.16: Crystal Structures of a triangular metal organic framework, utilizing a palladium(II) metal center, synthesized by Uehara[51].

From the above it is clear that the selected ligands have been applied in a wide variety of metal organic frameworks, which shows that these ligands are versatile and can be applied to various areas. The large number of different combination of ligands and metals that can be combined to from various species is one of the major advantages of this research area.

(1) Copéret, C.; Chaudret, B. *Surface and Interfacial Organometallic Chemistry and Catalysis*; Springer-Verlag: Berlin/Heidelberg, **2005**; Vol. 16.

(2) Rosoff, M. *Nano-surface chemistry*; Marcel Dekker: New York, **2001**.

(3) De Vries, J.; Tucker, C. *Innovations in Pharmaceutical Technology* **2000**, 125-130.

(4) Garrett, C. E.; Prasad, K. *Advanced Synthesis & Catalysis* **2004**, *346*, 889–900.

(5) Poole, C. *Introduction to nanotechnology*; J. Wiley: Hoboken NJ, **2003**.

(6) Nabok, A. *Organic and inorganic nanostructures*; Artech House: Boston, **2005**.

(7) Astruc, D. *Nanoparticles and catalysis*; Wiley-VCH: Weinheim, **2008**.

(8) Pitkethly, M. J. *Nanotoday* **2003**, 36-42.

(9) Kurihara, K.; Fendler, J. H. *J. Am. Chem. Soc.* **1983**, *105*, 6152-6153.

(10) Toshima, N.; Yonezawa, T. *New J. Chem.* **1998**, *22*, 1179-1201.

(11) Zhou, B. *Nanotechnology in Catalysis 3.*; Springer: New York, **2007**.

(12) Patnaik, P. *Handbook of inorganic chemicals*; McGraw-Hill: New York, **2003**.

(13) Tsuji, J. *Palladium reagents and catalysts: new perspectives for the 21st century*; Wiley: Hoboken NJ, **2004**.

(14) Greenwood, N. *Chemistry of the elements*; 2nd ed.; Butterworth-Heinemann: Oxford; Boston, **1997**.

(15) Nishimura, S. *Handbook of heterogeneous catalytic hydrogenation for organic synthesis*; J. Wiley: New York, **2001**.

(16) Cotton, S. *Chemistry of precious metals*; 1st ed.; Blackie Academic & Professional: London; New York, **1997**.

(17) Olmsted, J. *Chemistry*; 4th ed.; Wiley: Hoboken NJ, **2006**.

(18) Clark, J.; Royal Society of Chemistry (Great Britain) *Clean synthesis using porous inorganic solid catalysts and supported reagents*; Royal Society of Chemistry: Cambridge, **2000**.

(19) Naicker, P. K.; Cummings, P. T.; Zhang, H.; Banfield, J. F. *J. Phys. Chem. B* **2005**, *109*, 15243-15249.

(20) Wu, F.; Zhang, Q.; Yang, H. *Journal of Alloys and Compounds* **2009**.

(21) Wu, B.; Guo, C.; Zheng, N.; Xie, Z.; Stucky, G. D. *J. Am. Chem. Soc.* **2008**, *130*, 17563-17567.

(22) Sikhwivhilu, L. M.; Coville, N. J.; Pulimaddi, B. M.; Venkatreddy, J.; Vishwanathan, V. *Catalysis Communications* **2007**, *8*, 1999–2006.

(23) Li, Y.; Xu, B.; Fan, Y.; Feng, N.; Qiu, A.; He, J. M.; Yang, H.; Chen, Y. *Journal of Molecular Catalysis. A, Chemical* **2004**, *216*, 107–114.

(24) Maaza, M.; Franklyn, P. J.; Levendis, D. C.; Coville, N. J. *S. Afr. J. Chem.* **2007**, 71–75.

(25) Niederberger, M.; Bartl, M. H.; Stucky, G. D. *Chem. Mater*. **2002**, *14*, 4364-4370.

(26) Niederberger, M.; Bartl, M. H.; Stucky, G. D. *J. Am. Chem. Soc*. **2002**, *124*, 13642-13643.

(27) Garnweitner, G.; Antonietti, M.; Niederberger, M. *Chem. Commun.* **2005**, 397.

(28) James, S. L. *Chemical Society Reviews* **2003**, *32*, 276–288.

(29) Long, J. R.; Yaghi, O. M. *Chem. Soc. Rev.* **2009**, *38*, 1213.

(30) McCleverty, J. *Comprehensive coordination chemistry.*; 2nd ed.; Pergamon: Oxford, **2003**; Vol. 7.

(31) Leininger, S.; Olenyuk, B.; Stang, P. J. *Chem. Rev.* **2000**, *100*, 853-908.

(32) Bruckner, C.; Powers, R. E.; Raymond, K. N. *Angew. Chem., Int. Ed. Engl.* **1998**, 37, 1837.

(33) Lever, A. *Fundamentals ligands, complexes, synthesis, purification, and structure*; 1st ed.; Elsevier: Amsterdam, **2004**.

(34) Vlád, G.; Horváth, I. T. *J. Org. Chem.* **2002**, *67*, 6550-6552.

(35) Bly, D. D.; Mellon, M. G. *J. Org. Chem.* **1962**, *27*, 2945-2946.

(36) Inagaki, A.; Yatsuda, S.; Edure, S.; Suzuki, A.; Takahashi, T.; Akita, M. *Inorg. Chem.* **2007**, *46*, 2432-2445.

(37) Kawakami, D.; Yamashita, M.; Matsunaga, S.; Takaishi, S.; Kajiwara, T.; Miyasaka, H.; Sugiura, K.; Matsuzaki, H.; Okamoto, H.; Wakabayashi, Y.; Sawa, H. *Angew. Chem. Int. Ed.* **2006**, *45*, 7214-7217.

(38) Klein, A. *Inorganica Chimica Acta* **1997**, *264*, 269-278.

(39) MacQueen, D. B.; Petersen, J. D. *Inorg. Chem.* **1990**, *29*, 2313-2320.

(40) Sahai, R.; Rillema, D. P.; Shaver, R.; Van Wallendael, S.; Jackman, D. C.; Boldaji, M. *Inorg. Chem.* **1989**, *28*, 1022-1028.

(41) Bridgewater, J. *Inorganica Chimica Acta* **1993**, *208*, 179-188.

(42) Swavey, S.; Fang, Z.; Brewer, K. J. *Inorg. Chem.* **2002**, *41*, 2598-2607.

(43) Benkstein, K. D.; Hupp, J. T.; Stern, C. L. *J. Am. Chem. Soc.* **1998**, *120*, 12982-12983.

(44) Kumazawa, K.; Biradha, K.; Kusukawa, T.; Okano, T.; Fujita, M. *Angew. Chem. Int. Ed.* **2003**, *42*, 3909-3913.

(45) Willermann, M.; Mulcahy, C.; Sigel, R. K. O.; Cerdà, M. M.; Freisinger, E.; Sanz Miguel, P. J.; Roitzsch, M.; Lippert, B. *Inorg. Chem.* **2006**, *45*, 2093-2099.

(46) Schweiger, M.; Seidel, S. R.; Arif, A. M.; Stang, P. J. *Angewandte Chemie (International ed. in English)* **2001**, *40*, 3467.

(47) Stang, P. J.; Cao, D. H.; Saito, S.; Arif, A. M. *J. Am. Chem. Soc.* **1995**, *117*, 6273-6283.

(48) Schnebeck, R.; Freisinger, E.; Lippert, B. *European Journal of Inorganic Chemistry* **2000**, 1193-1200.

(49) Fujita, M.; Sasaki, O.; Mitsuhashi, T.; Fujita, T.; Yazaki, J.; Yamaguchi, K.; Ogura, K. *Chem. Commun.* **1996**, 1535.

(50) Slone, R. V.; Yoon, D. I.; Calhoun, R. M.; Hupp, J. T. *J. Am. Chem. Soc.* **1995**, *117*, 11813-11814.

(51) Uehara, K.; Kasai, K.; Mizuno, N. *Inorg. Chem.* **2007**, *46*, 2563-2570.

3 Synthesis of Platinum and Palladium Compounds

3.1 Introduction

As mentioned in Section 2.7, various ligands were chosen to construct bridged metal organic frameworks utilizing platinum(II) and palladium(II). The synthesis and characterization of these complexes are discussed in this chapter as well as attempted experimental procedures. The compounds synthesized were characterized by means of Nuclear Magnetic Resonance (NMR) spectroscopy and single crystal X-ray diffraction. Some crystalline titanium and tungsten oxide supports were also synthesized and characterized by means of Infra Red Spectroscopy. Although many of the compounds explored in this chapter have been successfully synthesized, obtaining crystals of these complexes remains challenging.

3.2 Chemicals and apparatus

All reagents utilized for the synthesis of compounds were of analytical grade and were purchased from Sigma-Aldrich, South Africa. Reagents were used as received without further purification. All experiments were performed in air unless otherwise stated. Infrared spectra of the complexes were recorded on a Bruker Tensor 27 Standard System ATR spectrophotometer with a laser range of 4000 – 370 cm^{-1}. Data was collected at ambient temperature in air and reported in cm^{-1}. The ^{1}H NMR data was obtained from a Bruker 300 MHz spectrometer using the mentioned deuterated solvent. All chemical shifts, δ, are reported in ppm using ^{1}H-TMS as internal standard. Coupling constants, J, are reported in Hertz. The powders that were collected from the reported synthetic procedures were air dried with mild heating. The yields reported for products were reported under the assumption that all solvents were removed in the drying process. The crystal structures obtained are discussed in Chapter 4.

3.3 Synthesis of compounds

3.3.1 Dichlorido-(2,2'-bipyridine)-palladium(II)[1]

This compound was prepared by the modification of the literature procedure. $PdCl_2$ (0.20 g, $1.13x10^{-3}$ mol) was dissolved in boiling acetonitrile (30.0 ml). 2,2'-Bipyridine (0.176 g, $1.13x10^{-3}$ mol) was added. Upon addition a yellow precipitate formed. The solvent was evaporated in the fume hood. Yield: 0.243 g (64 %). ^{1}H NMR ($(CD_3)_2SO$): δ 7.8 (t, J = 6.7 Hz, 2 H), 8.3 (t, J = 7.8 Hz, 2H), 8.5 (d, J = 7.8 Hz, 2H), 9.1 (d, J = 5.4 Hz, 2H). IR (ATR): 1599 (ν_{C-H}), 1162 (ν_{C-N}), 802 (ν_{Ar-H}).

3.3.2 Dichlorido-(2,2'-Bipyridine)-platinum(II)[2]

The title compound was prepared according to the published procedure. K_2PtCl_4 (0.160 g, $3.855x10^{-4}$ mol) was dissolved in H_2O (10 ml). To this 2,2'-bipyridine (0.0624 g, $4.0x10^{-4}$) and 2 M HCl (2 ml) was added. The solution was boiled, which resulted in the formation of a yellow precipitate, which was filtered. Yield: 0.122 g (75 %). ^{1}H NMR ($(CD_3)_2SO$): δ 7.8 (dd, J = 9.8, 3.7 Hz, 2H), 8.42 (dd, J = 11.1, 4.6 Hz, 1H), 8.59 (d, J = 8.0 Hz, 2H), 9.52 (t, J = 9.9 Hz, 2H). IR (ATR): 1604 (ν_{C-H}), 1163 (ν_{C-N}), 758 (ν_{Ar-H}).

3.3.3 Dichlorido-(1,10-phenanthroline)-platinum(II)[2]

The title compound was prepared by a modification to the published procedure. K_2PtCl_4 (0.100 g, $2.41x10^{-4}$ mol) was dissolved in H_2O (10 ml). To this 1,10-Phenanthroline (0.048 g, $2.42x10^{-4}$ mol) and 2 M HCl (1.25 ml) was added. The solution was boiled, which resulted in the formation of yellow powder, which was filtered off. Yield: 0.086 g (80 %). ^{1}H NMR ($(CD_3)_2SO$): δ 8.1 (m, 2 H), 8.3 (s, 2 H), 9.0 (d, J = 8.3 Hz, 2 H), 9.7 (d, J = 4.8 Hz, 2 H). IR (ATR): 1599 (ν_{C-H}), 1153 (ν_{C-N}), 802 (ν_{Ar-H}).

3.3.4 cis-Dichlorido-diammine-platinum(II)[3]

KI (2.4 g, $1.445x10^{-2}$ mol) was reacted with K_2PtCl_4 (1.0 g, $2.42x10^{-3}$ mol) in H_2O (20 ml) and stirred in the dark for 30 min. NH_4OH (0.670 ml of 28 % sol.) was added drop wise over 15 min and the solution stirred for another 15 min in the dark. The precipitate was centrifuged and the supernatant collected. $AgNO_3$ (0.552 g, $3.25x10^{-3}$ mol) was added to the supernatant and stirred for 1 hour in the dark. AgI was removed by centrifuge and KCl (1.0 g, $1.445x10^{-2}$ mol) was added to the solution. A yellow powder was obtained, which was washed with methanol and diethyl ether. Yield: 0.293 g (40 %).^{1}H NMR (D_2O): δ 4.77 (s). IR (ATR): 3279 (ν_{N-H}), 1625 (ν_{N-H}).

3.3.5 Dichlorido-(2,2'-bipyrimidine)-platinum(II)[2]

The title compound was prepared by a modification to the published procedure. K_2PtCl_4 (0.160 g, $3.855x10^{-4}$ mol) was dissolved in H_2O (10 ml). To this 2,2'-bipyrimidine (0.0630 g, $4.0x10^{-4}$ mol) and 2 M HCl (2 ml) was added. The solution was boiled, which resulted in the formation of an orange powder. Yield: 0.122 g (74 %). ^{1}H NMR ($(CD_3)_2SO$): δ 8.00 (t, J = 5.3 Hz, 2H), 9.35 (d, J = 3.4 Hz, 2H), 9.7 (d, J = 5.9 Hz, 2H). IR (ATR): 1582 (ν_{C-H}), 1239 (ν_{C-N}), 791 (ν_{Ar-H}).

3.3.6 (μ_2-2,2'-Bipyrimidine)-tetrachlorido-palladium(II)[1]

This compound was prepared by the modification of the published procedure. $PdCl_2$ (0.200 g, $1,13x10^{-3}$ mol) was dissolved in boiling acetonitrile (30 ml). 2,2'-Bipyridine (0.092 g, $5.71x10^{-4}$ mol) was added to the solution. Upon addition a yellow precipitate formed. The solvent was evaporated in the fume hood. Yield: 0.244 g (85%). ^{1}H NMR ($(CD_3)_2SO$): δ 7.9 (t, J = 5.2 Hz, 2H), 9.3 (dd, J = 5.1 Hz, 4H). IR (ATR): 1589 (ν_{C-H}), 1137 (ν_{C-N}), 813 (ν_{Ar-H}). A typical NMR of the compound is displayed in Figure 3.1.

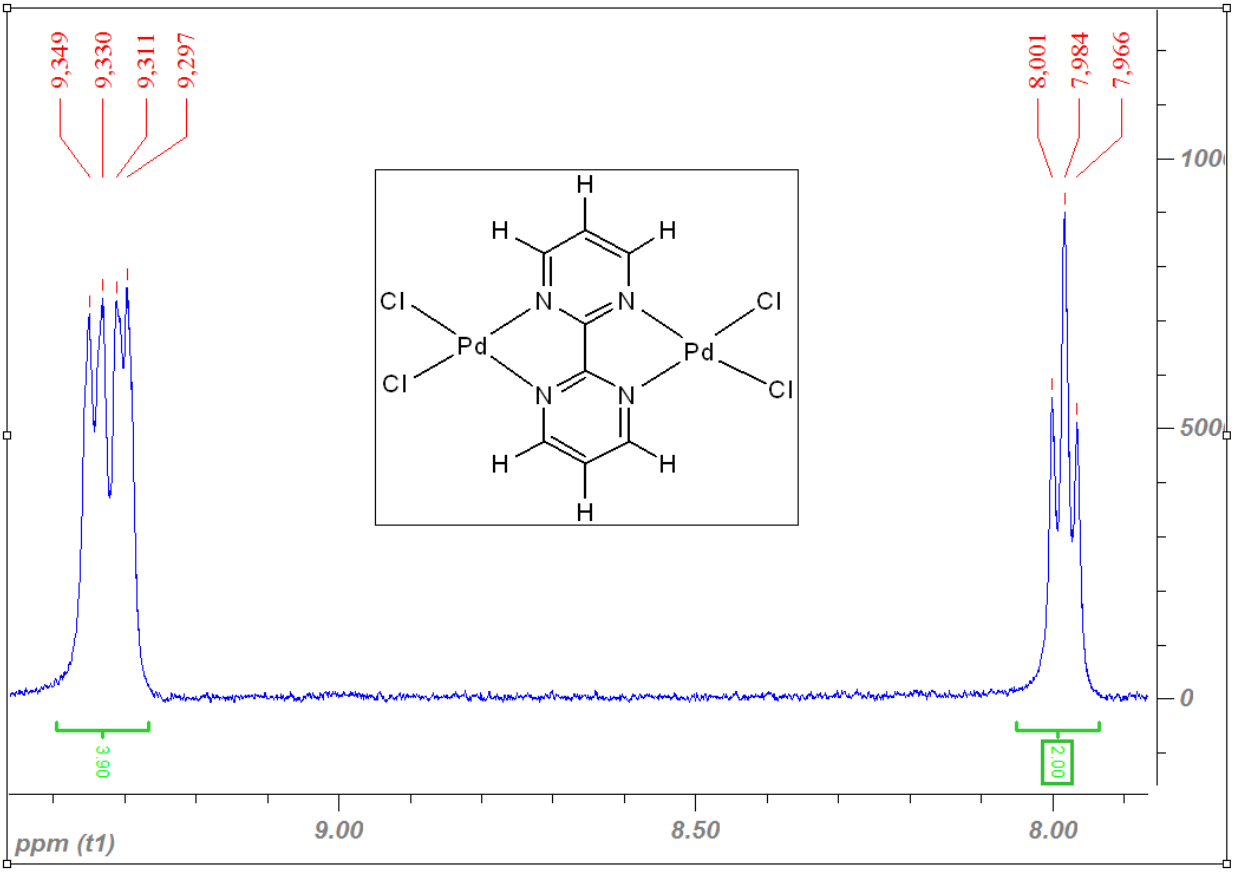

Figure 3.1: NMR spectrum obtained for (μ_2-2,2'-Bipyrimidine)-tetrachlorido-palladium(II).

3.3.7 4,5-Diazafluoren-9-one[4]

$KMnO_4$ (4.0 g, 0.0256mol) in H_2O (250ml) was heated and added drop wise to a solution of 1,10-phenanthroline (1.6 g, $8.8x10^{-3}$ mol) , KOH (8.0 g, $2.91x10^{-2}$ mol) and H_2O (250ml). The solution was refluxed for three hours and the product extracted with chloroform and dried over anhydrous $MgSO_4$. Yield: 0.673 g (41 %). ^1H NMR ($CDCl_3$): δ 7.4 (t, 2H, J = 5.1 Hz), 8.0 (d, J = 7.5 Hz, 2H), 8.8 (d, J = 4.4 Hz, 2H). IR (ATR): 1714 (ν_{C-O}), 1258 (ν_{C-N}), 838 (ν_{Ar-H}).

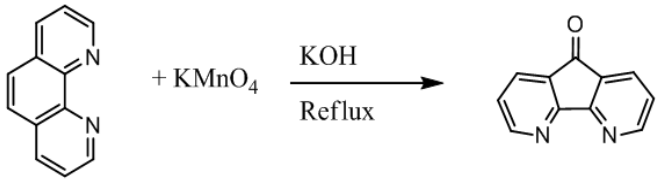

Scheme 3.1: Synthesis of 4,5-diazafluoren-9-one

3.3.8 Dichlorido-bis-(5-diazafluoren-9-one)-platinum(II)[2]

The title compound was prepared through a modification of the procedure published by Morgan[2]. K_2PtCl_4 (0.160 g, $3.855x10^{-4}$ mol) was dissolved in H_2O (10 ml). To this 4,5-diazafluoren-9-one (0.074 g, $0.403x10^{-4}$) and 2 M HCl (2ml) was added. The solution was boiled, which resulted in the formation of orange powder. Yield: 0.085 g (35 %). ^{1}H NMR ($(CD_3)_2SO$): δ 7.5 (t, J = 6 Hz, 1H), 7.7-7.8 (m, 1H), 8.0 (d, 1H), 8.2-8.3 (dd, J = 7.7 Hz, 1H), 8.8 (d, J = 7.5 Hz, 1H), 9.1-9.3 (dd, J = 15 Hz, 1H). IR (ATR): 1735 (ν_{C-O}), 1219 (ν_{C-N}), 827 (ν_{Ar-H}).

3.3.9 Dichlorido-bis-(5-diazafluoren-9-one)-palladium(II)[1]

This compound was prepared by the modification of the procedure used by Boyle[1]. $PdCl_2$ (0.100 g, $5.64x10^{-4}$ mol) was dissolved in boiling acetonitrile (20 ml). 4,5-diazafluoren-9-one (0.205g, $1.12\ x10^{-3}$ mol) was added. Upon addition a yellow precipitate formed. The solvent was evaporated. Yield: 0.258 g (85%). ^{1}H NMR ($(CD_3)_2SO$): δ 7.5 (1H), 7.7 (1 H), 8.0 (1H), 8.3 (1 H), 8.8 (1H), 9.1-9.3 (1H). IR (ATR): 1737 (ν_{C-O}), 1221 (ν_{C-N}), 827 (ν_{Ar-H}).

3.3.10 Dichlorido-1,5-cyclooctadien-platinum(II)

K_2PtCl_4 (0.4 g, $9.64x10^{-4}$ mol) was dissolved in a mixture of distilled water (6.5 ml) and n-propanol (5.5 ml). To this 1,5-Cyclooctadiene (0.8 ml) and $SnCl_2$ (0.015 g, $2.4x10^{-3}$ mol,) were added. The reaction mixture was stirred at room temperature for 48 hours. The solvent was evaporated overnight. The product was extracted with boiling dichloromethane. The

solution was allowed to evaporate slowly overnight forming light yellow crystals. Yield: 0.341 g (94.0 %). ^{1}H NMR ($CDCl_3$)**:** δ 2.20-2.30 (m, 4H), 2.60-2.80 (m, 4H), 5.59 (m, 4H).

3.3.11 Dichlorido-1,5-cyclooctadien-palladium(II)

$PdCl_2$ (1.0 g, $5.65x10^{-3}$ mol) was dissolved in hot concentrated HCl (10 M, 2.5 ml). The solution was cooled to room temperature, diluted with ethanol (75 ml) and filtered. 1,5-Cyclooctadiene ($1,13x10^{-2}$ mol, 3ml) was added to the filtrate with rapid stirring. The yellow product precipitated immediately and was stirred for a further 10 minutes. The solution was filtered and the precipitate was washed with diethyl ether (50 ml). Yield: 1.42 g (91.0 %). ^{1}H NMR ($CDCl_3$): δ 2.6 (m, 4H), 2.9 (m, 4H), 5.3 (m, 4H).

3.3.12 Dichlorido-bis-(triphenylphosphino)-palladium(II)[1]

This compound was prepared by the modification of the procedure used by Boyle[1]. $PdCl_2$ (0.150 g, $8.467x10^{-4}$ mol) was dissolved in boiling acetonitrile (25.0 ml). Triphenylphosphine (0.45 g, $1.71x10^{-3}$ mol) was added. Upon evaporation of the solvent a yellow precipitate formed. The solvent was evaporated in the fume hood. Yield: 0.433 g (72%). ^{1}H NMR ($(CD_3)_2SO$): δ 7.74 – 7.37 (m). IR (ATR): 1434 (ν_{P-C}), 743 (ν_{Ar-H}).

3.3.13 cis-[Bis-(diphenylphosphino)]-dinitrato-palladium(II)

$Pd_2BpymCl_4$ (0.050 g, $9.76x10^{-5}$ mol) and $AgNO_3$ (0.067 g, $3.95x10^{-4}$ mol) were reacted in nitromethane. After filtering PPh_3 (0.105 g, $4.0x10^{-4}$ mol) was added drop wise to the solution. The resulting yellow powder was dissolved in acetone for crystal growth. The crystal structure of this compound is discussed in Chapter 4. Yield: 0.012 g (16 %). ^{1}H NMR ($(CD_3)_2SO$): δ 7.86 – 7.22 (m). IR (ATR): 1436 (ν_{P-C}), 1268 (ν_{N-O}), 800 (ν_{Ar-H}).

3.3.14 cis-[Bis-(triphenylphosphino)]-4,5-diazafluoren-9-one-palladium(II)

$Pd(PPh_3)_2Cl_2$ (0.053 g, 7.55 $x10^{-5}$ mol) was dissolved in nitromethane (15ml). AgTrif (0.040 g, $1.5x10^{-4}$ mol) was added to the solution and the solution stirred for 30 minutes. The AgCl was filtered off and 4,5-diazafluoren-9-one (0.014g, 7.7 $x10^{-5}$ mol) was added to the solution. The solution was left to evaporate. The crystal structure of the title compound is discussed in Chapter 4. Yield: 0.063 g (63 %). ^{1}H NMR ($(CD_3)_2SO$): δ 7 .74 – 7.28 (m), 8.32 (d, J = 6.9 Hz, 2H), 9.60 (s, 2H). IR (ATR): 1733 (ν_{C-O}), 1435(ν_{P-C}), 1254 (ν_{C-N}), 745 (ν_{Ar-H}).

3.3.15 (μ_2-2,2'-Bipyrimidine)-bis-2,2-bipyridine-palladium(II)

$Pd_2BpymCl_4$ (0.060 g, $9.76x10^{-5}$ mol) and silver triflate (0.120 g, $4.67x10^{-4}$ mol) were reacted in acetonitrile. AgCl was filtered off and 2,2'-bipyridine (0.037 g, $2.35x10^{-4}$ mol) was added to the solution. A yellow precipitate was formed, which was filtered and weighed. Yield: 0.016 g (23%). ^{1}H NMR ($(CD_3)_2SO$): δ 7.8 (t, J = 4.6 Hz, 2H), 7.9 (m, 4H), 8.5 (m, 4H), 8.7 (d, J = 7.4 Hz, 4H), 8.8 (d, J = 4.7), 9.1 (d, J = 3.7 Hz, 4 H). IR (ATR): 1605 (ν_{C-H}), 1121 (ν_{C-N}), 817 (ν_{Ar-H}).

3.3.16 Crystalline Titanium Oxide[5]

$TiCl_4$ (0.5 ml, $4.5x10^{-3}$ mol) and benzyl alcohol (20 ml) was stirred at 40°C for 7 days. The white powder was filtered from the solution and washed with nitromethane to yield an off white crystalline material. Yield: 0.243 g (68 %). IR (ATR): 500-820 (ν_{max} = 595).

3.3.17 Crystalline Tungsten Oxide[6]

WCl_6 (0.153 g, 3.8 $x10^{-4}$ mol) was added to benzyl alcohol (4 ml) and stirred for 2 days at 100 ° C. The yellow crystalline product was centrifuged and washed with ethanol. Yield: 0.053g (59.5 %). IR (ATR): 530-780 (ν_{max} = 604).

3.4 Unsuccessful synthesis

3.4.1 PdBpymPtCl$_4$

PtBypmCl$_2$ (0.081 g, 1.91 x10^{-4} mol) was dissolved in acetonitrile. To this PdCl$_2$ (0.035 g, 1.97 x10^{-4} mol), dissolved in boiling acetonitrile, was added. A brownish powder was obtained. The NMR data was identical to the starting PtBypmCl$_2$ compound. ^{1}H NMR ((CD$_3$)$_2$SO): δ 8.00 (t, J = 5.3 Hz, 2H), 9.35 (d, J = 3.4 Hz, 2H), 9.7 (d, J = 5.9 Hz, 2H).

3.4.2 *cis*-[Pt-(NH$_3$)$_2$(pz)}$_4$](NO$_3$)$_8$3.67H$_2$O [7].

Cisplatin (0.0502 g, 0.167x10^{-3} mol) was suspended in H$_2$O (4 ml) and AgNO$_3$ (0.057 g, 3.34 x10^{-3} mol) and stirred with daylight excluded for 24 hours. The solution was filtered and pyrazine (0.0134 g, 0.168x10^{-3} mol) was added. The solution was stirred at 40°C for 2 days.

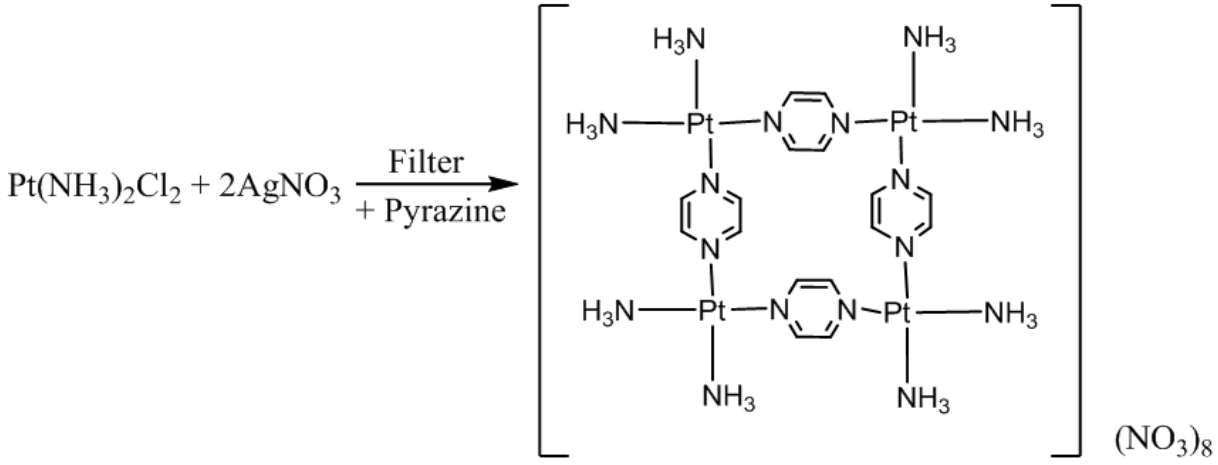

Scheme 3.2: Reported synthesis of platinum metal organic framework utilizing pyrazine as a bridging ligand[7].

Although this reaction was performed several times the title compound could not be isolated or characterized by NMR. The NH$_3$ ligands were replaced by ethylene diamine and 2,2-bipyridine with the same result. This synthesis was performed utilizing [PdBipyCl$_2$] but was also

unsuccessful. The overlapping of peaks makes characterization by means of NMR difficult. No access to elemental analysis was available.

3.4.3 $[Pd(en)(4,4'\text{-bipy})]_4(NO_3)_8]$[8,9,10]

Pde(n)Cl_2 (0.083 g, 3.5 x10^{-4} mol) and $AgNO_3$ (0.085 g, 7.0x10^{-4} mol) were stirred in a methanol-water (1:1) solution for 15 minutes and filtered. To this an ethanol (4 ml) solution of 4,4'-bipy (0.055g 3.5 x10^{-4} mol) was added at room temperature. The solution was stirred for 10 min at that temperature. Upon addition of ethanol (4 ml), a pale yellow powder immediately precipitated.

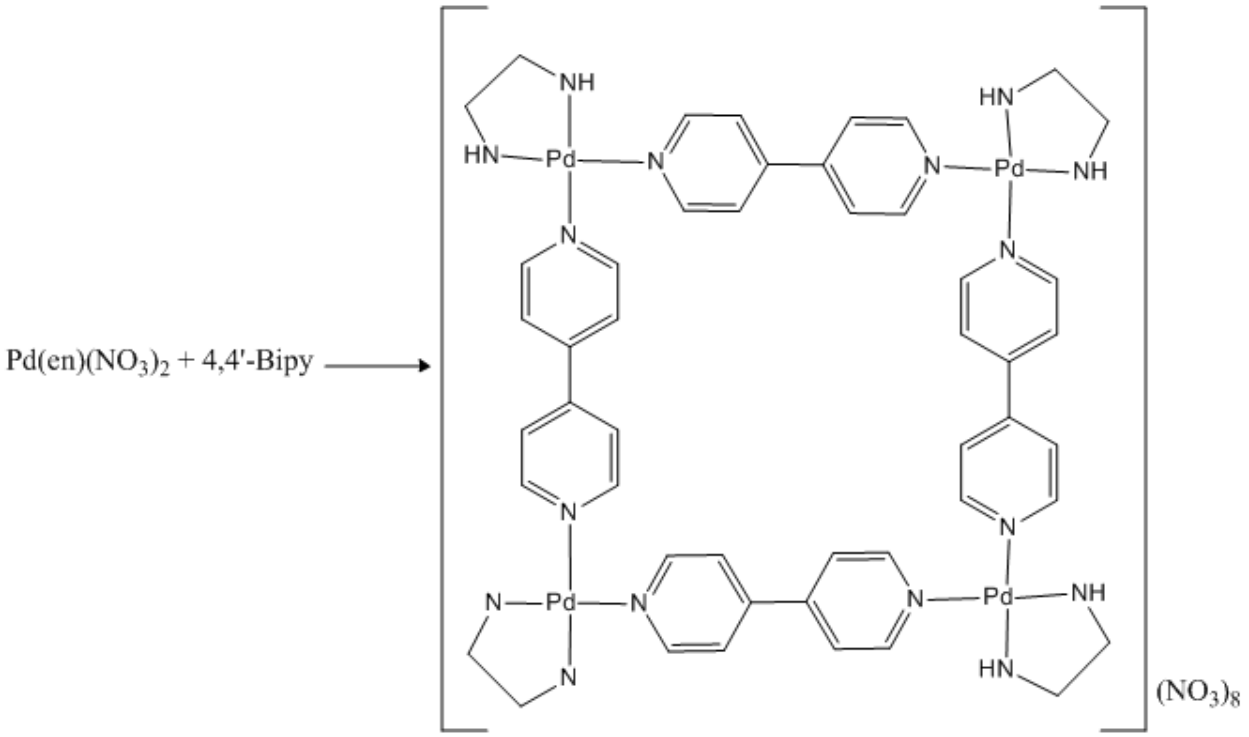

Scheme 3.3: Reported synthesis procedure for metal organic framework utilizing 4,4'-Bipy and palladium[8,9,10].

Although the above synthesis is listed in the unsuccessful section the reaction steps were identical to those mentioned in the references. The NMR data yielded the same peaks at ~7.6 and ~8.6 that are used to characterize the compounds. However, the rest of the NMR data was

not sufficient to conclude without a doubt that the compound had been synthesized. The non-bridging ligands were also varied, triphenylphosphine, 2,2-bipyridine, 4,5-diazafluoren-9-one and 1,10-Phenanthroline were investigated. These ligands are problematic in the sense that multiple overlapping peaks are formed when NMR analysis is done which makes the characterization even more challenging. Unfortunately, elemental analysis could not be performed on these samples. This is the primary characterization technique used in the references. Although the compounds were not sufficiently characterized several crystallization techniques were utilized to try to attain crystals.

3.5 Conclusions

In this chapter, the successful synthesis of various metal complexes as building blocks for bridged platinum(II) and palladium(II) complex are reported. The following compounds were successfully synthesized and characterized.

- An alternative bidentate ligand, 5-diazafluoren-9-one.
- Palladium dichlorido amine compounds: complexes of 2,2'-bipyridine and 45-diazafluoren-9-one.
- Palladium dichloride type phosphine compounds of triphenyl phosphine.
- Platinum dichlrido type amines: complexes of 2,2-bipyridine, 1,10, phenanthroline, 2,2-bipyrimidine, amine, ethylene diamine and 5-diazafluoren-9-one.

The above mentioned compounds were obtained in reasonable yields. In addition to the fact that the solid state crystal structures of *cis*-$[Pd(PPh_3)_2(Daf)_2].(Trif)_2.CH_3NO_2$ and *cis*-$[Pd(PPh_3)_2(NO_3)_2].CO(CH_3)_2$, were obtained and discussed in Chapter 4, these complexes were also characterized by means of NMR and IR spectroscopy. The complexes that were synthesized were used in the attempted synthesis of various metal organic frameworks and bridged platinum and palladium compounds. Two palladium centers were successfully bridged by 2,2-bipyrimidine and the complex was successfully characterized by means of NMR and IR. The crystal structure of this compound is also reported in Chapter 4.

Chapter 3

Some crystalline inorganic supports, namely titanium oxide and tungsten oxide were synthesized and characterized by IR as reported in literature. Unfortunately, these two compounds could not be further verified by any other techniques due to infrastructural problems. However, the reaction followed the specification of the mentioned literature accurately.

A number of unsuccessful attempts to synthesize a range of metal organic frameworks according to literature procedures were also reported. In most cases the reactions followed the same path as described in literature. Unfortunately, the NMR data was of such a nature that proper characterization could not be done using this technique. Elemental analysis was unavailable for this purpose. The complexes reported in this chapter were further studied as reported in the following chapters.

---

(1) Boyle, R. C.; Mague, J. T.; Fink, M. J. *Acta Crystallogr E Struct Rep Online* **2003**, *60*, m40-m41.

(2) Morgan, G.; Burstall, F. *J. Chem. Soc.* **1934**, 965−971.

(3) Alderden, R. A.; Hall, M. *Journal of Chemical Education* **2006**, *83*, 728-734.

(4) Zhu, Q. *Inorganica Chimica Acta* **2003**, *351*, 177-182.

(5) Niederberger, M.; Bartl, M. H.; Stucky, G. D. *Chem. Mater.* **2002**, *14*, 4364-4370.

(6) Niederberger, M.; Bartl, M. H.; Stucky, G. D. *J. Am. Chem. Soc.* **2002**, *124*, 13642-13643.

(7) Willermann, M.; Mulcahy, C.; Sigel, R. K. O.; Cerdà, M. M.; Freisinger, E.; Sanz Miguel, P. J.; Roitzsch, M.; Lippert, B. *Inorg. Chem.* **2006**, *45*, 2093-2099.

(8) Fujita, M.; Yazaki, J.; Ogura, K. *J. Am. Chem. Soc.* **1990**, *112*, 5645-5647.

(9) Fujita, M.; Sasaki, O.; Mitsuhashi, T.; Fujita, T.; Yazaki, J.; Yamaguchi, K.; Ogura, K. *Chem. Commun.* **1996**, 1535.

(10) Leininger, S.; Olenyuk, B.; Stang, P. J. *Chem. Rev.* **2000**, *100*, 853-908.

4 Single Crystal X-Ray Crystallographic Study of Palladium(II) Complexes

4.1 Introduction

The development of analytical tools from the 1960's onward has played an important role in the understanding of chemical systems. Although microscopy was developed extensively, observation of small particles was limited by the resolution which is determined by the wavelength of radiation used[1]. Two objects which are approximately 0.36 λ (λ = wavelength of radiation) apart cannot be sufficiently resolved in order to be separately observed by microscopy. In chemical substances a C-C bond is typically in the order of 1.5 Å, so in order for one to observe the two it is necessary to employ radiation with λ = 1 Å. Unfortunately, visible light does not fall within these parameters, which led to the employment of X-rays for this purpose. X-rays, like light, consists of an electromagnetic wave which can interact with matter on a nanometer scale. This makes X-rays ideal for the characterizing of molecules. In the Electron Microscope the electromagnetic wave is reflected by atoms and then focused by the lens system. However, when utilizing X-rays the electromagnetic waves are scattered and cannot easily be focused. As a result a microscope which can view atoms cannot be built, thus in order to 'see' atoms a different approach is needed. Consequently, diffraction rather than reflection is exploited to observe the atoms which are present in crystalline compounds[2].

A crystal can be described as a solid in which there is a three dimensional repetition of a particular unit which constitutes the molecule[1]. Walther Friedrich, Paul Knipping and Max van Laue were the first scientists that demonstrated that crystals refract X-rays in 1890. At the time scientists were unsure whether X-rays consisted of particles or electromagnetic radiation. After the discovery of X-ray diffraction, it was clear that X-rays have a wave property. Scientists were then able to calculate the relationship between the observed effect and experimental conditions using sound mathematical principles[2]. During an X-ray diffraction, experiment X-rays are scattered by electrons of atoms in various locations throughout the unit cell. This scattering is reinforced and captured as spots on photographic film. W. L. Bragg demonstrated that these

diffraction patterns hold information on the distribution of electron density within the unit cell. When performing an X-ray diffraction experiment the following steps are followed.

1. A suitable single crystal has to be obtained.
2. The crystal is then placed in a beam of monochromatic X-rays and the diffracted data collected by a diffractometer.
3. Interpretation of the results by making use of various software packages. The principles discussed later are then used to solve the crystal structure so results can be interpreted.

4.1.1 Bragg's Law

According to Bragg's law; when a beam of a certain wavelength radiation, λ, enters a crystal at a certain plane, defined by the Miller indexes (*hkl)*, the radiation will only be refracted if the following geometrical conditions are met:

$$n\lambda = 2d_{hkl} \sin \theta \qquad \textbf{...Eq 4.1.1}$$

Equation 4.1.1 is known as Bragg's law where n is an integer, λ is the wavelength of the radiation, d_{hkl} is the interplanar spacing of the hkl planes and θ is the diffraction angle or Bragg angle. Figure 4.1 illustrates the above mentioned relationship more clearly.

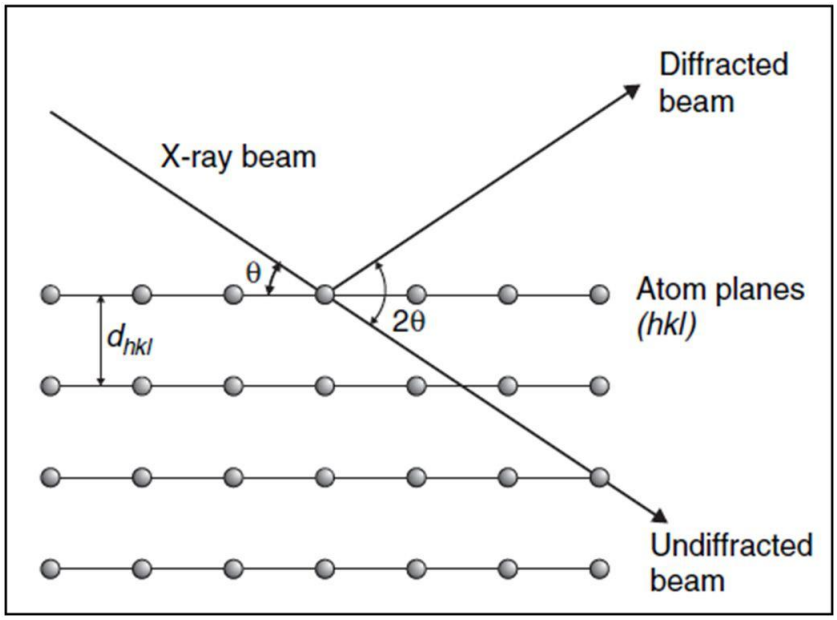

Figure 4.1: The diffraction of X-rays according to Bragg's Law.

It is important to note that Bragg's law is used to predict where the beam will be diffracted, however it does not give an indication to the intensity of the refracted beam. Although it might seem as though the geometry that is depicted in Figure 4.1 is identical to reflection there is a definite difference between the refraction and reflection angles. Another factor that separates diffraction from reflection is the fact that refraction will only occur when the atoms are irradiated at the angle, $\theta = \sin^{-1}(n\lambda/2d_{hkl})$, whereas light can be reflected from almost every angle.

4.1.2 The Structure Factor

The major factors that determine the intensity of the Bragg reflections are the following.

- The number of electrons that are present in the atoms.
- The degree to which the X-rays are scattered from one atom reinforces the X-rays scattered by another.

Chapter 4

The interaction of X-rays scattered by different atoms can be constructive or destructive. By combing the scattering from all the atoms in a unit cell, one is able to obtain the total intensity of the scattered radiation. In order to achieve this, the waves scattered by each individual set of planes are added together to obtain a value known as the structure factor for each plane. When observing atoms in a unit cell their position can be defined by equation 4.1.2:

$$r = hx + ky + lz \qquad \textbf{...Eq 4.1.2}$$

Using equation 4.1.2 the structure factor (F) can be defined as the following[3]:

$$F_{hkl} = \sum_{j=1}^{N} f_j \left(\frac{\sin\theta_{hkl}}{\lambda}\right) e^{2\pi i g_{hkl}\cdot r_j} = \sum_{j=1}^{N} f_j \left(\frac{\sin\theta_{hkl}}{\lambda}\right) e^{2\pi i(hx_j + ky_j + lz_j)} \qquad \textbf{...Eq 4.1.3}$$

where N is the number of units in the cell and f_j is the scattering factor for each of the atoms. F is a complex number which expresses the phase and amplitude of the resultant wave. The amplitude and resultant wave of a single electron is obtained from $|F|$[4].

$$|F| = \frac{Amplitude\ of\ the\ wave\ scattered\ by\ all\ atoms\ of\ the\ unit\ cell}{Amplitude\ of\ the\ wave\ scattered\ by\ one\ electron} \qquad \textbf{...Eq 4.1.4}$$

Using Equation 4.1.3 one can calculate the intensity of any *hkl* value, if the position of the atom is known. It is important to note that the phase difference between waves scattered by two atoms is constant for every unit cell and that the difference in phase increases, the deeper the crystal is penetrated as the Bragg angle is not exactly equal to the angle of the diffracted ray. When this difference between atoms A and B exists the structure factor changes to:

$$F_{hkl} = \sum_{j=1}^{N} f_j \left[\cos 2\pi(hx_j + ky_j + lz_j) + i \sin 2\pi(hx_j + ky_j + lz_j)\right] \qquad \textbf{...Eq 4.1.5}$$

4.1.3 The Phase Problem

In an X-ray diffractometer experiment the diffraction from the different planes within a crystal are measured. In order to obtain an image of the atoms from the diffracted rays, scientists make use of the structure factor functions and Bragg equations. Unlike an optical lens that recombines both the amplitude and phase of refracted rays, the reflections obtained from the X-ray diffractometer provide intensities which are proportional to the squares of the amplitudes of the diffracted waves. As a result there is a loss of information which is commonly known as the phase problem. The reconstruction of the actual image relies on models which seek to recapture the missing information. In the direct method mathematical calculations are used, but these calculations are best suited to structures that contain only light atoms. For the heavier atoms the Patterson function is employed.

4.1.4 The Patterson Function

Since the measured intensities in an X-ray diffraction experiment contains no information on the phase of the refractions a different solution is needed. In 1934 Patterson linked the Fourier transform (Equation 4.1.6) of the intensities with the electron density (Equation 4.1.7) of the atom.

$$P(u,v,w) = V^{-1} \sum_h \sum_k \sum_l (f_{hkl})^2 \exp[-2\pi i(hu + kv + lw)] \qquad \textbf{...Eq 4.1.6}$$

$$\mathrm{P(u)} = \int \rho(\mathrm{r})\rho(\mathrm{r} + \mathrm{u})\, \mathrm{d}^3\mathrm{r} \qquad \textbf{...Eq 4.1.7}$$

The Patterson function P(u) is an autocorrelation function of the density[5]. By plotting the Patterson function on the u, v and w axes one is able to construct a map with peaks that correspond to interatomic vectors. The peak heights are proportional to the product of the two atoms between which the vector is found. Consequently, one is able to obtain the position of the atoms relative to one another and the center of the unit cell. Unfortunately, the Patterson

function is not without fault. In systems where a large number of similar atoms are found, multiple overlapping peaks which cannot be resolved are generated.

4.1.5 Fourier Transformation

A reflection obtained from an X-ray diffraction can be described by the structure factor (F) equation which contains a term for each atom in the unit cell. In a similar fashion the structure factors can be converted to electron density (ρ). The mathematical manipulation used to achieve this is known as the Fourier transformation. The equation for the Fourier transformation is obtained as follows.

$$F(hkl) = \int_V \rho(xyz)\, e^{\phi} dV \qquad \textbf{...Eq 4.1.8}$$

Therefore:

$$\rho(xyz) = \left(\frac{1}{V}\right) \sum_{hkl} F(hkl) e^{-i\phi}\, dV \qquad \textbf{...Eq 4.1.9}$$

Where $\phi = 2\pi(hx + ky + lz)$. A Fourier transformation is a mathematical tool that can be used by a crystallographer to flip between real and diffracted space. Ultimately the Fourier transformation is applied to the Bragg equation to construct an electron density map. If electron density is expressed as the sum of cosine waves then its Fourier transform will be equal to the sum of the Fourier transform of each individual cosine wave.

4.1.6 Least-Squares Refinement

The least-squares refinement process is one of the most useful methods for obtaining valuable information from a single crystal X-ray diffraction (XRD) experiment. This method compares the experimental structure factors to the calculated ones. The final goal of XRD is to determine the correct atomic structure of the crystal. In order to achieve this, the least-squares refinement process constantly compares the experimental data to the calculated ones. These values converge as the correctness of the structure increases. This convergence is measured by the residual or R-factor and the so called weighted R: [6]

$$R = \frac{\sum_{hkl} ||F(hkl)|_o - |F(hkl)|_c|}{\sum |F(hkl)|_o} \quad \text{...Eq 4.1.10}$$

$$wR2 = \sqrt{\frac{\sum w\left(F_0^2 - F_c^2\right)^2}{\sum w(F_0^2)^2}} \quad \text{...Eq 4.1.11}$$

The smaller the wR2 and R value of the model being evaluated, the closer it is to the correct observed crystal structure. A wR2 or R value of 0 would indicate the perfect refinement of experimental data but this is rarely achieved.

In the past, the R value was used primarily. Consequently, refinement was performed against structure factors F; however this required that the measured intensities be transformed to structure factors. This action requires the extraction of a root as $I \propto F^2$ which leads to mathematical problems when dealing with weak and negative reflections. As a result these reflections need to be adjusted to equal to zero or a small positive number when refining to the structure factor. This results in bias in the solving of a crystal structure as the information contained in the weak reflections is lost. The estimation of σ is also problematic when refining towards F. On the other hand when refining towards F^2 these problems do not exist. Consequently the wR2 equation became the equation of choice. There are several other advantages when refining to F^2; the mathematical refinement of twinned structures is simpler, and refinement against F^2 is less likely to settle into a local minimum. It is accepted that F^2 is the superior refinement method[7].

4.1.7 The Charge Flipping Method

All the above mentioned refinement processes involve complex algorithms which have been extensively developed. However, in 2004 Gabor Oszlanyi and Andras Suto introduced a surprisingly simple method for structures solution, namely the Charge Flipping method[8]. The Charge Flipping method uses structure factors corresponding to real atoms at zero temperatures and avoids structure factors that correspond to point atoms. This is done to ensure that peaks are sufficiently defined but the effect of resolution cut-off is less severe. Irregular scattering is not

exploited and atomic scattering factors are taken to be strictly real. Furthermore, it is taken that the diffraction data is complete up to a given resolution, it is error free, the absolute scale and global isotropic temperature factor is known. The Fourier transform is used to relate real-space charge-density and reciprocal space structure factors. Charge density is represented on a grid structure after factors are limited by a given resolution. A certain positive threshold, δ, is assigned to charged pixels on the grid. Pixels above this threshold are taken to be those of atoms and are unchanged. Pixels below this value are multiplied by -1. Temporary structure factors, G(h), are then calculated by a FFT. Structure factors, F(h), are constructed by accepting phases and replacing the moduli by $F_{obs}(h)$. It is accepted that F(0) = G(0) and F(h) for h > H are reset to zero. Finally, the F(h) amplitudes are inverted to obtain the new approximation of the charge density[8]. This process is repeated until convergence is achieved.

4.2 Crystal structure Determination of Selected Complexes

4.2.1 Introduction

One of the aims of this study was to synthesize complexes, and then co-crystallize the metal complexes with crystalline supports. Consequently, the compounds that were synthesized were investigated and characterized by means of single crystal X-ray crystallography. The crystals of the complexes that were synthesized, namely *cis*-$[Pd(PPh_3)_2(Daf)_2].(Trif)_2.CH_3NO_2$ (**1**), *cis*-$[Pd_2BipmCl_4]$.DMF (**2**) and *cis*-$[Pd(PPh_3)_2(NO_3)_2].CO(CH_3)_2$ (**3**) are discussed in this section. The term, Daf, is used to describe 4,5-diazafluoren-9-one, bpym refers to 2,2'-bipyrimidine and nq to describe (2,3-η)-1,4-naphthoquinone.

4.2.2 Experimental

A Bruker X8 ApexII 4K diffractometer[9] using graphite monochromated Mo *K*α radiation with ω-and-φ-scans at 100K was used to obtain reflection data. COSMO[10] was used for optimum collection of more than a hemisphere of reciprocal space. The first 50 frames were repeated periodically to ensure that no decomposition of the crystals took place. The crystals remained stable throughout the data collection. The cell refinement was performed with SAINT-Plus[11] and data reduction with SAINT-Plus and XPREP[10]. Data corrections for absorption effects were performed using the multi-scan technique SADABS[12]. The structures were solved by the direct method package SIR97[13] and refined using the software package WinGX[14], incorporating SHELXL[15]. Graphical representations of crystal structures were created by DIAMOND[16]. All structures are shown with thermal ellipsoids drawn at 50% probability level and refined anisotropically, unless otherwise stated. Methyl and aromatic hydrogen atoms were placed in geometrically idealized positions (C-H = 0.95 – 0.98 Å) and constrained to ride on their parent atoms (U_{iso}(H) = 1.5 U_{eq}(C) and 1.2 U_{eq}(C)). Table 4.1 indicates that (**1**) and (**3**) have R_{int} values of 11.87 % and 11.37% respectively. This is higher than the accepted norm and could be as a result of poor crystal quality or faulty centering of the crystal in the experimental data collection. Molecule (**2**) has a high goodness-of-fit value as a result of one carbon atom not being placed on the disordered DMF molecule. The SIMU, EADP, FLAT and SAME restraints were used to solve the disorder on the phenyl ring and the triflate counter ion in (**1**).

Table 4.1: Crystal Data parameters for *cis*-$[Pd(PPh_3)_2(Daf)_2].(Trif)_2.CH_3NO_2$, *cis*-$[Pd_2BpymCl_4].DMF$ and *cis*-$[Pd(PPh_3)_2(NO_3)_2].CO(CH_3)_2$.

Compound	$[Pd(PPh_3)_2(Daf)_2].(Trif)_2.CH_3NO_2$	$[Pd_2BpymCl_4].DMF$	$[Pd(PPh_3)_2(NO_3)_2].CO(CH_3)_2$
Emperical formula	$C_{61}\ H_{40}\ F_6\ N_5\ O_{10}\ P_2\ Pd\ S_2$	$C_8\ H_6\ Cl_4\ N_2\ Pd_2$	$C_{75}\ H_{30}\ N_4\ O_{13}\ P_4\ Pd_2$
F.W.	1338.44	484.75	1501.47
Crystal system	Monoclinic	Monoclinic	Monoclinic
Space group	P2/n	C2/m	C2/c
a (Å)	15.1843(10)	10.7299(6)	40.343(2)
b (Å)	17.1115(12)	14.2399(7)	9.7490(4)
c (Å)	22.2575(14)	5.9381(3)	19.7802(10)
α(°)	90	90	90
β(°)	99.676(4)	108.229(2)	115.5140(10)
γ(°)	90	90	90
Volume ($Å^3$)	5700.8(7)	861.76(8)	7021.0(6)
Z	4	2	4
ρ_{calc} ($g\ cm^{-3}$)	1.559	1.868	1.420
μ (mm^{-1})	0.539	2.684	0.668
F(000)	2710	456	2936
Crystal Colour	Yellow	Red	Yellow
Morphology	Cuboid	Cuboid	Plate
Crystal size (mm)	0.247x0.251x 0.301	0.076x0.087x0.089	0.075x0.181x0.192
Theta range (°)	1.51 to 27.00	2.46 to 28.26	1.12 to 28.29
Completeness	99.20%	99.90%	99.00%
Limiting indices	-19<=h<=19	-12<=h<=14	-53<=h<=53
	-21<=k<=21	-18<=k<=18	-12<=k<=7
	28<=l<=26	-7<=l<=7	-26<=l<=26
Reflections collected	72760	6121	42875
Unique reflections	12345	1110	8638
R_{int}	0.1187	0.041	0.1137
Refinement method	Full-matrix least-squares on F^2	Full-matrix least-squares on F^2	Full-matrix least-squares on F^2
Data / restraints / parameters	12345 / 61 / 816	1110 / 0 / 68	8638 / 0 / 435
Goodness-of-fit on F^2	1.049	1.328	1.007
Final R indices [I>2sigma(I)]	R1 = 0.0750	R1 = 0.0320	R1 = 0.0773
	wR2 = 0.1930	wR2 = 0.0893	wR2 = 0.1873
R indices (all data)	R1 = 0.1417	R1 = 0.0441	R1 = 0.1585
	wR2 = 0.2620	wR2 = 0.1327	wR2 = 0.2652
Temperature	100 K	100 K	100 K

4.3 Crystal Structure of *cis*-$[Pd(PPh_3)_2(Daf)_2].(Trif)_2 .CH_3NO_2$

The compound, *cis*-$[Pd(PPh_3)_2(Daf)_2].(Trif)_2.CH_3NO_2$ (**1**) crystallized in the primitive monoclinic P2/n space group with four molecules per unit cell. The crystals were obtained as described in Section 3.3.14. One of the triflate counter ions showed a problematic disorder which will be briefly discussed later. The numbering scheme for the complex cation is illustrated in Figure 4.2. Selected bond angles and lengths are presented in and Table 4.2 and 4.3 respectively. Atomic coordinates, anisotropic displacement parameters, all bond distances, angles and torsion angles are given in Appendix A.

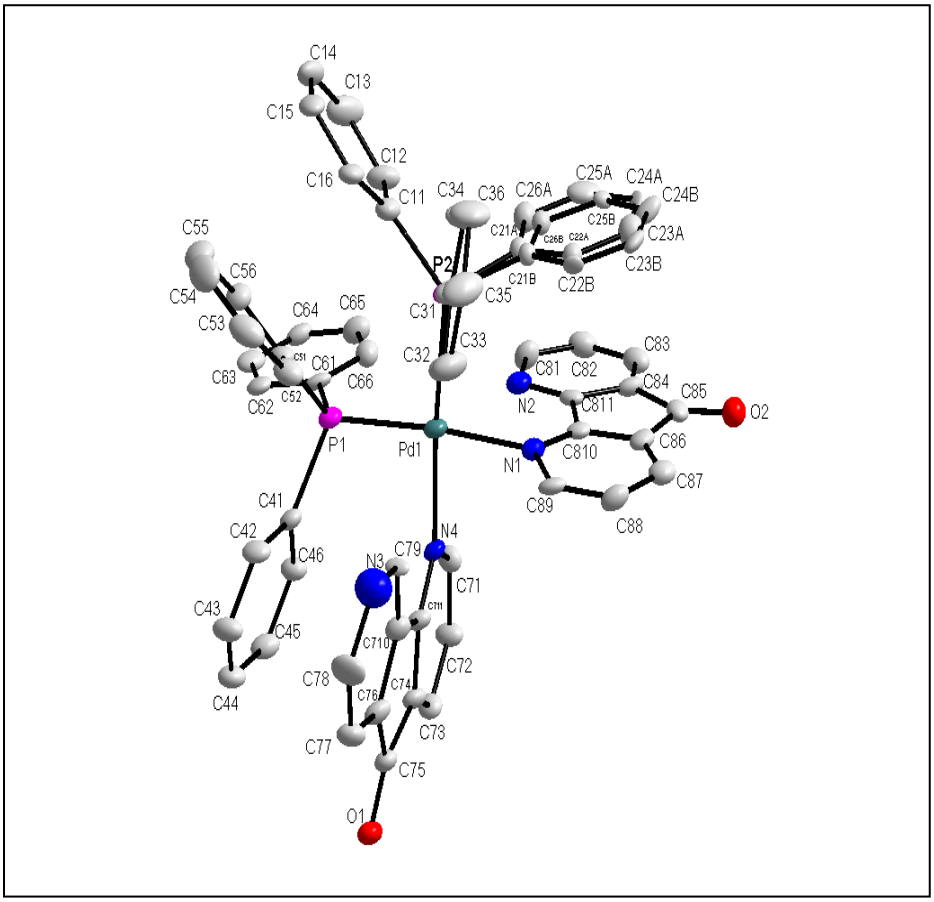

Figure 4.2: Diamond representation of *cis*-$[Pd(PPh_3)_2(Daf)_2].(Trif)_2.CH_3NO_2$ at 50 % probability level, displaying the numbering scheme employed: the first digit represents the ring and the second digit the number of the atom in the ring. The disorder on the phenyl ring defined by C21-C26 is also shown. Both triflate counter ions, the CH_3NO_2 solvate molecule and hydrogen atoms are omitted for clarity.

The complex cation consists of a palladium(II) center to which two Daf ligands and two triphenyl phosphine ligands have bonded in a *cis* fashion. The geometry around the palladium metal center is slightly distorted from the square plane as illustrated by the angle of P(1)-Pd(1)-P(2) and N(4)-Pd(1)-N(1) being 95.3° and 86.4° respectively. Interestingly enough the crystals that were obtained did not show the bidentate ligands binding to the palladium center with both nitrogen atoms. Rather, the two bidentate ligands coordinate adjacent to each other with the free ends facing in opposite directions. Upon closer investigation of the complex in Figure 4.3 it is clear that the free nitrogens have an interaction with the vacant orbital of the palladium(II) species in order to form a pseudo octahedral structure. The angles of the non-coordinating nitrogen ligands with respect to the xy are therefore of interest. The N2-Pd1-N1 and N2-Pd1-P2 are 67.412(2)° and 92.861(2)° respectively. For N3 the N3-Pd1-P2 and N3-Pd1-N1 angles are 113.0919(2)° and 90.01(1)° respectively. In a proper octahedral structure, one would expect all these angles to be approximately 90°. From the above one can deduce that the octahedral structure is distorted by approximately 20°. The N2-Pd1-N3 bond angle is 147.1° and deviates from the true octahedral geometry by approximately 30°.

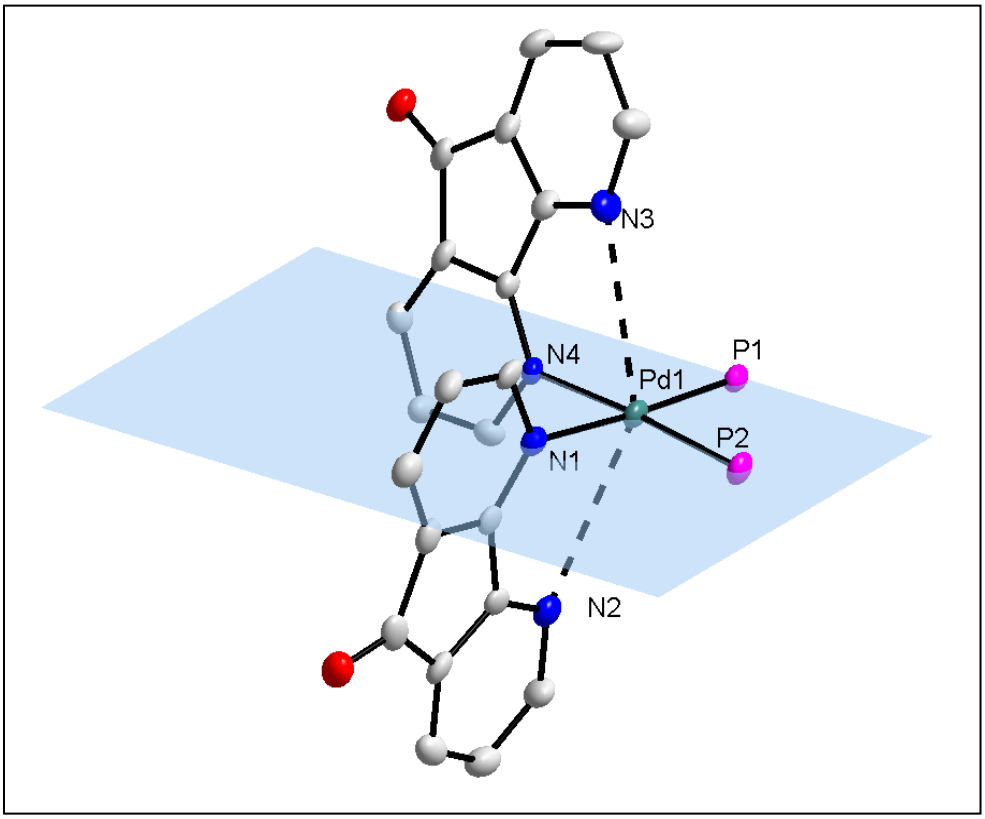

Figure 4.3: Diamond representation of *cis*-[Pd(PPh$_3$)$_2$(Daf)$_2$].(Trif)$_2$.CH$_3$NO$_2$ at 50 % probability level, displaying the formation of a pseudo octahedral structure. The phosphine ligands, the solvate CH$_3$NO$_2$, hydrogen atoms and counter ions are omitted for clarity.

Table 4.2 : Selected bond Lengths for *cis*-[Pd(PPh$_3$)$_2$(Daf)$_2$].(Trif)$_2$.CH$_3$NO$_2$

Atoms	Bond Lengths (Å)	Atoms	Bond Lengths(Å)
P(2)-Pd(1)	2.3227(17)	C(81)-N(2)	1.356(8)
P(1)-Pd(1)	2.3020(17)	C(71)-N(4)	1.350(8)
N(1)-Pd(1)	2.136(5)	C(810)-N(1)	1.346(8)
N(2)-Pd(1)	3.2248(2)	C(811)-N(2)	1.335(8)
N(3)-Pd(1)	3.1113(2)	C(89)-N(1)	1.360(8)
N(4)-Pd(1)	2.131(5)	C(79)-N(3)	1.334(9)
C(11)-P(2)	1.836(7)	C(711)-N(4)	1.333(8)
C(41)-P(1)	1.828(7)	C(710)-N(3)	1.331(8)
C(61)-P(1)	1.818(6)	C(85)-O(2)	1.227(8)
C(31)-P(2)	1.813(7)	C(75)-O(1)	1.217(7)
C(51)-P(1)	1.809(6)		

Table 4.3: Selected bond angles for *cis*-$[Pd(PPh_3)_2(Daf)_2].(Trif)_2.CH_3NO_2$

Atoms	Angle (◦)	Atoms	Angle (◦)
P(1)-Pd(1)-P(2)	95.3(6)	C(32)-C(31)-P(2)	121.8(5)
C(31)-P(2)-C(21B)	95.0(5)	C(66)-C(61)-P(1)	120.8(5)
N(1)-Pd(1)-P(2)	89.4(1)	C(16)-C(11)-P(2)	120.4(5)
N(4)-Pd(1)-P(1)	88.8(1)	C(22B)-C(21B)-P(2)	120.2(9)
N(4)-Pd(1)-N(1)	86.5(2)	C(12)-C(11)-P(2)	120.2(5)
N(4)-Pd(1)-P(2)	175.4(1)	C(34)-C(31)-P(2)	119.9(6)
N(1)-Pd(1)-P(1)	175.2(1)	C(62)-C(61)-P(1)	119.9(5)
N(2)-Pd(1)-P(2)	92.86(1)	C(46)-C(41)-P(1)	119.6(5)
N(2)-Pd(1)-N(1)	67.41 (1)	C(71)-N(4)-Pd(1)	119.6(4)
N(3)-Pd(1)-P(2)	113.1(2)	C(89)-N(1)-Pd(1)	119.0(4)
N(3)-Pd(1)-N(4)	69.18(2)	C(51)-P(1)-Pd(1)	117.8(2)
C(21A)-P(2)-C(21B)	13.9(5)	C(711)-N(4)-C(71)	117.5(5)
N(1)-C(810)-C(811)	128.3(6)	C(810)-N(1)-C(89)	115.9(5)
O(1)-C(75)-C(76)	128.1(6)	C(41)-P(1)-Pd(1)	113.2(2)
N(4)-C(711)-C(710)	127.9(6)	C(31)-P(2)-Pd(1)	112.5(2)
O(1)-C(75)-C(74)	127.1(6)	C(11)-P(2)-C(21B)	110.9(5)
O(2)-C(85)-C(86)	126.1(6)	C(61)-P(1)-Pd(1)	110.5(2)
C(810)-N(1)-Pd(1)	125.0(4)	C(51)-P(1)-C(61)	109.3(3)
C(26A)-C(21A)-P(2)	124.4(10)	C(31)-P(2)-C(21A)	108.3(5)
C(711)-N(4)-Pd(1)	123.0(4)	C(21A)-P(2)-Pd(1)	106.5(5)
C(42)-C(41)-P(1)	122.9(5)	C(31)-P(2)-C(11)	103.8(3)
C(56)-C(51)-P(1)	122.7(5)	C(11)-P(2)-C(21A)	103.0(5)
N(1)-C(810)-C(86)	122.5(6)	C(51)-P(1)-C(41)	102.7(3)
C(11)-P(2)-Pd(1)	121.9(2)	C(61)-P(1)-C(41)	102.0(3)

A 50% positional disorder is observed for ring two of the triphenylphosphine ligands. This disorder is also experienced in one of the triflate ions. There is an interaction between a fluorine on the triflate anion and the hydrogen atoms of the disordered phenyl as illustrated in Figure 4.4. The crystal packing of (**1**), displayed in Figure 4.5, shows the four palladium centers in the unit cell. The complex crystallizes diagonally across the ac plane in a typical head to tail fashion.

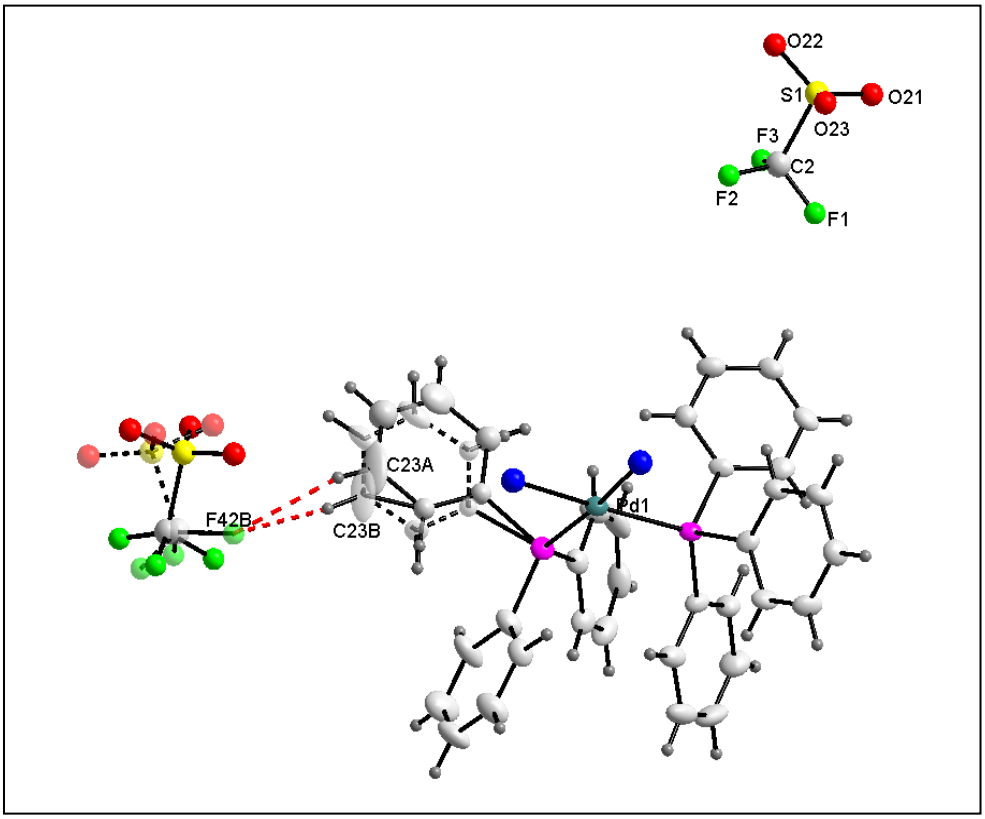

Figure 4.4: Diamond representation of *cis*-[Pd(PPh_3)$_2$(Daf)$_2$].(Trif)$_2$.CH_3NO_2 at 50 % probability level, displaying the disorders in the one phenyl ring of the PPh3 and the triflate counter anion. The interaction between the phenyl ring's hydrogen atoms and the flourines of the triflate counter ion is shown. The triflate anion which has no disorder is also indicated. The Daf ligands are omitted for clarity.

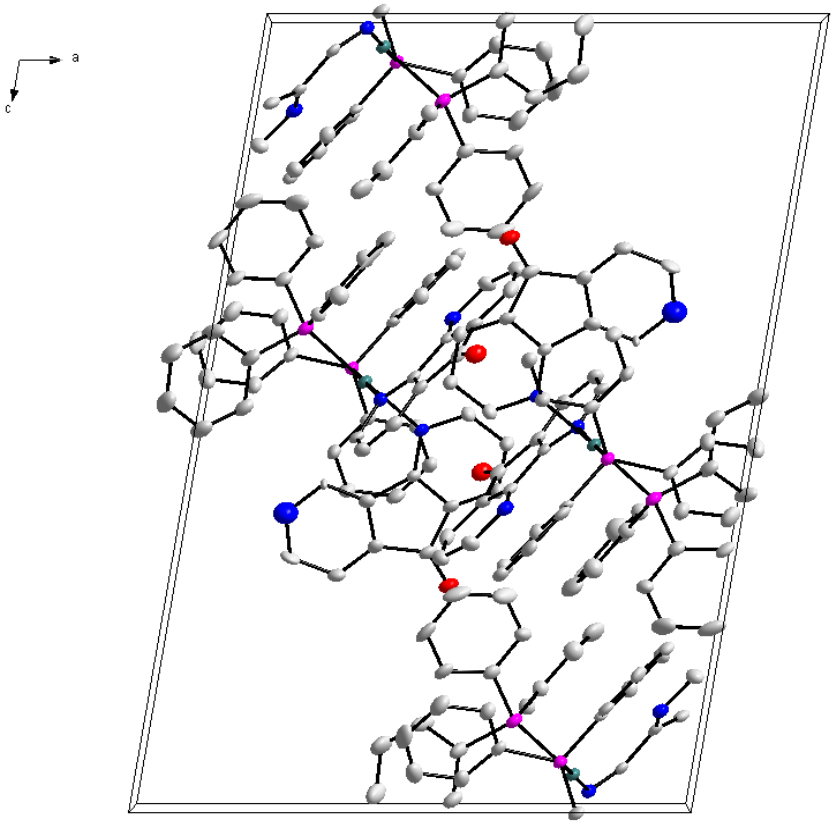

Figure 4.5: Diamond representation of *cis*-[Pd(PPh$_3$)$_2$(Daf)$_2$], at 50 % probability level, displaying the packing in the unit cell along the b axis. The triflate counter ions and nitromethane solvate are omitted for clarity.

The coordination mode demonstrated by the Daf ligand has been reported previously for palladium(II) centers[17]. A comparison of the bond distances and angles of the published structure is indicated in Table 4.4. The bond lengths between the palladium and coordinating nitrogens in (**1**) of 2.13 Å are slightly shorter than those that have reported complex which has bond lengths of 2.16 Å. The distances of 3.11 Å and 3.22 Å between the uncoordinated nitrogen atoms of (**1**) and the palladium center are significantly longer than for the reported complex, in which has a length of 3.07 Å. This could be as a result of the large steric demands of the triphenylphosphine ligands which are absent in the Pd(Daf)(nq)$_2$ complex. The palladium-phosphorus and palladium-nitrogen bonds are comparable to those of similar complexes found in literature[18].

Table 4.4: Comparison of bond lengths between $[Pd(Daf)(nq)_2]$[19] and $[Pd(PPh_3)_2(Daf)_2]$.

$[Pd(Daf)(nq)_2]$		$[Pd(PPh_3)_2(Daf)_2]$			
Pd(1)- N(1A)	2.1646(6)	Pd(1)-N(1)	2.136(5)	Pd(1)-N(4)	2.131(5)
Pd(1)-N(2A)*	3.070(5)	Pd(1)-N(2)*	3.2248(2)	Pd(1)-N(3)*	3.1113(2)
* = non-coordinating nitrogen interactions lengths					

4.4 Crystal Structure of *cis*-$[Pd_2BpymCl_4]$.DMF

Red crystals of the compound were obtained according to the procedure described in Section 3.3.6. The compound crystallized in a monoclinic C2/m space group with two palladium dinuclear complexes and a DMF solvate per unit cell. The graphical representation of the numbering and packing are illustrated in Figure 4.6 and Figure 4.7 respectively. The DMF molecule has a 25% disorder, which is omitted for clarity. Selected bond lengths and angles are represented in Table 4.5 and Table 4.6. Hydrogen bonding is illustrated in Figure 4.8 and described in Table 4.7. Atomic coordinates, anisotropic displacement parameters, all bond distances and angles are given in Appendix A. Bpym refers to 2,2'-bipyrimidine.

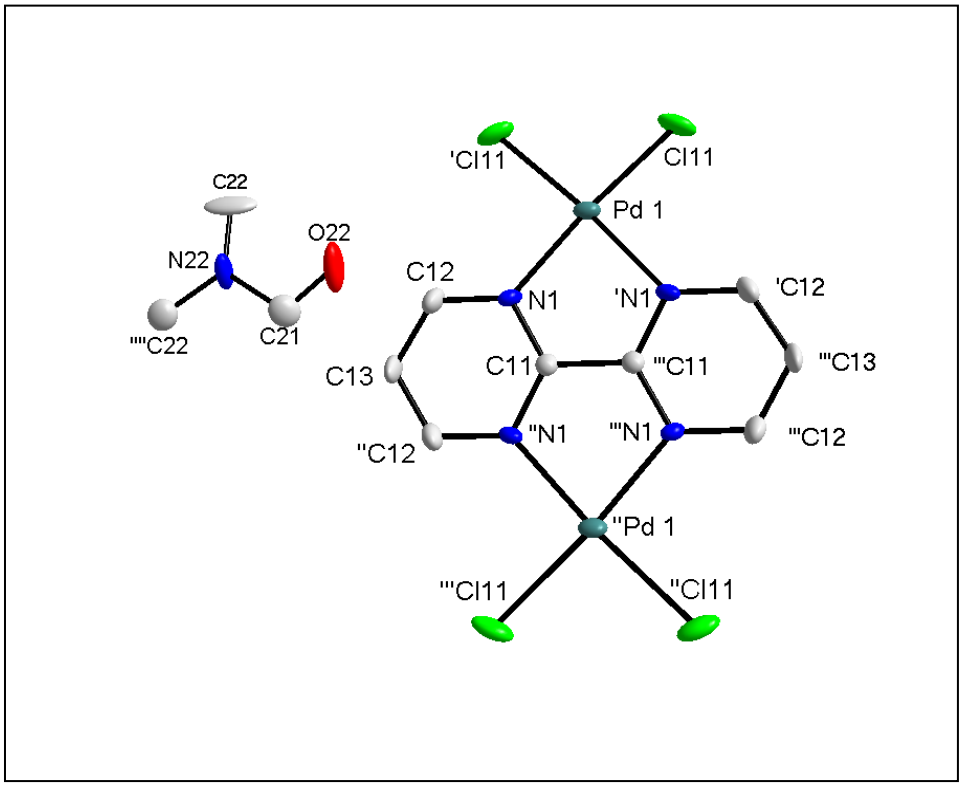

Figure 4.6: Diamond representation of *cis*-[Pd$_2$BpymCl$_4$].DMF, at 50 % probability level, displaying the numbering scheme employed. The disorder on the solvent DMF molecule and the hydrogen atoms are omitted for clarity. Symmetry operations used ' x, 2-y, z, '' –x, y, 1-z, ''' –x, 2-y, 1-z, '''' x, 1-y, z.

The molecular structure of *cis*-[Pd$_2$BpymCl$_4$].DMF (**2**) consists of two palladium(II) centers which are linked by a bpym ligand. The complex is neutral as the four chlorido ligands compensate for the charge on the metals. Both palladium atoms lie on a special position (two fold rotation axis) and two carbon atoms, namely C11 and C13, lie on a mirror plane. The nitrogen and oxygen atoms from the solvent are also on special positions which make the solving of the solvent molecule extremely difficult. As a result of the symmetry in the molecule there are only twelve atoms, including the hydrogen atoms, in the asymmetric unit. The rest of the structure is generated by the two fold rotation axis and a mirror plane.

The geometry of the palladium centers is slightly distorted from the square planar geometry. This is illustrated by the N(1)-Pd(01)-'N(1) and Cl(11)-Pd(01)-'Cl(11) angles which are 81.8° and 91.6° respectively. The square planar nature of the palladium metal centers results in the formation of an almost completely flat molecule. Figure 4.7 illustrates the packing of (**2**) in the centrosymmetric space group. Parts of five different molecules form part of the unit cell. The molecules in the center of the unit cell stack on top of each other with an inter-molecular distance of 3.37 Å.

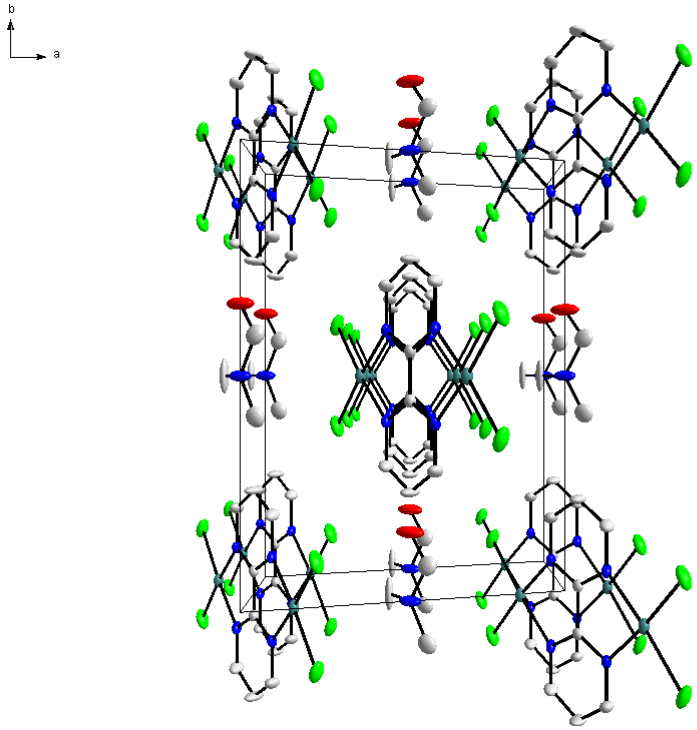

Figure 4.7: Diamond representation of *cis*-[Pd_2BpymCl$_4$].DMF, at 50 % probability level, displaying the packing in the unit cell along the c axis. The disorder on the solvent DMF molecule and the hydrogen atoms are omitted for clarity.

Table 4.5: Bond Lengths for *cis*-[Pd_2BpymCl$_4$].DMF.

Atoms	Bond lengths (Å)	Atoms	Bond lengths (Å)
C(11)-N(1)	1.334(5)	N(22)-C(21)	1.46 (2)
C(12)-N(1)	1.335(6)	O(22)-C(21)	1.26(4)
C(12)-C(13)	1.362(6)	C(21)-C(22)	1.380(4)
N(1)-Pd(1)	2.056(4)	Pd(1)-Pd(1)#3	5.468(1)
Cl(11)-Pd(1)	2.267(1)	Pd(1)-Pd(1)#6	3.373(1)
N(22)-C(22)	1.42(2)		
Symmetry transformations used to generate equivalent atoms: #3 -x, 2-y, z; #6 0.5-x, -0.5+y, 2-z.			

Table 4.6: Bond Angles for *cis*-[Pd_2BpymCl$_4$].DMF

Atoms	Bond angles (°)	Atoms	Bond angles (°)
N(1)#1-C(11)-N(1)	124.8(6)	C(12)-N(1)-Pd(1)	131.2(3)
N(1)#1-C(11)-C(11)#2	117.6(3)	N(1)-Pd(01)-N(1)#3	81.8(2)
N(1)-C(12)-C(13)	120.5(5)	N(1)-Pd(01)-Cl(11)	175.0(1)
C(12)-C(13)-C(12)#1	119.5(6)	N(1)#3-Pd(01)-Cl(11)	93.3(2)
C(11)-N(1)-C(12)	117.4(4)	Cl(11)-Pd(01)-Cl(11)#3	91.6(1)
C(11)-N(1)-Pd(1)	111.3(3)		
Symmetry transformations used to generate equivalent atoms: #1 -x, y, -z+1 #2 -x, -y+2, -z+1 #3 x, -y+2, z			

Figure 4.8 illustrates the hydrogen bonding for (**2**). The hydrogen atoms found on C12 interact with the chlorine atoms found on the palladium center and with the oxygen atom of the solvate molecule. No visible distortions are present as a result of these interactions as the molecule is symmetrical. The hydrogen bond properties are displayed in Figure 4.8 and are summarized in Table 4.7.

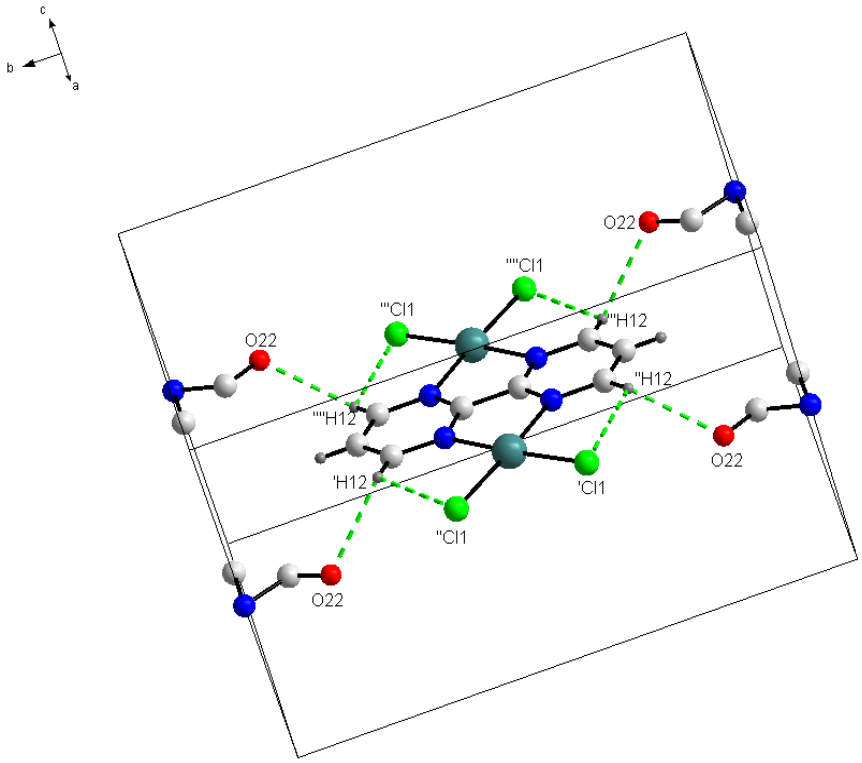

Figure 4.8: Diamond representation of the hydrogen bonding in the *cis*-[Pd_2BpymCl$_4$]·DMF molecule, at 50 % probability level. The disorder on the DMF solvent molecule and hydrogen atoms not involved in hydrogen bonding have been omitted. Symmetry operations used ' 0.5-x, 1.5-y, 1-z, '' 0.5 –x, -0.5+y, 1-z, ''' 0.5+x, -0.5+y, z, '''' 0.5+x, 1.5-y, z.

Table 4.7: Hydrogen bonds for *cis*-[Pd_2BpymCl$_4$].DMF

D-H...A	d(D-H)	d(H...A)	d(D...A)	<(DHA)
C(12)-H(12)...O(22)	0.93	2.56	3.116(9)	118.7
C(12)-H(12)...Cl(11)#3	0.93	2.79	3.313(6)	116.5
Symmetry transformations used to generate equivalent atoms: #3 x, -y+2, z				

The bond lengths and angles for (**2**) are comparable to those in literature[20,21]. The palladium-nitrogen bonds of 2.05 Å are slightly longer than the mono-coordinated palladium complex[22] which has a bond length of 1.99 Å. The palladium-palladium intra-molecular bond distances of 5.47 Å, is slightly shorter than the 5.62 Å for the platinum counterpart[23]. A comparison of these bond lengths is shown in Table 4.8.

Table 4.8: Comparison between $[Pd_2BpymCl_4]$, $[Pdbpym(NO_3)_2]$[22], $[PdBpymRu(Bipy)_2]$[24] and $[Pt_2Bpym(en)_2]$[23].

Compound	$[Pd_2BpymCl_4]$	$[PdBpymCl_2]$	$[PdBpymRu(Bipy)_2]$	$[Pt_2Bpym(en)_2]$
Pd-Cl	2.2673(13)	----------	----------	----------
Pd-N	2.056(4)	1.990(4)	2.0494(93)	----------
Pd-Pd/ Pd-Ru/ Pt-Pt*	5.4681(3)	----------	5.6199(45)	5.534
* Intra-molecular distance				

4.5 Crystal structure of *cis*-$[Pd(PPh_3)_2(NO_3)_2].CO(CH_3)_2$

Yellow crystals of *cis*-$[Pd(PPh_3)_2(NO_3)_2].CO(CH_3)_2$ were obtained as described in Section 3.3.13. The compound crystallized in a monoclinic C2/c space group with four molecules in the unit cell and an acetone solvate. The acetone solvate molecule lies on a special position (mirror) and consequently has a problematic disorder. The disorder is omitted from figures for clarity. The compound orientation and numbering is illustrated in Figure 4.9, while selected bond lengths, bond angles and hydrogen bonding are reported in Table 4.9, 4.10 and 4.11 respectively. Atomic coordinates, anisotropic displacement parameters, all bond distances, angles and torsion angles are given in Appendix A. The abbreviation dppe and dppm are used for 1,2-bis(diphenylphosphino)ethane and 1,2-bis(diphenylphosphino)methane respectively.

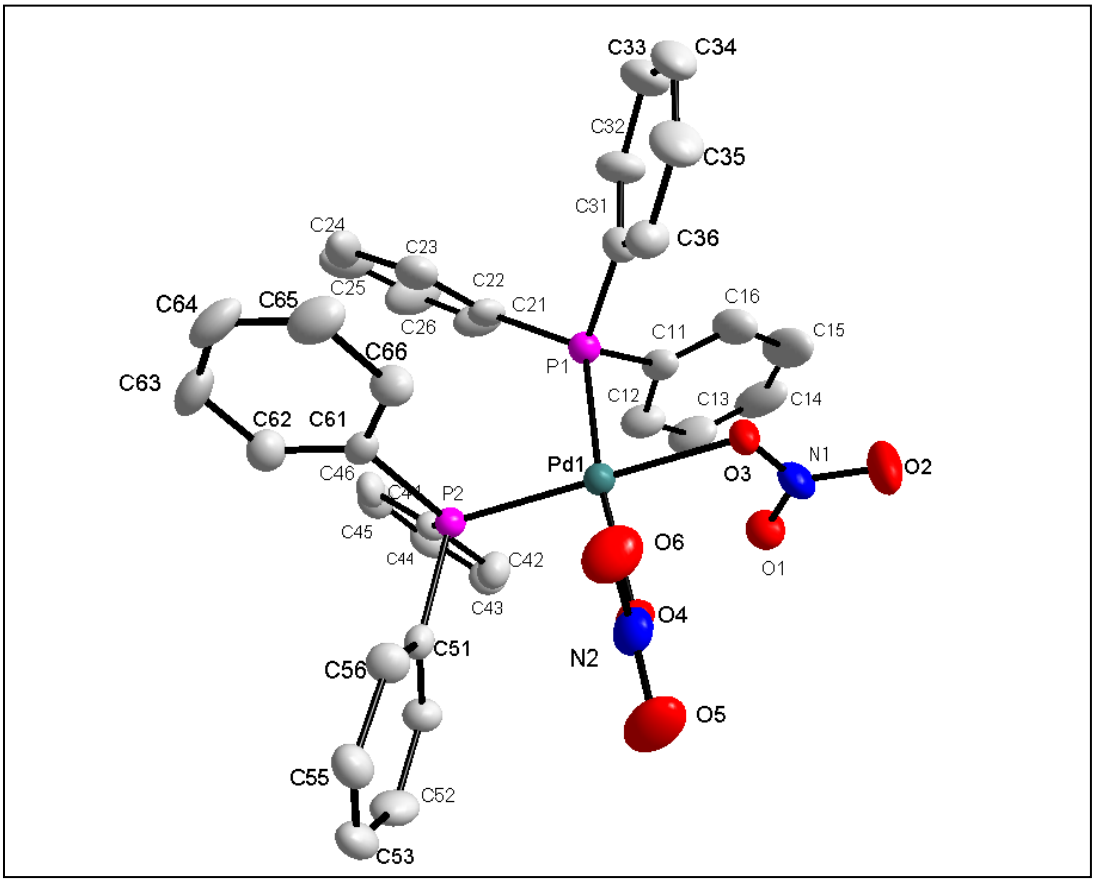

Figure 4.9: Diamond representation of the *cis*-$[Pd(PPh_3)_2(NO_3)_2].CO(CH_3)_2$ molecule, at 30 % probability level, displaying the numbering scheme employed: the first digit represents the ring and the second digit the number of the atom in the ring. The disordered acetone solvate and hydrogen atoms have been omitted for clarity.

The title compound consists of a palladium(II) center to which two phosphorous and two nitrogen atoms have bonded in a distorted square planar orientation. The two phosphine and nitrate ligands are bonded to the palladium in a *cis* fashion. The palladium has a distorted square planar bonding mode, which is illustrated by the O(3)-Pd(1)-P(1) and P(2)-Pd(1)-P(1) bond angles being 85.7 and 96.6 respectively. A plane was constructed between the two phosphorous atoms and the palladium atoms in Figure 4.10. O3 and O4 deviate from the plane by approximately 0.15 Å and 0.25 Å respectively. O4 might be more distorted from the plane as a result of H64 having a hydrogen interaction with N1 which is absent for N2. Figure 4.11 and Table 4.11 more clearly illustrate the hydrogen bonding which is present in the compound.

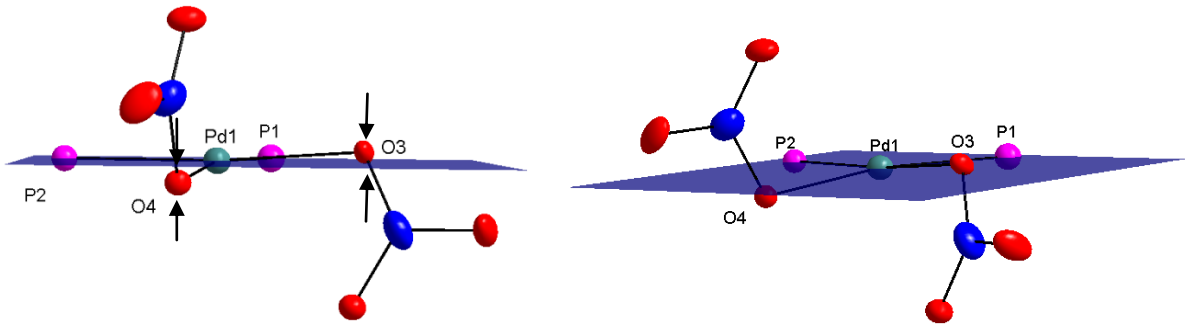

Figure 4.10a and b: Different viewing angles Diamond representation of the *cis*-$[Pd(PPh_3)_2(NO_3)_2.CO(CH_3)_2$ molecule, at 20 % probability level, displaying the deviation from the plane by the nitrate oxygen atoms. The phenyl rings and disordered acetone solvent molecule have been omitted for clarity.

Table 4.9: Selected bond lengths for *cis*-$[Pd(PPh_3)_2(NO_3)_2].CO(CH_3)_2$

Atoms	Bond lengths (Å)	Atoms	Bond length (Å)
P(1)-Pd(1)	2.2761(19)	C(21)-P(1)	1.816(7)
P(2)-Pd(1)	2.2491(18)	C(31)-P(1)	1.813(7)
O(3)-Pd(1)	2.131(5)	N(2)-O(4)	1.281(8)
O(4)-Pd(1)	2.110(5)	N(1)-O(2)	1.247(8)
C(11)-P(1)	1.834(8)	N(1)-O(3)	1.238(8)
C(51)-P(2)	1.829(7)	N(2)-O(5)	1.233(8)
C(61)-P(2)	1.822(7)	N(1)-O(1)	1.218(8)
C(41)-P(2)	1.821(7)	N(2)-O(6)	1.212(8)

Table 4.10: Selected Bond Angles for *cis*-$[Pd(PPh_3)_2(NO_3)_2].CO(CH_3)_2$

Atoms	Bond angles (°)	Atoms	Bond angles (°)
P(2)-Pd(1)-P(1)	96.63(7)	C(52)-C(51)-P(2)	122.4(5)
O(6)-N(2)-O(5)	123.4(7)	C(51)-P(2)-Pd(1)	114.2(2)
O(6)-N(2)-O(4)	119.4(7)	C(46)-C(41)-P(2)	127.9(6)
O(5)-N(2)-O(4)	117.2(7)	C(42)-C(41)-P(2)	113.0(5)
O(4)-Pd(1)-P(2)	89.83(14)	C(41)-P(2)-Pd(1)	110.0(2)
O(4)-Pd(1)-P(1)	170.53(14)	C(41)-P(2)-C(61)	112.4(3)
O(4)-Pd(1)-O(3)	88.36(19)	C(41)-P(2)-C(51)	105.4(3)
O(3)-Pd(1)-P(2)	175.27(13)	C(36)-C(31)-P(1)	122.8(6)
O(3)-Pd(1)-P(1)	85.72(15)	C(32)-C(31)-P(1)	118.0(6)
O(3)-N(1)-O(2)	117.8(6)	C(31)-P(1)-Pd(1)	111.6(3)
O(1)-N(1)-O(3)	122.5(7)	C(31)-P(1)-C(21)	101.7(3)
O(1)-N(1)-O(2)	119.6(7)	C(31)-P(1)-C(11)	107.9(4)
N(2)-O(4)-Pd(1)	113.2(4)	C(26)-C(21)-P(1)	119.3(6)
N(1)-O(3)-Pd(1)	113.5(4)	C(22)-C(21)-P(1)	123.7(7)
C(66)-C(61)-P(2)	117.2(6)	C(21)-P(1)-Pd(1)	125.1(2)
C(62)-C(61)-P(2)	123.2(6)	C(21)-P(1)-C(11)	106.7(4)
C(61)-P(2)-Pd(1)	112.9(2)	C(16)-C(11)-P(1)	120.3(7)
C(61)-P(2)-C(51)	101.5(3)	C(12)-C(11)-P(1)	119.7(7)
C(56)-C(51)-P(2)	118.6(5)	C(11)-P(1)-Pd(1)	102.9(2)

There are three different prominent groups of hydrogen bond interactions. The hydrogen atoms H63 and H64 of ring six interact with two of the oxygens of both the nitrate ions. There is also an interaction between the H56 and O6. O6 does not interact with the hydrogen atoms on ring six and no visible distortions are present as a result of the hydrogen bond interactions.

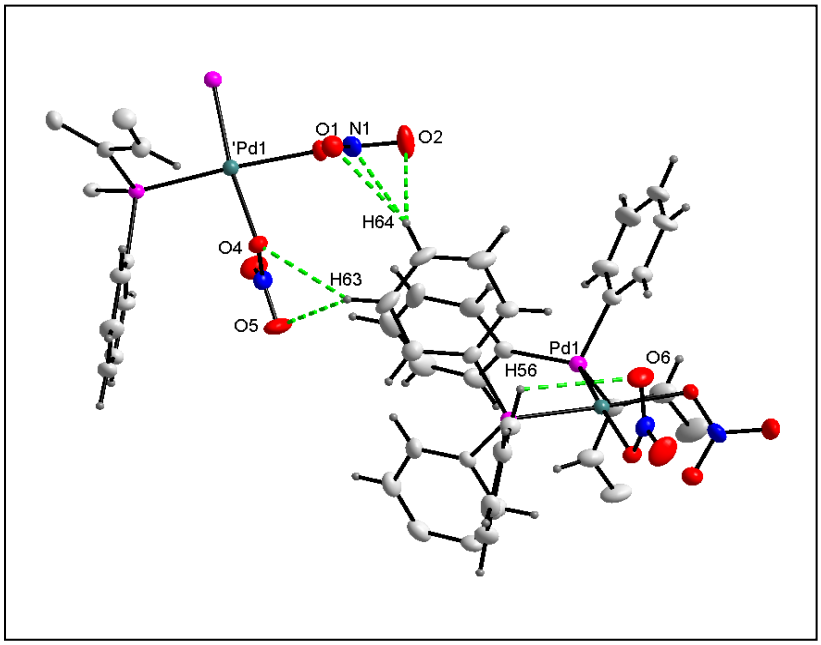

Figure 4.11: Diamond representation of the hydrogen bonding in the *cis*-$[Pd(PPh_3)_2(NO_3)_2].CO(CH_3)_2$ molecule, at 50 % probability level. The disordered acetone solvent molecule has been omitted. ' x, -y, z+1/2.

Table 4.11: Selected hydrogen bonds in *cis*-$[Pd(PPh_3)_2(NO_3)_2].CO(CH_3)_2$

D-H...A	d(D-H)	d(H...A)	d(D...A)	<(DHA)
C(56)-H(56)...O(6)	0.93	2.89	3.321(11)	109.9
C(23)-H(23)...O(1)#1	0.93	2.84	3.646(13)	145.2
C(23)-H(23)...O(2)#1	0.93	2.98	3.816(15)	150.3
C(63)-H(63)...O(4)#2	0.93	2.8	3.507(10)	133.5
C(63)-H(63)...O(5)#2	0.93	2.6	3.156(12)	119.1
C(64)-H(64)...N(1)#2	0.93	2.9	3.533(11)	126.5
C(64)-H(64)...O(1)#2	0.93	2.62	3.431(10)	146.5
C(64)-H(64)...O(2)#2	0.93	2.84	3.360(11)	116.7
Symmetry transformations used to generate equivalent atoms: #1 x, -y+1, z+1/2, #2 x, -y, z+1/2				

A comparison of the palladium phosphor and palladium-oxygen bonds to similar structures in literature[25,26] has been made in Table 4.12. It is clear that the palladium-oxygen bond lengths are all approximately 2.1 Å with no major deviations. The palladium-phosphor bonds of 2.25 and 2.28 Å for (**3**) are slightly longer than those that have been reported. From Figure 4.9 one is able to deduce a trend. One palladium phosphor and one palladium-oxygen bond are slightly longer than their counterparts.

Table 4.12: Comparison between the bond lengths of $[Pd(PPh_3)_2(NO_3)_2]$, $[Pd(dppm)(NO_3)_2]$[25] and $[Pd(PPh_3)_2(NO_3)_2]$[26].

Compound	$[Pd(PPh_3)_2(NO_3)_2]$	$[Pd(dppe)(NO_3)_2]$	$[Pd(dppm)(NO_3)_2]$
Pd – P1	2.25(2)	2.2148(8)	2.2241(8)
Pd – P2	2.287(2)	2.224(1)	2.2345(7)
Pd – O1	2.110(5)	2.103(2)	2.103(2)
Pd – O2	2.131(5)	2.114(2)	2.130(2)

4.6 Correlations between palladium(II) structures

Not many correlations can be drawn between the three crystals that have been discussed in the previous sections; however similar complexes to which these can be compared have been reported in literature.

Compound (**1**) has two bidentate Daf ligands, which are mono-coordinated to the palladium metal center. This coordination mode has been previously reported by Klein[17]. The complex reported however is not a square planar complex, it has trigonal geometry with one Daf and two quinone ligands. This makes the comparison of bond angles obsolete. The reported palladium-nitrogen bond lengths of 2.16 Å are slightly longer in (**3**), whereas the uncoordinated palladium-nitrogen bond lengths are slightly shorter. Table 4.13 shows a comparison between the crystallographic data, bond distances and bond angles $[Pd(PPh_3)_2(Daf)_2]$ and $[Pd(PPh_3)_2(NA)_2]$[18] (NA = nicotinamide).

Table 4.13: Comparison of the crystallographic data, bond distances and bond angles of *cis*-$[Pd(PPh_3)_2(Daf)_2]$ and *cis*-$[Pd(PPh_3)_2(NA)_2]$[18].

Compound	$[Pd(PPh_3)_2(Daf)_2]$	$[Pd(PPh_3)_2(NA)_2]$
Crystal system	Monoclinic	Triclinic
Space group	P2/n	$P\bar{1}$
a (Å)	15.1843(10)	12.4775(7)
b (Å)	17.1115(12)	12.870 75(5)
c (Å)	22.2575(14)	17.5888(6)
α(°)	90	71.835(2)
β(°)	99.676(4)	88.993(3)
γ(°)	90	86.174(3)
Volume $(Å)^3$	5700.8(7)	2677.9(2)
Z	4	2
ρ_{calc} (g cm^{-3})	1.559	1.527
Bond Lengths (Å)		
P(2)-Pd(1)	2.323(2)	2.322(3)
P(1)-Pd(1)	2.302(2)	2.297(3)
N(1)-Pd(1)	2.136(5)	2.082(8)
N(4)-Pd(1)	2.131(5)	2.128(4)
Bond Angles (°)		
N(1)-Pd-N(2)	86.45(19)	84.7(3)
N(1)-Pd-P(1)	88.84(14)	92.1(2)
N(2)-Pd-P(2)	89.44(14)	89.1(3)
P(1)-Pd-P(2)	95.30(6)	94.1(1)
N(1)-Pd-P(2)	175.41(14)	176.7(3)
N(2)-Pd-P(1)	175.19(14)	173.8(2)

There are very little differences in the bond lengths and no significant differences in bond angles. The larger N-Pd-P bond angles for $[Pd(PPh_3)_2(NA)_2]$ is probably due to the different steric demands of the amine ligands and the interaction of the Me_2CO with its triflate counter ions. All the bond lengths of $[Pd(PPh_3)_2(Daf)_2]$ are longer than the reported structure. This is probably due to the pseudo octahedral geometry displayed in the complex, which results in the donation of electron density to the palladium center from the non-coordinating nitrogen atoms.

This reduces the back bonding for the coordinating nitrogen and phosphorus atoms and results in longer bond lengths.

There are no bridged palladium counter parts in the Cambridge Structural Database for compound (**2**). There is, however a platinum complex to which the palladium-nitrogen coordination and the intra-metal distances can be correlated[23]. These bonds are also comparable to the non-bridged palladium compound; [Pd(bpym)$(NO_3)_2$].

Table 4.14: Comparison between the crystal data, bond distances and bond angles of *cis*-[Pd_2bpymCl_4], [Pt_2bpym$(CH_3)_8$][23] and [Pd(bpym)$(NO_3)_2$][22].

Compound	[Pd_2bpymCl_4]	[Pt_2bpym$(CH_3)_8$]	[Pd(bpym)$(NO_3)_2$]
Crystal system	Monoclinic	Orthorhombic	Triclinic
Space group	C2/m	*Pbca*	$P\bar{1}$
a (Å)	10.7299(6)	12.830(2),	7.605(5)
b (Å)	14.2399(7)	11.502(2)	8.791(4)
c (Å)	5.9381(3)	12.877(2)	12.632(5)
α(°)	90	90	85.11(3)
β(°)	108.229(2)	90	78.79(4)
γ(°)	90	90	77.45(4)
Volume $(Å)^3$	861.76(8)	1900.3(5)	807.7(7)
Z	2	4	2
ρ_{calc} (g cm^{-3})	1.868	2.337	1.84
Bond Lengths (Å)			
Pd-N/ Pt-N	2.056(4)	2.149	1.990(4)
Pd-Pd/ Pt-Pt	5.468(3)	5.534	----------
Bond Angles (°)			
N(1)-Pd(1)-N(2)	81.8(2)	77.2(3)	81.0(2)
C(11)-N(1)-Pd(1)	111.3(3)	114.73	114.51
C(12)-N(1)-Pd(1)	131.2(3)	129.75	128.12

The comparison of bond lengths shows that the Pd-N bond (2.06 Å) is slightly shorter than the Pt-N bond (2.15 Å). This is probably due to the difference in the size between the platinum and palladium. The Pd-N bond (1.99 Å) where the palladium is coordinated to one side of the

bridging ligand is only slightly shorter than for the bridged complex. There are only subtle differences in bond angles. The bond angle between the N(1)-Pd(1)-N(2) of 77.2° in the platinum complex is slightly less than for the other two compounds. This is probably due to the larger intra-molecular distance of the platinum molecules.

The crystal structure of compound (**3**) also crystallized with two triphenylphosphine ligands coordinated *cis* to each other and two nitrate anions coordinated opposite the phosphine ligands. A comparison of crystallographic data, bond lengths and angles between (**3**) and similar reported structures[25,26] is shown in Table 4.15.

All three compounds crystallized in the monoclinic crystal system with four molecules in the unit cell. The bond lengths for the three compared structures correlate well and there are no significant differences in bond lengths. The bond angles are also very similar with two exceptions. The P(2)-Pd(1)-P(1) angle of 72.5°, for [Pd(dppm)(NO_3)$_2$], is smaller than for the other two compounds which have angles of 96.6° and 98.7°. This is as a result of smaller bite angle for phosphine ligand. The O(4)-Pd(1)-P(2) angle is skewed in the same way.

Table 4.15: Comparison between the crystallographic data, bond distances and bond angles of $[Pd(PPh_3)_2(NO_3)_2]$, $[Pd(dppm)(NO_3)_2]$[25] and $[Pd(PPh_3)_2(NO_3)_2]$[26].

Compound	$[Pd(PPh_3)_2(NO_3)_2]$	$[Pd(dppm)(NO_3)_2]$	$[Pd(dppe)(NO_3)_2]$
Crystal system	Monoclinic	Monoclinic	Monoclinic
Space group	C2/c	*P21/c*	Cc
a (Å)	40.343(2)	13.9841 (2)	10.383 (5)
b (Å)	9.7490(4)	16.8118(2) ,4,	15.442 (5)
c (Å)	19.7802(10)	16.8033 (2)	16.278 (5)
α(°)	90	90	90
β(°)	115.5140(10)	93.858 (1)	101.135 (16)
γ(°)	90	90	90
Volume (Å)	7021.0(6)	3941.47 (9)	2560.7 (16)
Z	4	4	4
ρ_{calc} (g.cm^{-3})	1.420	1.645	1.631
Bond Lengths (Å)			
P(1)-Pd(1)	2.249(2)	2.224(1)	2.215(1)
P(2)-Pd(1)	2.276(2)	2.235(1)	2.224(1)
O(3)-Pd(1)	2.110(5)	2.103(2)	2.103(2)
O(4)-Pd(1)	2.131(5)	2.130(2)	2.114(2)
Bond Angles (°)			
P(2)-Pd(1)-P(1)	96.63(7)	72.52(3)	98.66 (6)
O(4)-Pd(1)-P(2)	89.83(14)	104.72 (6)	90.02 (6)
O(4)-Pd(1)-P(1)	170.53(14)	169.78(7)	171.82 (5)
O(4)-Pd(1)-O(3)	88.36(19)	85.26 (9)	86.94 (7)
O(3)-Pd(1)-P(2)	175.27(13)	177.04(6)	175.42 (6)
O(3)-Pd(1)-P(1)	85.72(15)	97.54 (7)	84.73 (3)

4.7 Conclusions

In this chapter, three compounds were successfully characterized by single crystal X-ray diffraction. The crystal structures of *cis*-$[Pd(PPh_3)_2(Daf)_2].(Trif)_2.CH_3NO_2$, *cis*-$[Pd_2BpymCl_4].DMF$ and *cis*-$[Pd(PPh_3)_2(NO_3)_2].CO(CH_3)_2$ were discussed and compared to similar complexes in literature.

Important information on the orientation of the Daf ligands in the crystal structure of *cis*-$[Pd(PPh_3)_2(Daf)_2].(Trif)_2.CH_3NO_2$ were obtained. Prior to crystal data collection of the crystals it was believed that the ligands would bond in a bidentate manner to the palladium(II) center. The coordination of the Daf ligands in a monodentate fashion resulted in the formation of a pseudo octahedral geometry which was discussed earlier. This was interesting because the palladium(II) species is known for forming square planar structures. The interaction between the un-coordinating ligands with axial orbitals was confirmed as the bond lengths between the phosphine ligands and nitrogen atoms were longer than counterparts in literature; this is indicative of less back bonding.

X-ray diffraction was used in addition to NMR and IR to characterize the bridged palladium complex; *cis*-$[Pd_2BpymCl_4].DMF$. One of the aims of this project was to co-crystallize planar molecules with inorganic supports. Investigation of the crystal structure of this compound confirmed the planarity of the compound, which could not be verified by NMR. The crystal structure also confirmed that palladium atoms attached to both sides of the bridging ligand. The structure could be correlated to similar complexes in literature.

The crystal structure of *cis*-$[Pd(PPh_3)_2(NO_3)_2].CO(CH_3)_2$ was used to deduce valuable information about the coordination properties of bpym. The crystal of this compound was obtained in an attempt to synthesize a bridged compound similar to the *cis*-$[Pd_2BpymCl_4].DMF$ crystals where the chlorido ions were substituted by four triphenylphosphine ligands. Unfortunately the addition of the phosphine ligands to the bridged palladium complex resulted in the loss of the bpym ligand and the formation of the of the dinitrato complex instead. This was probably as a result of the loss in bacisity of the bpym ligand when bridged which decreases its ability to form sigma bonds.

(1) Schwarzenbach, D. *Crystallography*; John Wiley: New York, **1996**.

(2) Glusker, J. *Crystal structure analysis for chemists and biologists*; VCH: New York, **1994**.

(3) De Graef, M. *Structure of materials: an introduction to crystallography, diffraction and symmetry*; Cambridge University Press: Cambridge, **2007**.

(4) Cullity, B. *Elements of X-ray diffraction*; 3rd ed.; Prentice Hall: Upper Saddle River NJ, 2001.

(5) Rossmann, M.; International Union of Crystallography. *Crystallography of biological macromolecules*; 1st ed.; Published for the International Union of Crystallography by Springer: Dordrecht; London, **2006**.

(6) Rhodes, G. *Crystallography made crystal clear: a guide for users of macromolecular models*; 2nd ed.; Academic Press: San Diego, **2000**.

(7) Muller, P. *Crystal structure refinement: a crystallographers guide to SHELXL*; Oxford University Press: Oxford; New York, **2006**.

(8) Oszlányi, G.; Suto, A. *Acta Crystallographica Section A: Foundations of Crystallography* **2004**, *60*, 134–141.

(9) *Bruker, APEX2 (Version 1.0-27), Bruker AXS Inc., Madison, Wisconsin, USA,* **2005**.

(10) *Bruker, COSMO, (Version 1.48), Bruker AXS Inc., Madison, Wisconsin, USA,* **2003**.

(11) *Bruker, SAINT-Plus (Version 7.12) (Including XPREP), Bruker AXS Inc., Madison, Wisconsin, USA,* **2004**.

(12) *Bruker, SADABS, (Version2004/1), Bruker AXS Inc., Madison, Wisconsin, USA,* **1998**.

(13) Altomare, A.; Burla, M. C.; Camalli, M.; Cascarano, G. L.; Giacovazzo, C.; Guagliardi, A.; Moliterni, A. G.; Polidori, G.; Spagna, R. *Journal of Applied Crystallography* **1999**, *32*, 115-119.

(14) Farrugia, L. J. *Journal of Applied Crystallography* **1999**, *32*, 837-838.

(15) M. Sheldrick, *SHELXL97, Program for Solving Crystal Structures, University of Göttigen, Germany,* **1997**.

(16) K. Brandenburg, *H. Putz, DIAMOND, Release 3.0c, Crystal Impact GbR, Bonn, Germany,* **2005**.

(17) Klein, A. *Inorganica Chimica Acta* **1997**, *264*, 269-278.

(18) Qin, Z.; Jennings, M. C.; Puddephatt, R. J. *Inorg. Chem.* **2001**, *40*, 6220-6228.

(19) Schnebeck, R.; Freisinger, E.; Lippert, B. *European Journal of Inorganic Chemistry* **2000**, 1193-1200.

(20) Maekawa, M.; Munkata, M.; Kuroda-Sowa, T.; Motokawa, M. *Analytical Sciences* **1994**, *10*, 977–978.

(21) Inagaki, A.; Yatsuda, S.; Edure, S.; Suzuki, A.; Takahashi, T.; Akita, M. *Inorg. Chem.* **2007**, *46*, 2432-2445.

(22) Hudgens, T.; Johnson, D.; Cordes, W.; Barclay, T.; Jeter, D. *Journal of Chemical Crystallography* **1997**, *27*, 247–250.

(23) Kawakami, D.; Yamashita, M.; Matsunaga, S.; Takaishi, S.; Kajiwara, T.; Miyasaka, H.; Sugiura, K.; Matsuzaki, H.; Okamoto, H.; Wakabayashi, Y.; Sawa, H. *Angew. Chem. Int. Ed.* **2006**, *45*, 7214-7217.

(24) Bridgewater, J. *Inorganica Chimica Acta* **1993**, *208*, 179-188.

(25) Adrian, R. A.; Zhu, S.; Daniels, L. M.; Tiekink, E. R. T.; Walmsley, J. A. *Acta Crystallogr E Struct Rep Online* **2006**, *62*, m1422-m1424.

(26) Rath, N. P.; Stockland, R. A.; Anderson, G. K. *Acta Crystallogr C Cryst Struct Commun*. **1999**, *55*, 494-496.

5 Preliminary Catalytic Evaluation of Selected Platinum and Palladium Compounds

5.1 Introduction

The importance of catalysis and catalyst development has already been highlighted in Chapter 2. Palladium shows the best catalytic properties of the platinum group metals[1], particularly in carbon-carbon bond formation reactions such as the Heck, Suzuki, Sonogashira, Stille, Negishi, and Kumada coupling reactions[2]. One of the aims of this project was to synthesize bridged metallic complexes, consequently it was decided to evaluate the catalytic capabilities of *cis*-[$Pd_2BpymCl_4$]. Preliminary investigations were performed for Heck coupling and the Wacker oxidation reaction.

5.1.1 Heck Coupling

The Heck reaction uses palladium as a catalyst and forms carbon-carbon bonds between an alkyl, aryl or vinyl group and an alkene. The palladium complex acts as the coupling species which is generated by a halide which ultimately adds to the olefin substrate. In a classical reaction a palladium salt is stabilized by a ligand like triphenylphosphine and regenerated by a variety of bases like triethylamine or potassium carbonate. The typical catalytic cycle of a Heck reaction can be defined by the following four steps[3] (Scheme 5.1).

1. Formation of an arylpalladium complex by means of oxidative addition.
2. Addition of the complex to the alkene.
3. β-elimination reaction from complex, releasing the substituted alkene.
4. Regeneration of the palladium(0) complex by the utilized base.

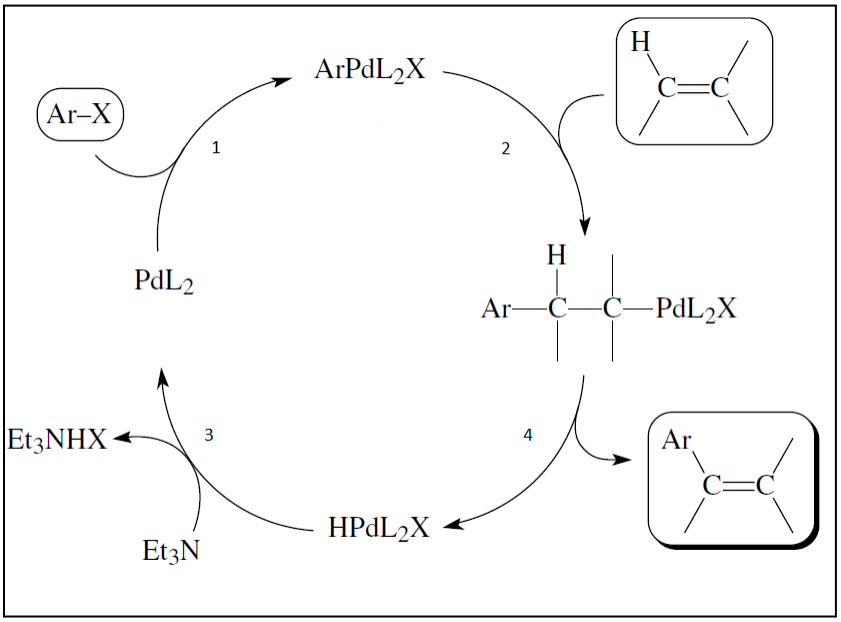

Scheme 5.1: The typical catalytic cycle for the Heck reaction

Triphenylphosphine is not the only ligand that has been used to stabilize the palladium metal center, in the catalytic process, various nitrogen based ligands have been investigated to perform the same function[4,5,6,7,8].

5.1.2 Wacker Oxidation

In the Wacker oxidation process, a terminal alkene is converted to an aldehyde by palladium(II), which is reduced to palladium(0). In order for the reaction to proceed a stoichiometric amount of copper(I) chloride is introduced into to the system. The copper reoxidizes the palladium(0) to palladium(II) so the catalytical process can continue. The copper is reoxidized to copper(II) by air. The three major steps in a typical catalytic cycle are represented in Scheme 5.2[1].

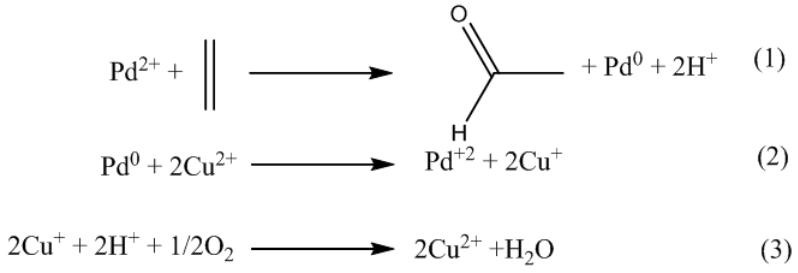

Scheme 5.2: Catalytic cycle for the Wacker Oxidation reaction with ethene as an example.

5.2 Experimental procedures for preliminary catalytic testing

5.2.1 Experimental Procedure for the Heck Coupling

Bromobenzene (0.79g, 5.0 $x10^{-3}$ mol), methyl acrylate (0.602 g, 7.06 $x10^{-3}$ mol), Et_3N (0.607 g, $6.0x10^{-3}$ mol) and $Pd_2BpymCl_4$ (0.051 g, $1.0x10^{-4}$ mol) was placed in DMF (50 ml). The reaction mixture was stirred at 120° C and analyzed by GC. After two days an excess of H_2O was added and the organic phase extracted with dichloromethane and dried of anhydrous magnesium sulphate.

5.2.2 Experimental Procedure for the Wacker Oxidation

In a reaction flask DMF (20 ml), H_20 (2ml), [$Pd_2BpymCl_4$] (0.045 g, 8.8 $x10^{-5}$ mol) and CuCl (0.882 g, 8.9 $x10^{-3}$ mol) was heated to 80°C. 1-Octene (1.0 g, 8.9 $x10^{-3}$ mol) in DMF (5ml) was added drop wise over 30 minutes. From half way through the addition of the substrate molecular oxygen (balloon) was bubbled through the solution. The reaction progress was monitored by GC.

5.3 Results and discussion

The Heck reaction was performed at different temperatures and the base used for the reoxidation of the palladium(0) to palladium(II) was varied. Sodium acetate and potassium carbonate were utilized as alternative bases. The temperature was also varied between 80 and 140°C. All the reactions where characterized by a rapid formation of palladium(0) at temperatures above 60°C.

The reactions were still continued according to the above mentioned procedure. Unfortunately NMR investigations into the products obtained indicated the absence of the two methene hydrogens which are formed as a result of the carbon-carbon bond formation reaction. This may be due to polymerization or catalyst deactivation. However, the above performed investigations were only preliminary. There are various combinations of solvents and bases mentioned in references 1-5 which were not investigated. The development of the optimum conditions for the selected compound was not allowed in the time scale of this project and hindered by infrastructural restraints.

The Wacker oxidation reaction is a homogenous process. However, when utilizing *cis*-[$Pd_2BpymCl_4$] the addition of water results in the precipitation of the palladium compound from the solution. At higher temperatures the solubility of the catalyst increases slightly but unfortunately this results in the liberation of the substrate which has a boiling point of 120°C. Initial GC investigations show the formation of the desired product, 2-octanone, but also the subsequent decrease of its concentration. The reason for this is unknown. Unfortunately the addition of water is vital to for the Wacker oxidation process, to proceed, so it cannot be eliminated from the reaction mixture to solve the solubility problems. In future investigations the chlorido ions may be replaced by BF_4^- or triphlate ions to increase the solubility of the compound. Benzoquinone should also be employed instead of oxygen as oxidant.

---

(1) Tsuji, J. *Palladium reagents and catalysts: new perspectives for the 21st century*; Wiley: Hoboken NJ, **2004**.

(2) Astruc, D. *Nanoparticles and catalysis*; Wiley-VCH: Weinheim, **2008**.

(3) Bhaduri, S. *Homogeneous catalysis mechanisms and industrial applications*; Wiley-Interscience,: New York :, **2000**.

(4) Pelagatti, P.; Carcelli, M.; Costa, M.; Ianelli, S.; Pelizzi, C.; Rogolino, D. *Journal of Molecular Catalysis. A, Chemical* **2005**, *226*, 107–110.

(5) Buchmeiser, M. R.; Schareina, T.; Kempe, R.; Wurst, K. *Journal of Organometallic Chemistry* **2001**, *634*, 39–46.

(6) Dodd, D.; Toews, H.; Carneiro, F.; Jennings, M.; Jones, N. *Inorganica Chimica Acta* **2006**, *359*, 2850-2858.

(7) Srinivas, P.; Likhar, P.; Maheswaran, H.; Sridhar, B.; Ravikumar, K.; Kantam, M. L. *Chem. Eur. J.* **2009**, *15*, 1578-1581.

(8) Eberhardt, J. K.; Fröhlich, R.; Würthwein, E. *J. Org. Chem.* **2003**, *68*, 6690-6694.

6 Critical Evaluation of the Study

6.1 Scientific relevance of the results obtained

The aim of the study was synthesize two dimensional square planar, Pt(II) and Pd(II) metal organic nano frameworks and bridged metallic complexes with a variety of bridging ligands, starting from simple synthons as building blocks. The non-bridging ligands would also be varied in order to change the electronic properties of the platinum(II) and palladium(II) metal centers. Crystalline supports such as titanium and tungsten oxide would also be synthesized. The optimum conditions for the crystallization of the compounds would then be determined in order to co-crystallize the complexes with the above mentioned supports, utilizing the principle of crystal engineering to selectively modify aspects that would change the solid state characteristics and properties of the compounds. The advantage of this process would be to exploit the fact that the metal organic frameworks would ensure that the metal atoms are optimally dispersed; a problem in many heterogeneous catalysts. Furthermore, the conjugated nature of the metal organic frameworks could also alter the electronic properties of the metal centers in such a way, as to modify the catalytic abilities of the metals. A further advantage of these types of systems would be the ability to characterize the above mentioned complexes by means of single X-ray diffraction and in so doing gain an understanding of the factors affecting these systems. With a good understanding of these co-crystals, one would in theory be able to engineer catalyst and support on a nano-scale basis.

The above mentioned aims of the study were perhaps slightly idealistic but due to the novelty of the research project, needed to be investigated in order to determine the advantages and disadvantages of the research area. Unfortunately not many of the aims of this study were completely attained. However, there are valid reasons for the lack of success:

1. The bridging ligands that were chosen namely, pyrazine, 4,4'-bipyridine and 2,2'-bipyrimidine, are some of the most rigid bridging ligands available. Originally the ligands were chosen for their rigidity to ensure that the metal organic frameworks, that were to be synthesized, would be of a two dimensional nature. This would promote the formation of a network, by the metal organic frameworks, on the surface of the supports in the co-crystallization process. This unfortunately, acted as a solution to one problem, but be the source of another. The rigidity of the ligands resulted in significant solubility problems to the extent that optimum crystallization techniques could not be developed. In these planar systems, π-π stacking is often present, which could also have contributed to solubility problems that were encountered.

2. Titanium and tungsten oxide were chosen as crystalline supports and although it is possible to synthesize these supports as crystalline species, the strict classification as catalysts 'supports' already per se makes further modification difficult. By definition, a heterogeneous catalyst support, should be insoluble and resistant to chemical and physical modifications. The prospect of synthesizing a crystalline support and then re-dissolving it, for co-crystallization, will not easily be accomplished.

As a result of the above mentioned factors crystals of the metal organic frameworks and co-crystals with the supports were not successfully obtained, even after many vigorous attempts. Although the aim of the study was not attained, three new scientifically interesting crystal structures, with potential as catalysts, were successfully obtained. The crystals structures were solved and compared to counterparts in literature. In one of the structures namely, *cis*-$[Pd(PPh_3)_2(Daf)_2].(Trif)_2.CH_3NO_2$ a pseudo octahedral in a d^8 metal species was a rare and novel observation. Two palladium centers were linked in the highly symmetric structure of *cis*-$[Pd_2BpymCl_4]$.DMF. The geometry the complex was almost completely flat, which was a positive result with regards to the aims of the project.

As the overarching aim the project was to develop new nano-supported catalysts, some kinetic testing to evaluate the above mentioned compounds was necessary. Preliminary catalytic testing was performed for the Heck coupling reaction and the Wacker oxidation process. Unfortunately these reactions needed further optimization for various different ligand systems. Preliminary investigations into these reactions were performed but no reportable results were obtained due to infrastructural restraints.

6.2 Future research

The use of metal organic frameworks and bridged metallic systems as tools to attach metal centers to catalyst supports, as mentioned in the previous section is a concept which should, and will be exploited further. Approaching it from a crystallographic point of view however, is challenging. In future research the following will be investigated.

- The introduction of less rigid substituents on the bridging ligands could be used to make the crystallization of the metal organic frameworks less problematic.
- Non-crystalline supports should be investigated, and catalytically active complexes can be attached through support-metal or support-ligand interactions.
- Different metal centers like silver and copper can be combined with platinum and palladium.
- Metal organic frameworks can be introduced into the solution from which the crystalline supports are synthesized so as to ‘trap’ the complexes in the crystalline materials.
- Intensive catalytic evaluation of complexes should be performed to observe and develop the catalytic capabilities of these systems. This will include the evaluation and study of basic reactions of importance in the specific catalytic systems to be utilized.
- Powder X-ray Diffraction and SEM will be used to further investigate the properties of the support and metal catalyst interactions.

Appendix A

cis-$[Pd(PPh_3)_2(Daf)_2].(Trif)_2.CH_3NO_2$

Table A.1: Atomic coordinates (x 10^4) and equivalent isotropic Atomic coordinates (x 10^4) and equivalent isotropic displacement parameters (A^2 x 10^3) for *cis*-$[Pd(PPh_3)_2(Daf)_2].(Trif)_2.CH_3NO_2$. U(eq) is defined as one third of the trace of the orthogonalized U^{ij} tensor.

	x	y	z	U(eq)
C(22A)	1795(11)	4690(8)	3754(8)	25(5)
C(23A)	2105(13)	5373(9)	3522(9)	67(7)
C(24A)	2584(12)	5310(10)	3053(8)	43(4)
C(25A)	2771(11)	4601(10)	2809(8)	48(2)
C(26A)	2468(10)	3896(9)	3039(7)	34(4)
C(21A)	1986(10)	3949(8)	3518(7)	22(4)
C(22B)	1586(10)	4778(7)	3925(7)	23(3)
C(23B)	1846(12)	5509(9)	3730(8)	67(7)
C(24B)	2340(10)	5532(10)	3263(8)	39(2)
C(25B)	2605(10)	4886(9)	2977(7)	39(2)
C(26B)	2344(9)	4142(8)	3169(6)	21(3)
C(21B)	1843(9)	4104(8)	3635(6)	18(4)
C(711)	4020(4)	2187(4)	5799(3)	21(2)
C(11)	1049(4)	2494(4)	3297(3)	25(2)
C(12)	1492(5)	2288(5)	2818(3)	32(2)
C(13)	1042(6)	1885(5)	2322(4)	43(2)
C(14)	169(5)	1682(4)	2299(3)	38(2)
C(15)	-268(5)	1846(4)	2782(3)	35(2)
C(16)	176(4)	2256(4)	3282(3)	28(2)
C(31)	704(5)	3433(4)	4299(3)	32(2)
C(32)	744(5)	3349(4)	4930(3)	31(2)
C(33)	47(5)	3623(5)	5203(4)	41(2)
C(79)	2415(4)	2348(4)	5904(3)	15(1)
C(34)	-44(5)	3801(5)	3968(4)	40(2)
C(35)	-675(5)	3973(5)	4860(4)	39(2)
C(36)	-722(5)	4055(6)	4244(4)	48(2)
C(41)	3008(4)	754(4)	5074(3)	22(2)
C(42)	2488(4)	478(4)	5496(3)	26(2)
C(811)	4201(4)	4093(4)	4043(3)	21(1)
C(43)	2846(5)	28(5)	5984(3)	30(2)
C(44)	3751(5)	-180(4)	6063(3)	30(2)

C(45)	4270(5)	87(4)	5663(3)	28(2)
C(46)	3907(4)	544(4)	5168(3)	24(2)
C(51)	1403(4)	1061(4)	4254(3)	23(2)
C(52)	832(4)	1324(4)	4642(3)	30(2)
C(53)	-43(5)	1039(5)	4564(4)	40(2)
C(54)	-337(5)	548(5)	4098(4)	44(2)
C(89)	2875(4)	4205(4)	5305(3)	23(2)
C(55)	205(5)	298(5)	3702(4)	39(2)
C(56)	1088(4)	553(4)	3778(3)	28(2)
C(61)	3152(4)	1014(4)	3839(3)	20(1)
C(62)	3210(4)	207(4)	3741(3)	25(2)
C(710)	3246(4)	2141(4)	6121(3)	24(2)
C(63)	3687(4)	-70(4)	3309(3)	27(2)
C(64)	4115(4)	442(4)	2983(3)	25(2)
C(65)	4064(5)	1230(5)	3074(3)	30(2)
C(66)	3586(4)	1526(4)	3504(3)	25(2)
C(71)	4814(4)	2353(4)	5016(3)	22(1)
C(72)	5604(4)	2150(4)	5389(3)	27(2)
C(73)	5590(4)	1921(4)	5991(3)	24(2)
C(74)	4787(4)	1935(4)	6189(3)	21(1)
C(75)	4519(4)	1661(4)	6775(3)	24(2)
C(76)	3542(4)	1818(4)	6698(3)	24(2)
C(77)	2930(5)	1665(4)	7066(3)	28(2)
C(78)	2036(5)	1869(5)	6842(3)	35(2)
C(81)	4745(5)	3345(4)	3357(3)	27(2)
C(82)	5232(5)	3969(4)	3174(3)	29(2)
C(83)	5188(4)	4691(4)	3435(3)	28(2)
C(84)	4644(4)	4759(4)	3879(3)	23(2)
C(86)	3862(4)	5107(4)	4678(3)	24(2)
C(87)	3506(4)	5456(4)	5139(3)	28(2)
C(88)	3017(4)	4975(4)	5462(3)	27(2)
C(93)	2600(9)	7523(8)	6502(5)	87(4)
C(810)	3711(4)	4316(4)	4540(3)	20(1)
C(85)	4464(4)	5420(4)	4253(3)	25(2)
N(1)	3186(3)	3866(3)	4827(2)	20(1)
N(2)	4232(4)	3386(3)	3799(3)	25(1)
N(3)	1816(5)	2224(5)	6272(4)	54(2)
N(4)	4020(3)	2372(3)	5217(2)	19(1)
N(6)	2826(6)	7528(6)	5875(4)	66(2)
O(1)	4992(3)	1342(3)	7199(2)	27(1)
O(2)	4761(3)	6087(3)	4253(2)	32(1)

O(89)	2144(7)	7888(9)	5361(5)	57(4)
O(90)	3537(4)	7283(4)	5777(3)	53(2)
P(1)	2558(1)	1370(1)	4426(1)	20(1)
P(2)	1607(1)	3112(1)	3921(1)	24(1)
Pd(1)	2840(1)	2680(1)	4602(1)	20(1)
C(2)	6516(5)	676(5)	2096(4)	39(2)
F(1)	6049(3)	140(3)	2341(2)	53(1)
F(2)	6429(4)	1345(3)	2371(3)	71(2)
F(3)	6122(3)	771(3)	1516(3)	62(2)
O(21)	7591(3)	-391(3)	1862(2)	38(1)
O(22)	8040(3)	963(3)	1782(2)	39(1)
O(23)	8013(4)	389(4)	2781(2)	51(2)
S(1)	7672(1)	374(1)	2136(1)	31(1)
C(1A)	710(9)	7890(7)	3539(9)	41(2)
F(41A)	244(5)	8400(5)	3174(4)	72(3)
F(42A)	322(5)	7183(5)	3401(4)	62(3)
F(43A)	601(8)	8066(8)	4108(4)	60(3)
O(33A)	2154(7)	8655(7)	3577(5)	73(3)
O(31A)	1778(6)	7691(5)	2801(5)	48(2)
O(32A)	2247(7)	7324(6)	3869(5)	77(3)
S(2A)	1858(2)	7855(2)	3459(2)	41(1)
C(1B)	762(16)	7776(14)	3570(16)	41(2)
F(41B)	420(20)	8210(20)	3965(13)	68(5)
F(42B)	1048(13)	7097(12)	3843(9)	68(5)
F(43B)	85(14)	7652(15)	3112(10)	68(5)
O(32B)	2351(12)	8389(10)	3867(9)	28(4)
O(33B)	1304(16)	8972(14)	3061(11)	63(7)
O(31B)	2023(17)	7460(14)	3015(12)	50(6)
S(2B)	1717(5)	8209(5)	3298(4)	30(2)

Table A.2: Bond distances (Å) and angles (◦) for *cis*-[Pd(PPh$_3$)$_2$(Daf)$_2$].(Trif)$_2$.CH$_3$NO$_2$.

Bond	Distance (Å)	Bond Angle	Angle (◦)
C(22A)-C(23A)	1.392(15)	C(23A)-C(22A)-C(21A)	120.5(14)
C(22A)-C(21A)	1.421(15)	C(24A)-C(23A)-C(22A)	118.2(15)
C(23A)-C(24A)	1.373(17)	C(23A)-C(24A)-C(25A)	122.6(14)
C(24A)-C(25A)	1.378(16)	C(24A)-C(25A)-C(26A)	120.4(14)
C(25A)-C(26A)	1.417(15)	C(21A)-C(26A)-C(25A)	117.7(14)
C(26A)-C(21A)	1.393(15)	C(26A)-C(21A)-C(22A)	120.5(12)
C(21A)-P(2)	1.835(13)	C(26A)-C(21A)-P(2)	124.9(11)
C(22B)-C(23B)	1.403(15)	C(22A)-C(21A)-P(2)	114.5(10)
C(22B)-C(21B)	1.408(15)	C(23B)-C(22B)-C(21B)	118.3(14)
C(23B)-C(24B)	1.380(17)	C(24B)-C(23B)-C(22B)	118.5(15)
C(24B)-C(25B)	1.370(16)	C(25B)-C(24B)-C(23B)	124.4(15)
C(25B)-C(26B)	1.420(15)	C(24B)-C(25B)-C(26B)	117.7(14)
C(26B)-C(21B)	1.386(14)	C(21B)-C(26B)-C(25B)	118.9(12)
C(21B)-P(2)	1.870(12)	C(26B)-C(21B)-C(22B)	122.3(11)
C(711)-N(4)	1.333(8)	C(26B)-C(21B)-P(2)	117.3(10)
C(711)-C(74)	1.398(9)	C(22B)-C(21B)-P(2)	120.2(9)
C(711)-C(710)	1.477(9)	N(4)-C(711)-C(74)	122.8(6)
C(11)-C(16)	1.381(9)	N(4)-C(711)-C(710)	127.8(6)
C(11)-C(12)	1.398(9)	C(74)-C(711)-C(710)	109.2(6)
C(11)-P(2)	1.836(7)	C(16)-C(11)-C(12)	119.3(6)
C(12)-C(13)	1.381(10)	C(16)-C(11)-P(2)	120.5(5)
C(13)-C(14)	1.363(11)	C(12)-C(11)-P(2)	120.1(5)
C(14)-C(15)	1.384(10)	C(13)-C(12)-C(11)	119.9(7)
C(15)-C(16)	1.391(9)	C(14)-C(13)-C(12)	120.3(7)
C(31)-C(34)	1.394(10)	C(13)-C(14)-C(15)	120.7(7)
C(31)-C(32)	1.403(10)	C(14)-C(15)-C(16)	119.5(7)
C(31)-P(2)	1.810(7)	C(11)-C(16)-C(15)	120.2(7)
C(32)-C(33)	1.388(10)	C(34)-C(31)-C(32)	118.0(7)
C(33)-C(35)	1.364(10)	C(34)-C(31)-P(2)	120.4(6)
C(79)-C(710)	1.322(9)	C(32)-C(31)-P(2)	121.6(5)
C(79)-N(3)	1.339(9)	C(33)-C(32)-C(31)	119.7(7)
C(34)-C(36)	1.357(11)	C(35)-C(33)-C(32)	120.2(8)
C(35)-C(36)	1.367(11)	C(710)-C(79)-N(3)	116.1(6)
C(41)-C(46)	1.393(9)	C(36)-C(34)-C(31)	121.3(8)
C(41)-C(42)	1.405(9)	C(33)-C(35)-C(36)	120.6(7)
C(41)-P(1)	1.825(7)	C(34)-C(36)-C(35)	120.3(7)

C(42)-C(43)	1.369(10)	C(46)-C(41)-C(42)	117.3(6)
C(811)-N(2)	1.331(9)	C(46)-C(41)-P(1)	119.7(5)
C(811)-C(84)	1.402(9)	C(42)-C(41)-P(1)	122.9(5)
C(811)-C(810)	1.483(9)	C(43)-C(42)-C(41)	121.8(6)
C(43)-C(44)	1.402(10)	N(2)-C(811)-C(84)	125.6(6)
C(44)-C(45)	1.364(10)	N(2)-C(811)-C(810)	126.5(6)
C(45)-C(46)	1.385(10)	C(84)-C(811)-C(810)	107.9(6)
C(51)-C(56)	1.391(10)	C(42)-C(43)-C(44)	119.5(7)
C(51)-C(52)	1.397(10)	C(45)-C(44)-C(43)	119.6(7)
C(51)-P(1)	1.810(7)	C(44)-C(45)-C(46)	120.8(6)
C(52)-C(53)	1.398(10)	C(45)-C(46)-C(41)	120.9(6)
C(53)-C(54)	1.351(12)	C(56)-C(51)-C(52)	120.2(6)
C(54)-C(55)	1.372(12)	C(56)-C(51)-P(1)	122.7(5)
C(89)-N(1)	1.363(8)	C(52)-C(51)-P(1)	117.0(5)
C(89)-C(88)	1.371(10)	C(51)-C(52)-C(53)	119.2(7)
C(55)-C(56)	1.394(10)	C(54)-C(53)-C(52)	119.7(8)
C(61)-C(66)	1.387(9)	C(53)-C(54)-C(55)	122.1(7)
C(61)-C(62)	1.404(10)	N(1)-C(89)-C(88)	123.3(6)
C(61)-P(1)	1.814(7)	C(54)-C(55)-C(56)	119.5(8)
C(62)-C(63)	1.381(10)	C(51)-C(56)-C(55)	119.2(7)
C(710)-C(76)	1.401(10)	C(66)-C(61)-C(62)	119.4(6)
C(63)-C(64)	1.371(10)	C(66)-C(61)-P(1)	120.9(5)
C(64)-C(65)	1.367(10)	C(62)-C(61)-P(1)	119.6(5)
C(65)-C(66)	1.390(10)	C(63)-C(62)-C(61)	120.0(7)
C(71)-N(4)	1.355(8)	C(79)-C(710)-C(76)	125.4(6)
C(71)-C(72)	1.384(9)	C(79)-C(710)-C(711)	126.7(6)
C(72)-C(73)	1.398(10)	C(76)-C(710)-C(711)	107.9(6)
C(73)-C(74)	1.365(9)	C(64)-C(63)-C(62)	120.0(7)
C(74)-C(75)	1.504(9)	C(65)-C(64)-C(63)	120.6(7)
C(75)-O(1)	1.215(8)	C(64)-C(65)-C(66)	120.7(7)
C(75)-C(76)	1.490(9)	C(61)-C(66)-C(65)	119.4(7)
C(76)-C(77)	1.365(9)	N(4)-C(71)-C(72)	122.5(7)
C(77)-C(78)	1.409(10)	C(71)-C(72)-C(73)	119.6(6)
C(78)-N(3)	1.396(10)	C(74)-C(73)-C(72)	117.6(6)
C(81)-N(2)	1.354(9)	C(73)-C(74)-C(711)	120.0(6)
C(81)-C(82)	1.400(10)	C(73)-C(74)-C(75)	131.3(6)
C(82)-C(83)	1.372(10)	C(711)-C(74)-C(75)	108.5(6)
C(83)-C(84)	1.395(10)	O(1)-C(75)-C(76)	128.2(7)
C(84)-C(85)	1.457(10)	O(1)-C(75)-C(74)	127.1(6)
C(86)-C(87)	1.374(10)	C(76)-C(75)-C(74)	104.6(5)
C(86)-C(810)	1.398(9)	C(77)-C(76)-C(710)	118.8(6)

C(86)-C(85)	1.518(10)	C(77)-C(76)-C(75)	131.5(6)
C(87)-C(88)	1.388(10)	C(710)-C(76)-C(75)	109.6(6)
C(93)-N(6)	1.491(13)	C(76)-C(77)-C(78)	116.9(6)
C(810)-N(1)	1.345(8)	N(3)-C(78)-C(77)	119.9(7)
C(85)-O(2)	1.227(8)	N(2)-C(81)-C(82)	124.7(7)
N(1)-Pd(1)	2.136(5)	C(83)-C(82)-C(81)	119.8(7)
N(4)-Pd(1)	2.129(5)	C(82)-C(83)-C(84)	116.9(7)
N(6)-O(90)	1.212(10)	C(83)-C(84)-C(811)	118.9(6)
N(6)-O(89)	1.538(14)	C(83)-C(84)-C(85)	131.3(7)
P(1)-Pd(1)	2.3023(18)	C(811)-C(84)-C(85)	109.7(6)
P(2)-Pd(1)	2.3222(18)	C(87)-C(86)-C(810)	121.0(7)
C(2)-F(2)	1.314(9)	C(87)-C(86)-C(85)	131.7(6)
C(2)-F(1)	1.332(9)	C(810)-C(86)-C(85)	107.3(6)
C(2)-F(3)	1.339(10)	C(86)-C(87)-C(88)	116.2(7)
C(2)-S(1)	1.818(8)	C(89)-C(88)-C(87)	120.7(7)
O(21)-S(1)	1.441(6)	N(1)-C(810)-C(86)	122.5(6)
O(22)-S(1)	1.447(5)	N(1)-C(810)-C(811)	128.3(6)
O(23)-S(1)	1.443(6)	C(86)-C(810)-C(811)	109.2(6)
C(1A)-F(41A)	1.314(17)	O(2)-C(85)-C(84)	128.1(7)
C(1A)-F(43A)	1.34(2)	O(2)-C(85)-C(86)	126.0(7)
C(1A)-F(42A)	1.359(14)	C(84)-C(85)-C(86)	105.8(6)
C(1A)-S(2A)	1.784(13)	C(810)-N(1)-C(89)	116.0(6)
O(33A)-S(2A)	1.450(12)	C(810)-N(1)-Pd(1)	125.1(4)
O(31A)-S(2A)	1.476(11)	C(89)-N(1)-Pd(1)	118.9(4)
O(32A)-S(2A)	1.351(12)	C(811)-N(2)-C(81)	114.0(6)
C(1B)-F(41B)	1.33(3)	C(79)-N(3)-C(78)	122.8(7)
C(1B)-F(43B)	1.34(3)	C(711)-N(4)-C(71)	117.4(6)
C(1B)-F(42B)	1.35(2)	C(711)-N(4)-Pd(1)	123.1(4)
C(1B)-S(2B)	1.820(18)	C(71)-N(4)-Pd(1)	119.5(5)
O(32B)-S(2B)	1.49(2)	O(90)-N(6)-C(93)	121.2(10)
O(33B)-S(2B)	1.50(3)	O(90)-N(6)-O(89)	120.9(8)
O(31B)-S(2B)	1.54(3)	C(93)-N(6)-O(89)	117.9(9)
		C(51)-P(1)-C(61)	109.3(3)
		C(51)-P(1)-C(41)	102.7(3)
		C(61)-P(1)-C(41)	102.1(3)
		C(51)-P(1)-Pd(1)	117.8(2)
		C(61)-P(1)-Pd(1)	110.4(2)
		C(41)-P(1)-Pd(1)	113.2(2)
		C(31)-P(2)-C(21A)	108.3(5)
		C(31)-P(2)-C(11)	103.7(3)
		C(21A)-P(2)-C(11)	102.8(5)

		C(31)-P(2)-C(21B)	94.9(5)
		C(21A)-P(2)-C(21B)	14.0(5)
		C(11)-P(2)-C(21B)	110.8(5)
		C(31)-P(2)-Pd(1)	112.6(2)
		C(21A)-P(2)-Pd(1)	106.5(5)
		C(11)-P(2)-Pd(1)	122.0(2)
		C(21B)-P(2)-Pd(1)	109.4(5)
		N(4)-Pd(1)-N(1)	86.4(2)
		N(4)-Pd(1)-P(1)	88.89(15)
		N(1)-Pd(1)-P(1)	175.20(15)
		N(4)-Pd(1)-P(2)	175.37(15)
		N(1)-Pd(1)-P(2)	89.43(15)
		P(1)-Pd(1)-P(2)	95.31(6)
		F(2)-C(2)-F(1)	107.9(7)
		F(2)-C(2)-F(3)	106.3(7)
		F(1)-C(2)-F(3)	107.2(7)
		F(2)-C(2)-S(1)	113.3(6)
		F(1)-C(2)-S(1)	111.1(6)
		F(3)-C(2)-S(1)	110.7(6)
		O(21)-S(1)-O(23)	115.4(4)
		O(21)-S(1)-O(22)	114.5(3)
		O(23)-S(1)-O(22)	115.0(3)
		O(21)-S(1)-C(2)	103.0(3)
		O(23)-S(1)-C(2)	103.1(4)
		O(22)-S(1)-C(2)	103.5(4)
		F(41A)-C(1A)-F(43A)	107.3(10)
		F(41A)-C(1A)-F(42A)	106.5(14)
		F(43A)-C(1A)-F(42A)	107.2(12)
		F(41A)-C(1A)-S(2A)	113.2(10)
		F(43A)-C(1A)-S(2A)	112.4(12)
		F(42A)-C(1A)-S(2A)	110.0(8)
		O(32A)-S(2A)-O(33A)	115.2(7)
		O(32A)-S(2A)-O(31A)	119.7(7)
		O(33A)-S(2A)-O(31A)	109.3(7)
		O(32A)-S(2A)-C(1A)	106.2(7)
		O(33A)-S(2A)-C(1A)	103.2(6)
		O(31A)-S(2A)-C(1A)	100.8(8)
		F(41B)-C(1B)-F(43B)	105(2)
		F(41B)-C(1B)-F(42B)	109(3)
		F(43B)-C(1B)-F(42B)	111(2)
		F(41B)-C(1B)-S(2B)	115(2)

		F(43B)-C(1B)-S(2B)	111(2)
		F(42B)-C(1B)-S(2B)	106.7(16)
		O(32B)-S(2B)-O(33B)	106.9(13)
		O(32B)-S(2B)-O(31B)	108.9(14)
		O(33B)-S(2B)-O(31B)	135.9(15)
		O(32B)-S(2B)-C(1B)	103.9(14)
		O(33B)-S(2B)-C(1B)	99.3(13)
		O(31B)-S(2B)-C(1B)	96.3(13)

Table A.3: Anisotropic displacement parameters (A^2 x 10^3) for *cis*- $[Pd(PPh_3)_2(Daf)_2].(Trif)_2.CH_3NO_2$.

	U11	U22	U33	U23	U13	U12
C(23A)	86(14)	22(7)	68(14)	-17(8)	-58(11)	-3(8)
C(25A)	34(4)	73(6)	31(5)	7(4)	-9(3)	14(4)
C(22B)	28(8)	32(8)	8(8)	-1(6)	4(7)	2(6)
C(23B)	86(14)	22(7)	68(14)	-17(8)	-58(11)	-3(8)
C(24B)	24(3)	61(5)	30(4)	-13(3)	-2(3)	16(3)
C(25B)	24(3)	61(5)	30(4)	-13(3)	-2(3)	16(3)
C(711)	16(3)	32(4)	13(4)	-1(3)	-1(3)	-2(3)
C(11)	24(4)	30(4)	19(4)	1(3)	-4(3)	4(3)
C(12)	25(4)	54(5)	17(4)	2(3)	2(3)	7(3)
C(13)	48(5)	56(6)	24(5)	-9(4)	1(4)	25(4)
C(14)	57(5)	29(4)	23(4)	-6(3)	-13(4)	4(4)
C(15)	27(4)	37(4)	34(5)	10(4)	-17(3)	-6(3)
C(16)	25(4)	33(4)	20(4)	6(3)	-8(3)	1(3)
C(31)	26(4)	41(4)	23(4)	-4(3)	-6(3)	10(3)
C(32)	27(4)	36(4)	24(4)	-2(3)	-8(3)	5(3)
C(33)	36(4)	55(5)	27(5)	-12(4)	-7(4)	11(4)
C(79)	5(3)	29(3)	11(3)	5(3)	2(2)	2(2)
C(34)	41(5)	55(5)	20(4)	-4(4)	-3(4)	27(4)
C(35)	24(3)	61(5)	30(4)	-13(3)	-2(3)	16(3)
C(36)	34(4)	73(6)	31(5)	7(4)	-9(3)	14(4)
C(41)	19(3)	27(4)	17(4)	-2(3)	-4(3)	-5(3)
C(42)	14(3)	42(4)	21(4)	4(3)	-2(3)	1(3)
C(811)	15(3)	32(4)	13(3)	6(3)	-4(3)	0(3)
C(43)	22(4)	48(5)	19(4)	10(3)	1(3)	-1(3)
C(44)	27(4)	38(4)	21(4)	4(3)	-5(3)	3(3)
C(45)	19(3)	42(4)	21(4)	-4(3)	0(3)	3(3)
C(46)	18(3)	35(4)	18(4)	3(3)	0(3)	2(3)

C(51)	17(3)	31(4)	19(4)	6(3)	-4(3)	-2(3)
C(52)	20(4)	43(4)	26(4)	11(3)	2(3)	4(3)
C(53)	25(4)	60(6)	35(5)	19(4)	8(4)	10(4)
C(54)	22(4)	58(6)	50(6)	18(5)	2(4)	-13(4)
C(89)	18(3)	38(4)	12(4)	0(3)	-4(3)	1(3)
C(55)	27(4)	49(5)	37(5)	3(4)	-7(4)	-8(4)
C(56)	20(4)	34(4)	26(4)	2(3)	-1(3)	-1(3)
C(61)	15(3)	35(4)	10(3)	-5(3)	-3(3)	0(3)
C(62)	18(3)	35(4)	18(4)	0(3)	-8(3)	-3(3)
C(710)	24(4)	31(4)	15(4)	-4(3)	2(3)	0(3)
C(63)	18(3)	38(4)	23(4)	-2(3)	-5(3)	8(3)
C(64)	19(3)	36(4)	17(4)	-6(3)	-2(3)	1(3)
C(65)	23(4)	44(5)	21(4)	-1(3)	3(3)	-4(3)
C(66)	21(3)	27(4)	26(4)	1(3)	1(3)	0(3)
C(71)	18(3)	29(4)	21(4)	5(3)	6(3)	0(3)
C(72)	17(3)	43(4)	19(4)	6(3)	1(3)	-1(3)
C(73)	15(3)	32(4)	24(4)	2(3)	0(3)	-1(3)
C(74)	22(3)	26(4)	13(4)	-4(3)	-3(3)	1(3)
C(75)	24(4)	28(4)	17(4)	-1(3)	-5(3)	-4(3)
C(76)	20(3)	34(4)	17(4)	-8(3)	0(3)	-1(3)
C(77)	28(4)	39(4)	15(4)	3(3)	0(3)	4(3)
C(78)	34(4)	58(5)	17(4)	12(4)	12(3)	0(4)
C(81)	29(4)	33(4)	20(4)	-5(3)	6(3)	-4(3)
C(82)	26(4)	41(5)	21(4)	4(3)	4(3)	5(3)
C(83)	18(3)	38(4)	27(4)	10(3)	0(3)	-1(3)
C(84)	20(3)	35(4)	13(4)	-4(3)	-5(3)	3(3)
C(86)	18(3)	30(4)	20(4)	-2(3)	-8(3)	2(3)
C(87)	23(4)	36(4)	22(4)	0(3)	-3(3)	3(3)
C(88)	23(4)	40(4)	19(4)	-7(3)	1(3)	-1(3)
C(93)	100(10)	125(11)	48(8)	-3(7)	49(7)	-10(8)
C(810)	14(3)	29(4)	14(4)	2(3)	-5(3)	1(3)
C(85)	22(3)	25(4)	26(4)	7(3)	-8(3)	1(3)
N(1)	16(3)	26(3)	16(3)	0(2)	0(2)	3(2)
N(2)	21(3)	35(3)	18(3)	1(3)	-2(2)	0(2)
N(3)	50(5)	70(6)	42(5)	8(4)	6(4)	-4(4)
N(4)	16(3)	25(3)	14(3)	-2(2)	-1(2)	-4(2)
N(6)	68(6)	90(7)	44(5)	-7(5)	18(5)	-12(5)
O(1)	29(3)	32(3)	18(3)	0(2)	-4(2)	-2(2)
O(2)	35(3)	30(3)	28(3)	1(2)	0(2)	-4(2)
O(89)	18(6)	108(11)	40(8)	29(7)	-7(5)	17(6)
O(90)	41(4)	77(5)	44(4)	12(3)	19(3)	24(3)
P(1)	15(1)	30(1)	14(1)	-1(1)	-1(1)	-1(1)
P(2)	20(1)	30(1)	18(1)	0(1)	-5(1)	0(1)

Pd(1)	16(1)	29(1)	14(1)	0(1)	-2(1)	0(1)
C(2)	35(4)	42(5)	43(5)	-5(4)	12(4)	3(4)
F(1)	31(3)	71(4)	60(4)	3(3)	18(2)	-4(2)
F(2)	59(4)	64(4)	97(5)	-24(3)	30(3)	5(3)
F(3)	42(3)	85(4)	51(4)	14(3)	-11(3)	14(3)
O(21)	36(3)	47(3)	33(3)	0(3)	9(3)	5(2)
O(22)	39(3)	52(3)	26(3)	1(3)	10(2)	-11(3)
O(23)	43(3)	93(5)	16(3)	0(3)	-3(3)	-20(3)
S(1)	23(1)	51(1)	20(1)	3(1)	2(1)	-3(1)
F(41A)	60(5)	104(7)	46(5)	11(5)	-10(4)	41(5)
F(42A)	45(5)	84(6)	60(6)	-17(4)	22(4)	-37(4)
F(43A)	43(6)	123(9)	19(5)	-12(5)	16(4)	2(5)
F(41B)	65(10)	84(11)	58(10)	-6(8)	18(8)	-23(8)
F(42B)	65(10)	84(11)	58(10)	-6(8)	18(8)	-23(8)
F(43B)	65(10)	84(11)	58(10)	-6(8)	18(8)	-23(8)

Table A.4: Torsion angles (◦) for *cis*- $[Pd(PPh_3)_2(Daf)_2].(Trif)_2.CH_3NO_2$.

	Angle (◦)		Angle (◦)
C(21A)-C(22A)-C(23A)-C(24A)	1.1(15)	C(810)-C(811)-N(2)-C(81)	-178.9(6)
C(22A)-C(23A)-C(24A)-C(25A)	-0.4(16)	C(82)-C(81)-N(2)-C(811)	1.9(10)
C(23A)-C(24A)-C(25A)-C(26A)	0(2)	C(710)-C(79)-N(3)-C(78)	-2.6(11)
C(24A)-C(25A)-C(26A)-C(21A)	-1(2)	C(77)-C(78)-N(3)-C(79)	3.7(13)
C(25A)-C(26A)-C(21A)-C(22A)	1(2)	C(74)-C(711)-N(4)-C(71)	-3.8(9)
C(25A)-C(26A)-C(21A)-P(2)	-175.0(12)	C(710)-C(711)-N(4)-C(71)	-178.1(6)
C(23A)-C(22A)-C(21A)-C(26A)	-2(2)	C(74)-C(711)-N(4)-Pd(1)	175.7(5)
C(23A)-C(22A)-C(21A)-P(2)	175.0(11)	C(710)-C(711)-N(4)-Pd(1)	1.3(9)
C(21B)-C(22B)-C(23B)-C(24B)	0.1(14)	C(72)-C(71)-N(4)-C(711)	0.2(10)
C(22B)-C(23B)-C(24B)-C(25B)	-0.7(17)	C(72)-C(71)-N(4)-Pd(1)	-179.3(5)
C(23B)-C(24B)-C(25B)-C(26B)	1(2)	C(56)-C(51)-P(1)-C(61)	6.7(7)
C(24B)-C(25B)-C(26B)-C(21B)	-1(2)	C(52)-C(51)-P(1)-C(61)	-176.3(5)
C(25B)-C(26B)-C(21B)-C(22B)	0(2)	C(56)-C(51)-P(1)-C(41)	-101.1(6)
C(25B)-C(26B)-C(21B)-P(2)	-174.4(11)	C(52)-C(51)-P(1)-C(41)	75.8(6)
C(23B)-C(22B)-C(21B)-C(26B)	0.3(19)	C(56)-C(51)-P(1)-Pd(1)	133.8(5)
C(23B)-C(22B)-C(21B)-P(2)	174.5(10)	C(52)-C(51)-P(1)-Pd(1)	-49.3(6)
C(16)-C(11)-C(12)-C(13)	3.2(11)	C(66)-C(61)-P(1)-C(51)	122.2(5)
P(2)-C(11)-C(12)-C(13)	-174.0(6)	C(62)-C(61)-P(1)-C(51)	-60.7(6)
C(11)-C(12)-C(13)-C(14)	-0.5(12)	C(66)-C(61)-P(1)-C(41)	-129.6(5)
C(12)-C(13)-C(14)-C(15)	-2.7(12)	C(62)-C(61)-P(1)-C(41)	47.5(6)
C(13)-C(14)-C(15)-C(16)	3.2(11)	C(66)-C(61)-P(1)-Pd(1)	-9.0(6)
C(12)-C(11)-C(16)-C(15)	-2.7(10)	C(62)-C(61)-P(1)-Pd(1)	168.1(4)

P(2)-C(11)-C(16)-C(15)	174.5(5)	C(46)-C(41)-P(1)-C(51)	150.5(6)
C(14)-C(15)-C(16)-C(11)	-0.4(11)	C(42)-C(41)-P(1)-C(51)	-30.0(7)
C(34)-C(31)-C(32)-C(33)	0.7(12)	C(46)-C(41)-P(1)-C(61)	37.2(6)
P(2)-C(31)-C(32)-C(33)	178.2(6)	C(42)-C(41)-P(1)-C(61)	-143.2(6)
C(31)-C(32)-C(33)-C(35)	-0.1(12)	C(46)-C(41)-P(1)-Pd(1)	-81.5(6)
C(32)-C(31)-C(34)-C(36)	-1.5(13)	C(42)-C(41)-P(1)-Pd(1)	98.1(6)
P(2)-C(31)-C(34)-C(36)	-179.1(7)	C(34)-C(31)-P(2)-C(21A)	54.5(9)
C(32)-C(33)-C(35)-C(36)	0.4(13)	C(32)-C(31)-P(2)-C(21A)	-123.0(8)
C(31)-C(34)-C(36)-C(35)	1.8(14)	C(34)-C(31)-P(2)-C(11)	-54.3(7)
C(33)-C(35)-C(36)-C(34)	-1.2(14)	C(32)-C(31)-P(2)-C(11)	128.2(6)
C(46)-C(41)-C(42)-C(43)	0.7(11)	C(34)-C(31)-P(2)-C(21B)	58.6(8)
P(1)-C(41)-C(42)-C(43)	-178.9(6)	C(32)-C(31)-P(2)-C(21B)	-118.9(8)
C(41)-C(42)-C(43)-C(44)	-1.3(12)	C(34)-C(31)-P(2)-Pd(1)	172.0(6)
C(42)-C(43)-C(44)-C(45)	1.9(11)	C(32)-C(31)-P(2)-Pd(1)	-5.5(7)
C(43)-C(44)-C(45)-C(46)	-1.9(11)	C(26A)-C(21A)-P(2)-C(31)	-159.9(13)
C(44)-C(45)-C(46)-C(41)	1.3(11)	C(22A)-C(21A)-P(2)-C(31)	23.7(13)
C(42)-C(41)-C(46)-C(45)	-0.6(10)	C(26A)-C(21A)-P(2)-C(11)	-50.6(15)
P(1)-C(41)-C(46)-C(45)	178.9(5)	C(22A)-C(21A)-P(2)-C(11)	133.0(11)
C(56)-C(51)-C(52)-C(53)	3.3(10)	C(26A)-C(21A)-P(2)-C(21B)	-177(4)
P(1)-C(51)-C(52)-C(53)	-173.7(5)	C(22A)-C(21A)-P(2)-C(21B)	6(3)
C(51)-C(52)-C(53)-C(54)	-3.4(11)	C(26A)-C(21A)-P(2)-Pd(1)	78.8(14)
C(52)-C(53)-C(54)-C(55)	1.8(13)	C(22A)-C(21A)-P(2)-Pd(1)	-97.7(11)
C(53)-C(54)-C(55)-C(56)	0.0(13)	C(16)-C(11)-P(2)-C(31)	-12.4(7)
C(52)-C(51)-C(56)-C(55)	-1.5(10)	C(12)-C(11)-P(2)-C(31)	164.8(6)
P(1)-C(51)-C(56)-C(55)	175.4(6)	C(16)-C(11)-P(2)-C(21A)	-125.2(7)
C(54)-C(55)-C(56)-C(51)	-0.2(11)	C(12)-C(11)-P(2)-C(21A)	52.0(8)
C(66)-C(61)-C(62)-C(63)	-0.7(9)	C(16)-C(11)-P(2)-C(21B)	-113.2(7)
P(1)-C(61)-C(62)-C(63)	-177.8(5)	C(12)-C(11)-P(2)-C(21B)	64.0(8)
N(3)-C(79)-C(710)-C(76)	-0.8(11)	C(16)-C(11)-P(2)-Pd(1)	115.8(5)
N(3)-C(79)-C(710)-C(711)	177.3(7)	C(12)-C(11)-P(2)-Pd(1)	-67.0(6)
N(4)-C(711)-C(710)-C(79)	-6.8(12)	C(26B)-C(21B)-P(2)-C(31)	-162.9(11)
C(74)-C(711)-C(710)-C(79)	178.3(7)	C(22B)-C(21B)-P(2)-C(31)	22.6(12)
N(4)-C(711)-C(710)-C(76)	171.6(6)	C(26B)-C(21B)-P(2)-C(21A)	1(3)
C(74)-C(711)-C(710)-C(76)	-3.4(8)	C(22B)-C(21B)-P(2)-C(21A)	-174(4)
C(61)-C(62)-C(63)-C(64)	1.0(10)	C(26B)-C(21B)-P(2)-C(11)	-56.3(12)
C(62)-C(63)-C(64)-C(65)	-1.1(10)	C(22B)-C(21B)-P(2)-C(11)	129.2(11)
C(63)-C(64)-C(65)-C(66)	0.8(10)	C(26B)-C(21B)-P(2)-Pd(1)	81.0(11)
C(62)-C(61)-C(66)-C(65)	0.4(10)	C(22B)-C(21B)-P(2)-Pd(1)	-93.5(11)
P(1)-C(61)-C(66)-C(65)	177.5(5)	C(711)-N(4)-Pd(1)-N(1)	95.0(5)
C(64)-C(65)-C(66)-C(61)	-0.5(10)	C(71)-N(4)-Pd(1)-N(1)	-85.6(5)
N(4)-C(71)-C(72)-C(73)	2.8(11)	C(711)-N(4)-Pd(1)-P(1)	-84.1(5)

C(71)-C(72)-C(73)-C(74)	-2.1(10)	C(71)-N(4)-Pd(1)-P(1)	95.3(5)
C(72)-C(73)-C(74)-C(711)	-1.3(10)	C(711)-N(4)-Pd(1)-P(2)	120.6(18)
C(72)-C(73)-C(74)-C(75)	173.4(7)	C(71)-N(4)-Pd(1)-P(2)	-60(2)
N(4)-C(711)-C(74)-C(73)	4.4(10)	C(810)-N(1)-Pd(1)-N(4)	88.7(5)
C(710)-C(711)-C(74)-C(73)	179.7(6)	C(89)-N(1)-Pd(1)-N(4)	-90.0(5)
N(4)-C(711)-C(74)-C(75)	-171.3(6)	C(810)-N(1)-Pd(1)-P(1)	99.4(18)
C(710)-C(711)-C(74)-C(75)	3.9(7)	C(89)-N(1)-Pd(1)-P(1)	-79.2(18)
C(73)-C(74)-C(75)-O(1)	-1.9(12)	C(810)-N(1)-Pd(1)-P(2)	-89.3(5)
C(711)-C(74)-C(75)-O(1)	173.3(7)	C(89)-N(1)-Pd(1)-P(2)	92.0(4)
C(73)-C(74)-C(75)-C(76)	-178.1(7)	C(51)-P(1)-Pd(1)-N(4)	148.4(3)
C(711)-C(74)-C(75)-C(76)	-3.0(7)	C(61)-P(1)-Pd(1)-N(4)	-85.1(3)
C(79)-C(710)-C(76)-C(77)	3.1(11)	C(41)-P(1)-Pd(1)-N(4)	28.7(3)
C(711)-C(710)-C(76)-C(77)	-175.3(6)	C(51)-P(1)-Pd(1)-N(1)	137.7(18)
C(79)-C(710)-C(76)-C(75)	179.8(6)	C(61)-P(1)-Pd(1)-N(1)	-95.8(18)
C(711)-C(710)-C(76)-C(75)	1.4(8)	C(41)-P(1)-Pd(1)-N(1)	18.0(18)
O(1)-C(75)-C(76)-C(77)	0.9(13)	C(51)-P(1)-Pd(1)-P(2)	-33.5(3)
C(74)-C(75)-C(76)-C(77)	177.1(7)	C(61)-P(1)-Pd(1)-P(2)	93.0(2)
O(1)-C(75)-C(76)-C(710)	-175.3(7)	C(41)-P(1)-Pd(1)-P(2)	-153.3(2)
C(74)-C(75)-C(76)-C(710)	0.9(7)	C(31)-P(2)-Pd(1)-N(4)	-102.0(19)
C(710)-C(76)-C(77)-C(78)	-1.8(10)	C(21A)-P(2)-Pd(1)-N(4)	17(2)
C(75)-C(76)-C(77)-C(78)	-177.7(7)	C(11)-P(2)-Pd(1)-N(4)	133.9(19)
C(76)-C(77)-C(78)-N(3)	-1.3(11)	C(21B)-P(2)-Pd(1)-N(4)	2(2)
N(2)-C(81)-C(82)-C(83)	-1.9(11)	C(31)-P(2)-Pd(1)-N(1)	-76.4(3)
C(81)-C(82)-C(83)-C(84)	-0.1(10)	C(21A)-P(2)-Pd(1)-N(1)	42.2(5)
C(82)-C(83)-C(84)-C(811)	1.8(9)	C(11)-P(2)-Pd(1)-N(1)	159.4(3)
C(82)-C(83)-C(84)-C(85)	178.2(7)	C(21B)-P(2)-Pd(1)-N(1)	27.8(5)
N(2)-C(811)-C(84)-C(83)	-1.8(10)	C(31)-P(2)-Pd(1)-P(1)	102.9(3)
C(810)-C(811)-C(84)-C(83)	177.2(6)	C(21A)-P(2)-Pd(1)-P(1)	-138.5(5)
N(2)-C(811)-C(84)-C(85)	-179.0(6)	C(11)-P(2)-Pd(1)-P(1)	-21.3(3)
C(810)-C(811)-C(84)-C(85)	0.1(7)	C(21B)-P(2)-Pd(1)-P(1)	-152.9(5)
C(810)-C(86)-C(87)-C(88)	1.6(10)	F(2)-C(2)-S(1)-O(21)	174.7(6)
C(85)-C(86)-C(87)-C(88)	-176.4(7)	F(1)-C(2)-S(1)-O(21)	53.0(7)
N(1)-C(89)-C(88)-C(87)	-0.9(10)	F(3)-C(2)-S(1)-O(21)	-66.0(6)
C(86)-C(87)-C(88)-C(89)	-2.5(10)	F(2)-C(2)-S(1)-O(23)	54.4(7)
C(87)-C(86)-C(810)-N(1)	2.9(10)	F(1)-C(2)-S(1)-O(23)	-67.3(7)
C(85)-C(86)-C(810)-N(1)	-178.7(6)	F(3)-C(2)-S(1)-O(23)	173.7(6)
C(87)-C(86)-C(810)-C(811)	-177.8(6)	F(2)-C(2)-S(1)-O(22)	-65.7(7)
C(85)-C(86)-C(810)-C(811)	0.6(7)	F(1)-C(2)-S(1)-O(22)	172.5(6)
N(2)-C(811)-C(810)-N(1)	-2.2(11)	F(3)-C(2)-S(1)-O(22)	53.5(6)
C(84)-C(811)-C(810)-N(1)	178.8(6)	F(41A)-C(1A)-S(2A)-O(32A)	178.6(11)
N(2)-C(811)-C(810)-C(86)	178.6(6)	F(43A)-C(1A)-S(2A)-O(32A)	56.9(11)

C(84)-C(811)-C(810)-C(86)	-0.4(7)	F(42A)-C(1A)-S(2A)-O(32A)	-62.4(14)
C(83)-C(84)-C(85)-O(2)	0.6(12)	F(41A)-C(1A)-S(2A)-O(33A)	57.1(14)
C(811)-C(84)-C(85)-O(2)	177.3(7)	F(43A)-C(1A)-S(2A)-O(33A)	-64.6(11)
C(83)-C(84)-C(85)-C(86)	-176.4(7)	F(42A)-C(1A)-S(2A)-O(33A)	176.1(12)
C(811)-C(84)-C(85)-C(86)	0.3(7)	F(41A)-C(1A)-S(2A)-O(31A)	-55.9(13)
C(87)-C(86)-C(85)-O(2)	0.5(12)	F(43A)-C(1A)-S(2A)-O(31A)	-177.6(9)
C(810)-C(86)-C(85)-O(2)	-177.7(6)	F(42A)-C(1A)-S(2A)-O(31A)	63.1(13)
C(87)-C(86)-C(85)-C(84)	177.6(7)	F(41B)-C(1B)-S(2B)-O(32B)	55(3)
C(810)-C(86)-C(85)-C(84)	-0.6(7)	F(43B)-C(1B)-S(2B)-O(32B)	173.6(19)
C(86)-C(810)-N(1)-C(89)	-6.1(9)	F(42B)-C(1B)-S(2B)-O(32B)	-65(2)
C(811)-C(810)-N(1)-C(89)	174.7(6)	F(41B)-C(1B)-S(2B)-O(33B)	-55(3)
C(86)-C(810)-N(1)-Pd(1)	175.2(5)	F(43B)-C(1B)-S(2B)-O(33B)	63(2)
C(811)-C(810)-N(1)-Pd(1)	-4.0(9)	F(42B)-C(1B)-S(2B)-O(33B)	-175(2)
C(88)-C(89)-N(1)-C(810)	5.2(9)	F(41B)-C(1B)-S(2B)-O(31B)	166(3)
C(88)-C(89)-N(1)-Pd(1)	-176.0(5)	F(43B)-C(1B)-S(2B)-O(31B)	-75(2)
C(84)-C(811)-N(2)-C(81)	0.0(9)	F(42B)-C(1B)-S(2B)-O(31B)	46(2)

cis-[$Pd_2BpymCl_4$].DMF

Table B.1: Atomic coordinates (x 10^4) and equivalent isotropic Atomic coordinates (x 104) and equivalent isotropic displacement parameters (A^2 x 10^3) for *cis*-[$Pd_2BpymCl_4$].DMF. U(eq) is defined as one third of the trace of the orthogonalized U^{ij} tensor.

	x	y	z	U(eq)
C(11)	0	9488(4)	5000	15(1)
C(12)	693(5)	8117(3)	6976(10)	27(1)
C(13)	0	7635(5)	5000	38(2)
N(1)	692(4)	9054(3)	6989(7)	14(1)
Cl(11)	2297(1)	11142(1)	12398(2)	30(1)
Pd(01)	1503(1)	10000	9663(1)	16(1)
N(22)	0	5000	10000	29(2)
O(22)	0	6532(7)	10000	49(4)
C(21)	-523(11)	5855(9)	8678(19)	33(3)
C(22)	-671(17)	5000	7530(30)	55(6)

Table B.2: Bond distances (Å) and bond angles (◦) for *cis*-[$Pd_2BpymCl_4$].DMF.

Bond	Distance (Å)	Bond Angle	Angle (◦)
C(11)-N(1)#1	1.334(5)	N(1)#1-C(11)-N(1)	124.8(6)
C(11)-N(1)	1.334(5)	N(1)#1-C(11)-C(11)#2	117.6(3)
C(11)-C(11)#2	1.457(12)	N(1)-C(11)-C(11)#2	117.6(3)
C(12)-N(1)	1.335(6)	N(1)-C(12)-C(13)	120.5(5)
C(12)-C(13)	1.362(6)	C(12)-C(13)-C(12)#1	119.5(6)
C(13)-C(12)#1	1.362(6)	C(11)-N(1)-C(12)	117.4(4)
N(1)-Pd(01)	2.056(4)	C(11)-N(1)-Pd(01)	111.3(3)
Cl(11)-Pd(01)	2.2673(13)	C(12)-N(1)-Pd(01)	131.2(3)
Pd(01)-N(1)#3	2.056(4)	N(1)-Pd(01)-N(1)#3	81.8(2)
Pd(01)-Cl(11)#3	2.2673(13)	N(1)-Pd(01)-Cl(11)	175.01(10)
N(22)-C(22)#4	1.419(19)	N(1)#3-Pd(01)-Cl(11)	93.26(12)
N(22)-C(22)	1.419(19)	N(1)-Pd(01)-Cl(11)#3	93.26(12)
N(22)-C(21)#5	1.462(12)	N(1)#3-Pd(01)-Cl(11)#3	175.01(10)
N(22)-C(21)#6	1.462(12)	Cl(11)-Pd(01)-Cl(11)#3	91.62(8)
N(22)-C(21)	1.462(12)	C(22)#4-N(22)-C(22)	180.000(5)
N(22)-C(21)#4	1.462(12)	C(22)#4-N(22)-C(21)#5	57.3(5)
O(22)-C(21)	1.259(14)	C(22)-N(22)-C(21)#5	122.7(5)
O(22)-C(21)#5	1.259(14)	C(22)#4-N(22)-C(21)#6	122.7(5)
C(21)-C(22)	1.381(14)	C(22)-N(22)-C(21)#6	57.3(5)
C(21)-C(21)#5	1.62(2)	C(21)#5-N(22)-C(21)#6	180.0(5)

C(22)-C(21)#6	1.381(14)	C(22)#4-N(22)-C(21)	122.7(5)
		C(22)-N(22)-C(21)	57.3(5)
		C(21)#5-N(22)-C(21)	67.3(9)
		C(21)#6-N(22)-C(21)	112.7(9)
		C(22)#4-N(22)-C(21)#4	57.3(5)
		C(22)-N(22)-C(21)#4	122.7(5)
		C(21)#5-N(22)-C(21)#4	112.7(9)
		C(21)#6-N(22)-C(21)#4	67.3(9)
		C(21)-N(22)-C(21)#4	180.000(3)
		C(21)-O(22)-C(21)#5	80.0(12)
		O(22)-C(21)-C(22)	160.7(13)
		O(22)-C(21)-N(22)	106.4(8)
		C(22)-C(21)-N(22)	59.8(9)
		O(22)-C(21)-C(21)#5	50.0(6)
		C(22)-C(21)-C(21)#5	114.7(9)
		N(22)-C(21)-C(21)#5	56.4(5)
		C(21)-C(22)-C(21)#6	123.6(17)
		C(21)-C(22)-N(22)	62.9(9)
		C(21)#6-C(22)-N(22)	62.9(9)

Symmetry transformations used to generate equivalent atoms: #1 -x,y,-z+1 #2 -x,-y+2,-z+1 #3 x,-y+2,z #4 -x,-y+1,-z+2 #5 -x,y,-z+2 #6 x,-y+1,z

Table B.3: Anisotropic parameters (A^2 x 10^3) for *cis*-[$Pd_2BpymCl_4$]·DMF.

	U11	U22	U33	U23	U13	U12
C(11)	12(3)	16(3)	18(3)	0	4(3)	0
C(12)	23(3)	15(2)	35(3)	7(2)	-2(2)	1(2)
C(13)	35(5)	8(3)	52(6)	0	-12(4)	0
N(1)	11(2)	18(2)	12(2)	4(1)	0(2)	-1(2)
Cl(11)	21(1)	48(1)	18(1)	-14(1)	4(1)	-12(1)
Pd(01)	12(1)	25(1)	12(1)	0	2(1)	0
N(22)	54(7)	12(4)	30(5)	0	28(5)	0
O(22)	84(11)	16(5)	68(9)	0	55(8)	0
C(21)	35(7)	40(6)	32(7)	0(5)	20(6)	-4(5)
C(22)	8(7)	130(20)	28(10)	0	2(7)	0

Table B.4: Torsion angles (◦) for *cis*-[Pd_2BpymCl_4]·DMF.

	Angle (◦)		Angle (◦)
N(1)-C(12)-C(13)-C(12)#1	0.3(4)	C(21)#5-N(22)-C(21)-C(22)	165.3(13)
N(1)#1-C(11)-N(1)-C(12)	0.3(3)	C(21)#6-N(22)-C(21)-C(22)	-14.7(13)
C(11)#2-C(11)-N(1)-C(12)	-179.7(3)	C(21)#4-N(22)-C(21)-C(22)	-70(100)
N(1)#1-C(11)-N(1)-Pd(01)	-176.4(3)	C(22)#4-N(22)-C(21)-C(21)#5	14.7(13)
C(11)#2-C(11)-N(1)-Pd(01)	3.6(3)	C(22)-N(22)-C(21)-C(21)#5	-165.3(13)
C(13)-C(12)-N(1)-C(11)	-0.5(7)	C(21)#6-N(22)-C(21)-C(21)#5	180.000(8)
C(13)-C(12)-N(1)-Pd(01)	175.3(3)	C(21)#4-N(22)-C(21)-C(21)#5	125(100)
C(11)-N(1)-Pd(01)-N(1)#3	-4.3(3)	O(22)-C(21)-C(22)-C(21)#6	65(4)
C(12)-N(1)-Pd(01)-N(1)#3	179.7(4)	N(22)-C(21)-C(22)-C(21)#6	17.4(15)
C(11)-N(1)-Pd(01)-Cl(11)	6.9(14)	C(21)#5-C(21)-C(22)-C(21)#6	31(3)
C(12)-N(1)-Pd(01)-Cl(11)	-169.1(9)	O(22)-C(21)-C(22)-N(22)	48(4)
C(11)-N(1)-Pd(01)-Cl(11)#3	174.8(2)	C(21)#5-C(21)-C(22)-N(22)	13.5(11)
C(12)-N(1)-Pd(01)-Cl(11)#3	-1.2(5)	C(22)#4-N(22)-C(22)-C(21)	82(100)
C(21)#5-O(22)-C(21)-C(22)	-42(3)	C(21)#5-N(22)-C(22)-C(21)	-16.2(14)
C(21)#5-O(22)-C(21)-N(22)	0.000(2)	C(21)#6-N(22)-C(22)-C(21)	163.8(14)
C(22)#4-N(22)-C(21)-O(22)	14.7(13)	C(21)#4-N(22)-C(22)-C(21)	180.000(11)
C(22)-N(22)-C(21)-O(22)	-165.3(13)	C(22)#4-N(22)-C(22)-C(21)#6	-82(100)
C(21)#5-N(22)-C(21)-O(22)	0.000(2)	C(21)#5-N(22)-C(22)-C(21)#6	180.000(7)
C(21)#6-N(22)-C(21)-O(22)	180.000(2)	C(21)-N(22)-C(22)-C(21)#6	-163.8(14)
C(21)#4-N(22)-C(21)-O(22)	125(100)	C(21)#4-N(22)-C(22)-C(21)#6	16.2(14)
C(22)#4-N(22)-C(21)-C(22)	180.000(8)		

Symmetry transformations used to generate equivalent atoms: #1 -x,y,-z+1 #2 -x,-y+2,-z+1 #3 x,-y+2,z #4 -x,-y+1,-z+2 #5 -x,y,-z+2 #6 x,-y+1,z

cis-$[Pd(PPh_3)_2(NO_3)_2].CO(CH_3)_2$

Table C. 1: Atomic coordinates (x 10^4) and equivalent isotropic Atomic coordinates (x 10^4) and equivalent isotropic displacement parameters (A^2 x 10^3) for *cis*-$[Pd(PPh_3)_2(NO_3)_2].CO(CH_3)_2$. U(eq) is defined as one third of the trace of the orthogonalized U^{ij} tensor.

	x	y	z	U(eq)
C(1)	1113(4)	4210(18)	3192(7)	119(5)
C(2)	193(3)	-629(11)	4457(6)	86(3)
C(006)	1091(3)	1831(15)	2959(5)	86(3)
C(012)	-99(3)	-137(13)	3831(7)	95(4)
C(013)	2262(2)	541(7)	6276(4)	39(2)
C(014)	1720(2)	-37(7)	4814(4)	42(2)
C(015)	1948(2)	2894(7)	5311(4)	41(2)
C(017)	2013(2)	3898(8)	5857(5)	55(2)
C(018)	1027(2)	2741(8)	4039(4)	49(2)
C(019)	2122(2)	5544(9)	5112(6)	70(3)
C(020)	2917(2)	-620(9)	7308(5)	59(2)
C(022)	2110(2)	5207(8)	5769(5)	62(2)
C(023)	541(2)	1353(7)	4490(5)	51(2)
C(024)	1437(2)	-969(7)	4715(5)	54(2)
C(025)	1029(2)	1652(10)	3569(5)	67(3)
C(026)	2555(2)	1385(8)	6720(4)	51(2)
C(027)	1917(2)	-173(9)	4391(4)	59(2)
C(028)	1536(3)	-2085(10)	3754(5)	74(3)
C(029)	2876(2)	779(10)	7226(5)	68(2)
C(030)	2629(2)	-1436(8)	6885(5)	55(2)
C(031)	2299(2)	-891(7)	6383(4)	49(2)
C(032)	1968(2)	3250(9)	4655(5)	56(2)
C(033)	1066(3)	4056(11)	3816(5)	79(3)
C(034)	848(2)	4016(8)	5179(4)	53(2)
C(036)	512(2)	119(9)	4787(5)	59(2)
C(037)	1104(3)	5028(8)	5412(5)	72(3)
C(038)	248(2)	1852(12)	3874(5)	76(3)
C(039)	2054(2)	4600(10)	4574(6)	68(2)
C(040)	1128(3)	3130(20)	2768(7)	116(5)
C(041)	1823(3)	-1163(9)	3864(5)	75(3)
C(042)	1355(3)	-2000(10)	4178(5)	75(3)
C(043)	-76(3)	1101(15)	3534(7)	97(4)
C(044)	1045(4)	6259(9)	5684(6)	89(4)

C(045)	729(4)	6415(11)	5772(6)	100(5)
C(046)	542(3)	4150(10)	5273(5)	75(3)
C(047)	481(4)	5381(14)	5602(7)	113(5)
N(34)	1760(2)	-407(7)	7159(4)	56(2)
N(35)	1010(2)	2407(8)	6796(4)	62(2)
P(002)	1832(1)	1225(2)	5564(1)	35(1)
P(003)	957(1)	2375(2)	4869(1)	43(1)
Pd(01)	1386(1)	1460(1)	5951(1)	37(1)
O(45)	1548(2)	-1137(6)	6671(4)	82(2)
O(46)	1975(2)	-831(7)	7781(4)	96(2)
O(47)	797(2)	2427(8)	7107(4)	97(3)
O(48)	1247(2)	3294(6)	6956(3)	63(2)
O(90)	966(1)	1502(5)	6331(3)	46(1)
O(91)	1760(1)	876(5)	7043(3)	48(1)
C(21)	0	-4120(50)	2500	250(17)
O(1)	0	-5480(30)	2500	290(12)
C(22)	196(9)	-3660(30)	3238(19)	125(10)

Table C.2: Bond distances (Å) and bond angles (◦) for *cis*-$[Pd(PPh_3)_2(NO_3)_2].CO(CH_3)_2$.

Bond	Distance (Å)	Bond Angle	Angle (◦)
C(1)-C(033)	1.334(15)	C(033)-C(1)-C(040)	122.9(14)
C(1)-C(040)	1.37(2)	C(036)-C(2)-C(012)	120.4(10)
C(2)-C(036)	1.374(11)	C(025)-C(006)-C(040)	117.4(12)
C(2)-C(012)	1.377(15)	C(043)-C(012)-C(2)	120.3(10)
C(006)-C(025)	1.345(13)	C(026)-C(013)-C(031)	118.9(7)
C(006)-C(040)	1.347(16)	C(026)-C(013)-P(002)	122.4(5)
C(012)-C(043)	1.363(16)	C(031)-C(013)-P(002)	118.7(5)
C(013)-C(026)	1.398(10)	C(027)-C(014)-C(024)	119.8(7)
C(013)-C(031)	1.410(9)	C(027)-C(014)-P(002)	123.3(6)
C(013)-P(002)	1.828(7)	C(024)-C(014)-P(002)	116.7(6)
C(014)-C(027)	1.385(10)	C(032)-C(015)-C(017)	118.9(7)
C(014)-C(024)	1.406(10)	C(032)-C(015)-P(002)	127.5(6)
C(014)-P(002)	1.828(7)	C(017)-C(015)-P(002)	113.6(6)
C(015)-C(032)	1.380(10)	C(022)-C(017)-C(015)	121.7(8)
C(015)-C(017)	1.395(10)	C(033)-C(018)-C(025)	116.8(8)
C(015)-P(002)	1.821(7)	C(033)-C(018)-P(003)	123.5(7)
C(017)-C(022)	1.367(10)	C(025)-C(018)-P(003)	119.6(6)
C(018)-C(033)	1.387(12)	C(039)-C(019)-C(022)	120.8(8)
C(018)-C(025)	1.413(12)	C(030)-C(020)-C(029)	118.7(8)

C(018)-P(003)	1.818(8)	C(019)-C(022)-C(017)	118.4(8)
C(019)-C(039)	1.343(13)	C(036)-C(023)-C(038)	119.6(8)
C(019)-C(022)	1.363(12)	C(036)-C(023)-P(003)	122.8(7)
C(020)-C(030)	1.358(11)	C(038)-C(023)-P(003)	117.5(7)
C(020)-C(029)	1.376(12)	C(042)-C(024)-C(014)	118.7(9)
C(023)-C(036)	1.365(11)	C(006)-C(025)-C(018)	123.3(10)
C(023)-C(038)	1.370(12)	C(029)-C(026)-C(013)	118.6(7)
C(023)-P(003)	1.814(7)	C(041)-C(027)-C(014)	119.5(9)
C(024)-C(042)	1.397(12)	C(042)-C(028)-C(041)	120.0(9)
C(026)-C(029)	1.382(11)	C(020)-C(029)-C(026)	122.5(8)
C(027)-C(041)	1.349(11)	C(020)-C(030)-C(031)	121.5(8)
C(028)-C(042)	1.329(13)	C(030)-C(031)-C(013)	119.7(8)
C(028)-C(041)	1.408(14)	C(015)-C(032)-C(039)	117.8(8)
C(030)-C(031)	1.381(10)	C(1)-C(033)-C(018)	118.6(12)
C(032)-C(039)	1.388(12)	C(046)-C(034)-C(037)	119.8(9)
C(034)-C(046)	1.333(12)	C(046)-C(034)-P(003)	120.1(7)
C(034)-C(037)	1.358(11)	C(037)-C(034)-P(003)	119.4(7)
C(034)-P(003)	1.833(8)	C(023)-C(036)-C(2)	120.0(9)
C(037)-C(044)	1.378(13)	C(034)-C(037)-C(044)	122.0(11)
C(038)-C(043)	1.393(13)	C(023)-C(038)-C(043)	120.9(11)
C(044)-C(045)	1.365(18)	C(019)-C(039)-C(032)	122.2(9)
C(045)-C(047)	1.358(18)	C(006)-C(040)-C(1)	120.8(12)
C(046)-C(047)	1.437(13)	C(027)-C(041)-C(028)	120.9(9)
N(34)-O(45)	1.209(9)	C(028)-C(042)-C(024)	120.9(10)
N(34)-O(46)	1.231(9)	C(012)-C(043)-C(038)	118.8(12)
N(34)-O(91)	1.271(8)	C(045)-C(044)-C(037)	118.4(11)
N(35)-O(48)	1.226(8)	C(047)-C(045)-C(044)	121.0(10)
N(35)-O(90)	1.232(8)	C(034)-C(046)-C(047)	119.7(11)
N(35)-O(47)	1.253(8)	C(045)-C(047)-C(046)	118.7(12)
P(002)-Pd(01)	2.2485(19)	O(45)-N(34)-O(46)	123.5(8)
P(003)-Pd(01)	2.2760(19)	O(45)-N(34)-O(91)	119.3(7)
Pd(01)-O(91)	2.110(5)	O(46)-N(34)-O(91)	117.2(7)
Pd(01)-O(90)	2.130(5)	O(48)-N(35)-O(90)	122.9(7)
C(21)-O(1)	1.33(4)	O(48)-N(35)-O(47)	119.1(8)
C(21)-C(22)	1.40(3)	O(90)-N(35)-O(47)	118.0(7)
C(21)-C(22)#1	1.40(3)	C(015)-P(002)-C(013)	105.4(3)
		C(015)-P(002)-C(014)	112.5(3)
		C(013)-P(002)-C(014)	101.5(3)
		C(015)-P(002)-Pd(01)	109.9(2)
		C(013)-P(002)-Pd(01)	114.1(2)
		C(014)-P(002)-Pd(01)	113.0(2)

		C(023)-P(003)-C(018)	102.1(4)
		C(023)-P(003)-C(034)	107.8(4)
		C(018)-P(003)-C(034)	106.4(4)
		C(023)-P(003)-Pd(01)	111.5(3)
		C(018)-P(003)-Pd(01)	125.1(2)
		C(034)-P(003)-Pd(01)	102.9(3)
		O(91)-Pd(01)-O(90)	88.3(2)
		O(91)-Pd(01)-P(002)	89.89(14)
		O(90)-Pd(01)-P(002)	175.21(14)
		O(91)-Pd(01)-P(003)	170.53(15)
		O(90)-Pd(01)-P(003)	85.72(15)
		P(002)-Pd(01)-P(003)	96.63(7)
		N(35)-O(90)-Pd(01)	113.4(4)
		N(34)-O(91)-Pd(01)	113.3(5)
		O(1)-C(21)-C(22)	108(2)
		O(1)-C(21)-C(22)#1	108(2)
		C(22)-C(21)-C(22)#1	143(5)
Symmetry transformations used to generate equivalent atoms: #1 -x+2,y,-z+3/2			

Table C.3: Anisotropic parameters (A^2 x 10^3) for *cis*-$[Pd(PPh_3)_2(NO_3)_2].CO(CH_3)_2$.

	U11	U22	U33	U23	U13	U12
C(1)	130(11)	148(13)	65(8)	19(9)	30(8)	-7(10)
C(2)	69(7)	81(7)	109(9)	-33(6)	41(7)	-43(6)
C(006)	62(6)	155(11)	44(6)	-6(7)	27(5)	12(7)
C(012)	64(7)	129(10)	104(9)	-53(8)	47(7)	-56(7)
C(013)	43(4)	42(4)	37(4)	1(3)	21(3)	1(3)
C(014)	49(4)	43(4)	31(4)	1(3)	13(3)	11(3)
C(015)	38(4)	42(4)	44(4)	4(3)	17(3)	-5(3)
C(017)	66(5)	53(5)	53(5)	-1(4)	32(4)	-6(4)
C(018)	39(4)	61(5)	36(4)	10(3)	7(3)	-4(3)
C(019)	59(5)	52(5)	95(7)	20(5)	31(5)	-6(4)
C(020)	43(5)	80(6)	55(5)	16(5)	21(4)	16(4)
C(022)	66(5)	43(4)	72(6)	-10(4)	27(5)	-15(4)
C(023)	43(4)	50(5)	63(5)	-16(4)	26(4)	-8(3)
C(024)	53(5)	41(4)	65(5)	-9(4)	22(4)	1(3)
C(025)	50(5)	71(6)	64(6)	0(5)	9(4)	9(4)
C(026)	48(5)	52(5)	46(5)	2(3)	13(4)	-1(3)
C(027)	63(5)	57(5)	58(5)	0(4)	27(4)	7(4)

C(028)	114(9)	55(6)	41(5)	-14(4)	23(5)	8(6)
C(029)	50(5)	83(7)	55(5)	1(5)	7(4)	-7(5)
C(030)	50(5)	57(5)	63(5)	12(4)	29(4)	12(4)
C(031)	56(5)	38(4)	52(5)	10(3)	21(4)	6(3)
C(032)	52(5)	65(5)	64(6)	4(4)	36(4)	6(4)
C(033)	88(7)	76(7)	51(5)	24(5)	8(5)	-21(5)
C(034)	50(5)	48(4)	51(5)	-3(4)	12(4)	12(4)
C(036)	59(5)	65(5)	53(5)	-3(4)	23(4)	-18(4)
C(037)	83(7)	48(5)	64(6)	-3(4)	13(5)	-6(5)
C(038)	48(5)	84(7)	72(6)	-13(5)	4(5)	-8(5)
C(039)	71(6)	68(6)	75(7)	29(5)	42(5)	6(5)
C(040)	75(8)	214(17)	50(7)	38(9)	17(6)	-38(9)
C(041)	109(8)	74(6)	44(5)	-10(4)	34(5)	29(6)
C(042)	94(7)	47(5)	66(6)	-11(5)	17(6)	3(5)
C(043)	47(6)	146(11)	89(8)	-22(8)	21(6)	-26(6)
C(044)	116(10)	47(6)	76(7)	-14(5)	16(7)	-1(6)
C(045)	125(11)	65(7)	68(7)	-17(5)	2(7)	34(7)
C(046)	58(6)	67(6)	82(7)	-9(5)	13(5)	15(5)
C(047)	81(8)	119(10)	111(10)	-42(8)	15(7)	46(8)
N(34)	72(5)	51(4)	52(4)	-4(3)	33(4)	6(4)
N(35)	37(4)	81(5)	70(5)	4(4)	26(4)	-9(3)
P(002)	36(1)	37(1)	32(1)	-1(1)	14(1)	1(1)
P(003)	38(1)	42(1)	44(1)	-1(1)	14(1)	-3(1)
Pd(01)	39(1)	36(1)	38(1)	-1(1)	18(1)	-2(1)
O(45)	113(6)	51(4)	76(5)	-1(3)	35(4)	-12(4)
O(46)	135(7)	81(5)	63(4)	30(4)	35(4)	49(5)
O(47)	84(5)	132(7)	104(6)	-54(5)	69(5)	-37(4)
O(48)	62(4)	62(4)	67(4)	-10(3)	29(3)	-8(3)
O(90)	40(3)	56(3)	47(3)	-15(2)	25(2)	-11(2)
O(91)	53(3)	49(3)	39(3)	3(2)	18(2)	0(2)

Table C.4: Torsion angles (◦) for *cis*-$[Pd(PPh_3)_2(NO_3)_2].CO(CH_3)_2$.

	Angle (◦)		Angle (◦)
C(16)-C(11)-C(12)-C(13)	-5.8(13)	C(36)-C(31)-P(1)-Pd(1)	-6.1(7)
P(1)-C(11)-C(12)-C(13)	-176.8(7)	C(32)-C(31)-P(1)-Pd(1)	174.8(6)
C(11)-C(12)-C(13)-C(14)	4.5(15)	C(22)-C(21)-P(1)-C(31)	126.1(7)
C(12)-C(13)-C(14)-C(15)	0.6(18)	C(26)-C(21)-P(1)-C(31)	-52.1(7)
C(13)-C(14)-C(15)-C(16)	-4.3(18)	C(22)-C(21)-P(1)-C(11)	13.1(8)
C(12)-C(11)-C(16)-C(15)	1.9(14)	C(26)-C(21)-P(1)-C(11)	-165.1(6)
P(1)-C(11)-C(16)-C(15)	172.9(8)	C(22)-C(21)-P(1)-Pd(1)	-106.5(7)
C(14)-C(15)-C(16)-C(11)	3.0(16)	C(26)-C(21)-P(1)-Pd(1)	75.3(6)
C(26)-C(21)-C(22)-C(23)	-0.9(14)	C(16)-C(11)-P(1)-C(31)	16.3(8)
P(1)-C(21)-C(22)-C(23)	-179.1(9)	C(12)-C(11)-P(1)-C(31)	-172.8(7)
C(21)-C(22)-C(23)-C(24)	-2.1(18)	C(16)-C(11)-P(1)-C(21)	125.0(7)
C(22)-C(23)-C(24)-C(25)	2(2)	C(12)-C(11)-P(1)-C(21)	-64.1(7)
C(23)-C(24)-C(25)-C(26)	1.3(17)	C(16)-C(11)-P(1)-Pd(1)	-101.8(7)
C(24)-C(25)-C(26)-C(21)	-4.4(14)	C(12)-C(11)-P(1)-Pd(1)	69.1(7)
C(22)-C(21)-C(26)-C(25)	4.2(12)	C(46)-C(41)-P(2)-C(61)	-2.3(8)
P(1)-C(21)-C(26)-C(25)	-177.4(7)	C(42)-C(41)-P(2)-C(61)	176.4(5)
C(36)-C(31)-C(32)-C(33)	-1.7(14)	C(46)-C(41)-P(2)-C(51)	107.5(7)
P(1)-C(31)-C(32)-C(33)	177.5(8)	C(42)-C(41)-P(2)-C(51)	-73.8(6)
C(31)-C(32)-C(33)-C(34)	1.2(17)	C(46)-C(41)-P(2)-Pd(1)	-129.0(6)
C(32)-C(33)-C(34)-C(35)	-0.6(17)	C(42)-C(41)-P(2)-Pd(1)	49.7(6)
C(33)-C(34)-C(35)-C(36)	0.5(16)	C(62)-C(61)-P(2)-C(41)	42.3(7)
C(32)-C(31)-C(36)-C(35)	1.6(13)	C(66)-C(61)-P(2)-C(41)	-142.3(5)
P(1)-C(31)-C(36)-C(35)	-177.6(7)	C(62)-C(61)-P(2)-C(51)	-69.8(6)
C(34)-C(35)-C(36)-C(31)	-1.0(14)	C(66)-C(61)-P(2)-C(51)	105.5(6)
C(46)-C(41)-C(42)-C(43)	-2.3(12)	C(62)-C(61)-P(2)-Pd(1)	167.5(5)
P(2)-C(41)-C(42)-C(43)	178.9(7)	C(66)-C(61)-P(2)-Pd(1)	-17.2(6)
C(41)-C(42)-C(43)-C(44)	3.7(13)	C(52)-C(51)-P(2)-C(41)	23.9(7)
C(42)-C(43)-C(44)-C(45)	-2.3(13)	C(56)-C(51)-P(2)-C(41)	-156.5(5)
C(43)-C(44)-C(45)-C(46)	-0.6(14)	C(52)-C(51)-P(2)-C(61)	141.3(6)
C(42)-C(41)-C(46)-C(45)	-0.6(11)	C(56)-C(51)-P(2)-C(61)	-39.0(6)
P(2)-C(41)-C(46)-C(45)	178.0(6)	C(52)-C(51)-P(2)-Pd(1)	-96.9(6)
C(44)-C(45)-C(46)-C(41)	2.0(13)	C(56)-C(51)-P(2)-Pd(1)	82.8(6)
C(56)-C(51)-C(52)-C(53)	2.2(11)	N(2)-O(4)-Pd(1)-O(3)	84.3(5)
P(2)-C(51)-C(52)-C(53)	-178.1(6)	N(2)-O(4)-Pd(1)-P(2)	-91.4(4)
C(51)-C(52)-C(53)-C(54)	1.0(13)	N(2)-O(4)-Pd(1)-P(1)	135.5(8)
C(52)-C(53)-C(54)-C(55)	-1.9(13)	N(1)-O(3)-Pd(1)-O(4)	66.1(5)
C(53)-C(54)-C(55)-C(56)	-0.4(13)	N(1)-O(3)-Pd(1)-P(2)	133.7(15)
C(54)-C(55)-C(56)-C(51)	3.7(12)	N(1)-O(3)-Pd(1)-P(1)	-106.4(5)

C(52)-C(51)-C(56)-C(55)	-4.5(11)	C(41)-P(2)-Pd(1)-O(4)	-113.1(3)
P(2)-C(51)-C(56)-C(55)	175.8(6)	C(61)-P(2)-Pd(1)-O(4)	120.4(3)
C(66)-C(61)-C(62)-C(63)	2.6(11)	C(51)-P(2)-Pd(1)-O(4)	5.1(3)
P(2)-C(61)-C(62)-C(63)	177.9(6)	C(41)-P(2)-Pd(1)-O(3)	179(100)
C(61)-C(62)-C(63)-C(64)	-1.9(13)	C(61)-P(2)-Pd(1)-O(3)	53.0(17)
C(62)-C(63)-C(64)-C(65)	-0.5(14)	C(51)-P(2)-Pd(1)-O(3)	-62.3(17)
C(63)-C(64)-C(65)-C(66)	2.3(14)	C(41)-P(2)-Pd(1)-P(1)	60.0(2)
C(62)-C(61)-C(66)-C(65)	-0.9(11)	C(61)-P(2)-Pd(1)-P(1)	-66.5(2)
P(2)-C(61)-C(66)-C(65)	-176.4(6)	C(51)-P(2)-Pd(1)-P(1)	178.2(2)
C(64)-C(65)-C(66)-C(61)	-1.5(13)	C(31)-P(1)-Pd(1)-O(4)	-105.2(9)
O(1)-N(1)-O(3)-Pd(1)	8.1(9)	C(21)-P(1)-Pd(1)-O(4)	131.6(9)
O(2)-N(1)-O(3)-Pd(1)	-173.3(6)	C(11)-P(1)-Pd(1)-O(4)	10.2(9)
O(6)-N(2)-O(4)-Pd(1)	-2.7(9)	C(31)-P(1)-Pd(1)-O(3)	-53.8(3)
O(5)-N(2)-O(4)-Pd(1)	178.9(5)	C(21)-P(1)-Pd(1)-O(3)	-177.0(3)
C(36)-C(31)-P(1)-C(21)	129.6(7)	C(11)-P(1)-Pd(1)-O(3)	61.6(3)
C(32)-C(31)-P(1)-C(21)	-49.6(7)	C(31)-P(1)-Pd(1)-P(2)	122.1(3)
C(36)-C(31)-P(1)-C(11)	-118.3(7)	C(21)-P(1)-Pd(1)-P(2)	-1.1(3)
C(32)-C(31)-P(1)-C(11)	62.5(8)	C(11)-P(1)-Pd(1)-P(2)	-122.5(3)